INTERNATIONAL STUDIES IN SCIENCE AND MATHEMATICS

EDITORS
PROF. DR. AHMET AKSOY
PROF. DR. HASAN AKGÜL

March 2024

SERÜVEN YAYINEVİ

Genel Yayın Yönetmeni / Editor in Chief • C. Cansın Selin Temana

Kapak & İç Tasarım / Cover & Interior Design • Serüven Yayınevi

Birinci Basım / First Edition • © Mart 2024

ISBN • 978-625-6319-08-0

Serüven Yayınevi / Serüven Publishing
Türkiye Adres / Turkey Address: Kızılay Mah. Fevzi Çakmak 1. Sokak
Ümit Apt No: 22/A Çankaya/ANKARA
Telefon / Phone: 05437675765
web: www.seruvenyayinevi.com
e-mail: seruvenyayinevi@gmail.com

Baskı & Cilt / Printing & Volume
Sertifika / Certificate No: 47083

INTERNATIONAL STUDIES IN SCIENCE AND MATHEMATICS

March 2024

Editors

PROF. DR. AHMET AKSOY

PROF. DR. HASAN AKGÜL

CONTENTS

CHAPTER 1

THE BIG THREAT IN OUR LIVES: MICROPLASTICS

Mustafa Fatih ERGİN[1]
Hülya ÇELİK ONAR[2]
Hasniye YAŞA[3]

1 İstanbul University-Cerrahpaşa, Engineering Faculty, Chemical Engineering Department, Avcılar,İstanbul,Türkiye Assoc.Prof. Mustafa Fatih ERGİN ORCID:0000-0003-4158-368X
2 İstanbul University-Cerrahpaşa, Engineering Faculty, Chemistry Department, Avcılar,İstanbul,Türkiye, Assoc.Prof. Hülya ÇELİK ONAR ORCID:0000-0003-2573-5751
3 İstanbul University-Cerrahpaşa, Engineering Faculty, Chemistry Department, Avcılar,İstanbul,Türkiye , Assoc. Prof. Hasniye YAŞA ORCID:0000-0003-3171-9096

Plastics made of macromolecular organic chemicals, primarily derived from natural gas and oil, but also, more recently, from plant sources like corn and sugar cane, have become an essential part of human existence (Tsiropoulos et al., 2015; Ergin and Ergin, 2021a; Ergin and Ergin, 2021b). And the global plastic market is predicted to reach 721.14 billion US dollars by 2027. Europe, Asia, and the United States are the main producers of plastic. China, home to the most population on Earth, produced the greatest amount of plastic—nearly 62 million tonnes. With almost 39 million tonnes, the United States ranked second, and Brazil was third with 13 million tonnes. Unfortunately, the plastics we commonly use due to their advantages of low cost, processability and durability are considered one of today's biggest pollutants (Akçay et al., 2020; Bulat and Kılınç,2020) Because only 10% of plastic waste can be recycled (Yurtsever, 2015; Esmeray and armutçu, 2020).

Plastic materials break down into smaller sizes over time through different degradation mechanisms such as photodegradation, oxidation, hydrolytic degradation and biological degradation. They are called by different names depending on their size (GESAMP, 2016).

- Those with a size of 100 - 2.5 cm are Macroplastic (Visible with the naked eye),
- Those with a size of 2.5 - 0.1 cm (1000 μm) are Mesoplastic (Visible with the naked eye or an optical microscope)
- Those with a size of 0.1 cm - 1 μm are Microplastic (Can be seen with an optical microscope).
- < 1 μm in size are called Nanoplastic (visible with an electron microscope).

Thompson used the word "microplastic" for the first time in 2004 (Arı and Öğüt, 2021). In the publication made by Frias, a more detailed definition was made by saying that any artificial solid particles or polymeric matrices are considered microplastics that are insoluble in water, originating from primary or secondary production, ranging between 1 and 5 mm in size, and having regular or irregular shapes (Frias and Nash, 2019). Microplastics can be found in many morphological forms such as amorphous, spherical and long fiber forms (Yurtsever, 2015). Microplastics (MPs) also differ in many aspects such as size, composition, weight, physical and chemical properties. There are two types of microplastics: primary and secondary. Primary MPs are specially made plastic particles that are less than five millimeters. Secondary MPs are tiny plastic particles that are created when big plastics deteriorate and wear down over time due to several interaction mechanisms. Microplastics are categorized as thermoplastics, thermosets, or elastomers based on their chemical composition and temperature. Based on their

intended use, thermoplastics are further divided into ordinary plastics, engineering plastics, and special plastics. Standard or common plastics are used extensively because of their important qualities and low cost. This group of polymers includes polyethylene (PE), polypropylene (PP), polystyrene (PS), and polyvinyl chloride (PVC). The superior structures, clarity, self-lubrication, and thermal properties of engineering plastics make them useful. This group of polymers includes polyamide, polybutylene terephthalate, polyethylene terephthalate, polycarbonate, polyphenylene ether (Mishra et al. 2019). Special plastics, like Teflon, can endure changes in temperature and chemical products well, while polymethyl methacrylate (PMMA) has higher telligibility and more consistent brightness. The fourth type of plastics that can withstand temperatures up to 152 °C are elevated recital plastics, which have a high heat endurance. Polyphenylene sulfide (PPS), polysulfone (PSU), polyarylsulfone (PAS), polyethersulfone (PES), polyimide and liquid crystal polymers (LCP) are examples of high-performance plastics.

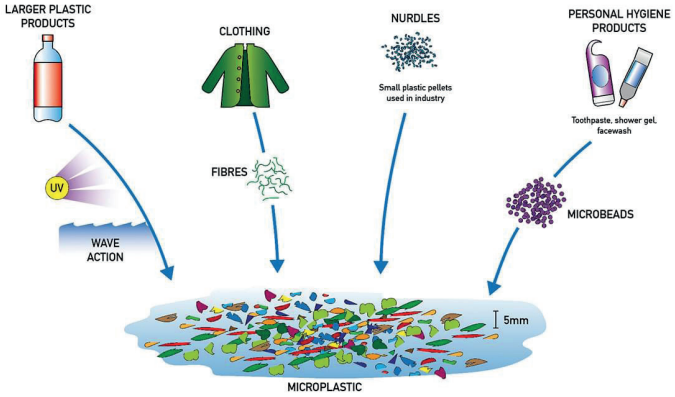

According to the results of statistical analyses, 92.4% of plastic waste consists of microplastics (MPs), which mainly consist of polystyrene (PS), polyethylene (PE) and polypropylene (PP).(Carr et al., 2016; Santana et al. 2016). The main origins of tiny plastic particles are microbeads, which are banned for use in cosmetics in some countries today (Yurtsever and Yurtsever, 2019), production pellet waste and/or waste of plastic factories and as secondary sources, microfibers (microfiber, MF) shed from synthetic textile products, vehicles, tire spills, road coating and paint spills, and in short, small debris that occurs when plastics break down in the environment over time.

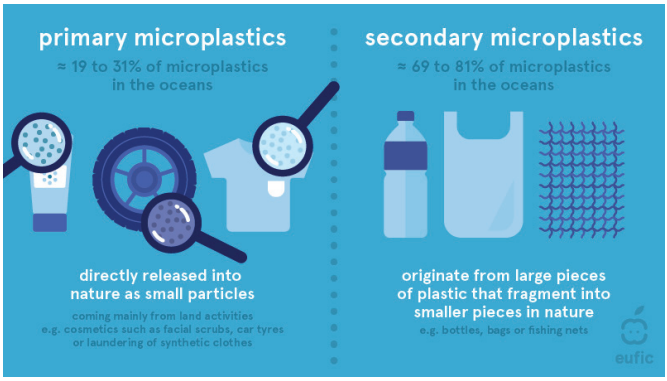

MPs are thought to be more hazardous persistent pollutants than plastics (Gaylarde et al., 2021). China and European nations have implemented rules and restrictions in the last ten years to limit the use of plastics and eliminate MP pollution at its source (Du et al., 2021). Persistent organic pollutants (POPs), which are polychlorinated biphenyls (PCB) and dichloro diphenyl trichloroethane (DDT), and some of the micropollutants are anthropogenic toxic substances that have a permanent effect in the environment because they do not biodegrade or degrade.

The ways in which humans are exposed to microplastics vary. These are commonly divided into three categories: oral route, skin contact (synthetic textile items), and inhalation (microplastics found in breathed air, city dust, powdered synthetic rubber compounds, etc.). Furthermore, eating or drinking tainted seafood, other foods, or water tainted with microplastics allows the particles to enter the gastrointestinal system directly. While human skin can block the entry of microplastics and other pollutants into the body during this process, there are still ways for microplastics to spread, including through open wounds, sweat glands, and the scalp (Toussaint et al., 2019). If microplastics in foods are examined, it is possible that these plastics can pass into foods in the basic raw materials for some products, in some during the production process, in others due to the packaging materials used in packaging, and during the consumption of the product (from the air, etc.). It has been established that consumption of microplastic alters human chromosomes, resulting in obesity, cancer, and infertility. Because they are biologically persistent, microplastics may cause adverse biological reactions in people, including genotoxicity, oxidative stress, necrosis of the tissue, cell apoptosis, and inflammation. These effects may also result in fibrosis, localized cell and tissue damage, and even cancer. Plastics are the most often utilized materials for packaging in the present food production system. The extensive usage of plastics in the food sector is assumed to be the reason for the growing inclusion of microplastics in the food chain (Van Raamsdonk et al., 2020). Studies have shown that acrylonitrile migration from disposable

plastic cups is carcinogenic, and bisphenol A migration from materials such as polycarbonate plastics, plastic plates and cutlery, glass container lids and the inner coating of aluminum cans causes breast cancer and prostate cancer. It has been observed that phthalate transfer from food packaging has an impact on the reproductive and nervous systems, and that styrene (also known as vinyl benzene) transfer from foam plates, cups and sandwich containers has carcinogenic effects. (Lu et al., 2019).

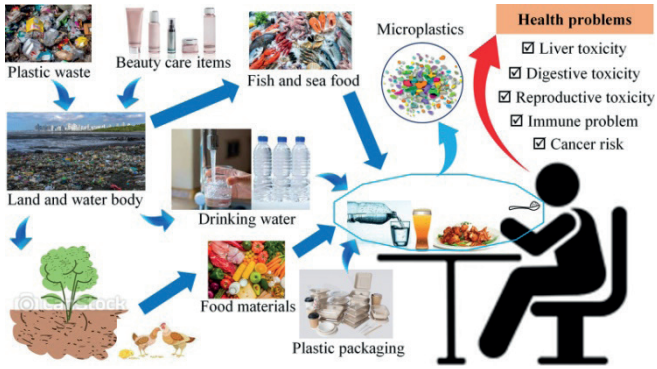

The aquatic ecology is the target of microplastics' most evident harmful effects. According to reports, without an effective management plan, plastic debris entering the oceans varies from 4.8 to 12.8 million metric tons. This dumping of plastic waste into the water has had a number of negative effects on both human and marine health and marine life (Anand et al., 2023). Because MPs are easily absorbed by aquatic plants and animals, they can have a negative impact on their growth, development, and reproduction (Qu et al., 2020; Ge et al., 2021; Mateos-Cardenas et al., 2019; Tanaka et al., 2020; Qiao et al., 2019; Cho et al., 2019). Pathogenic bacteria (Oberbeckmann and Labrenz, 2020; Stabnikova et al., 2021), antibiotics (Sathicq et al., 2021), polycyclic aromatic hydrocarbons (Sharma et al., 2020), heavy metals (Tang et al., 2021), organic chemicals (Rodrigues et al., 2019), and organic compounds (Tang et al., 2021) are only a few of the pollutants that MPs can absorb from the water. Additionally, they may serve as transporters of toxins that aquatic life consumes, enabling the pollutants to go inside the organisms. Plastics make up the bulk of the trash found in water resources (Koelmans et al., 2019). Particles of plastic may also be swallowed by water birds (seagulls, albatrosses) when they eat fish, mussels, and squid. Turtles may inadvertently swallow the plastic bags surrounding them when they are consuming jellyfish, thinking them to be food. Because microplastics are easily ingested and degraded, and because their color and structure are similar to those of food, most aquatic species can mistake them for food (Kirstein et al., 2016). Since the 1990s, it has been stated that over 140,000 marine species have perished annually as a result of ingesting plastic or from being wrapped in it (Valeria et al., 2012).

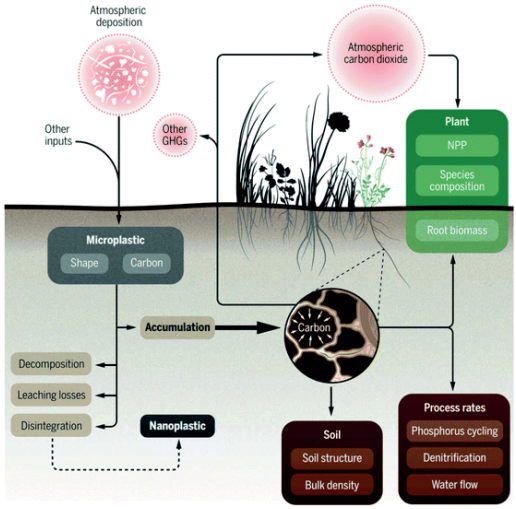

Terrestrial ecosystems also play an important role in transporting microplastics to aquatic ecosystems. Because the use of microplastics is predominantly in terrestrial ecosystems (He et al., 2018). Additionally, MPs have direct access to agricultural soils through sewage mud, water for irrigation, household water, and atmospheric buildup, or they might enter unintentionally by means of the degradation of plastic residues in agricultural processes. Plastic wastes affect soil macrofauna activities and microbial populations, and they also reduce the saturated hydraulic conductivity of soil. In turn, soil microbial communities play a critical part in the nutrition cycle and impact the behavior of pollutants, such as the mineralization, biodegradation, and detoxification of harmful substances. Microplastics that enter the soil can be stored in the soil and They can be moved to another location by erosion. Afterwards, they can be degraded by other environmental factors and even leak into groundwater. Many creatures living in the soil can also absorb these leaked microplastics into their bodies (Esmeray and Armutcu, 2020).

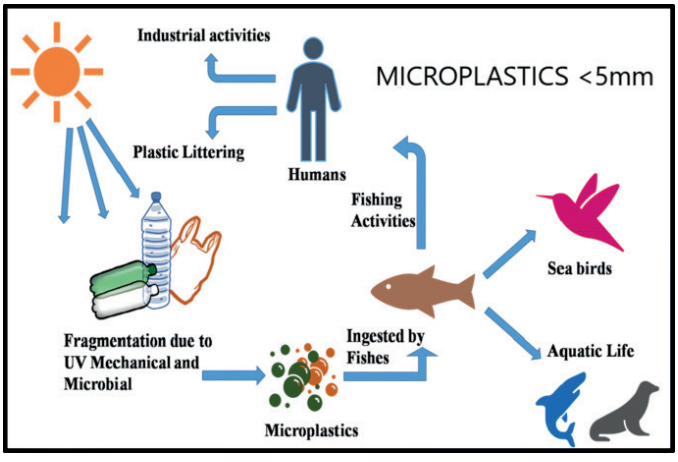

Optical microscopy, electron microscopy, raman spectroscopy, and Fourier transform spectroscopy (FTIR) can all be used to identify microplastics. After visually inspecting potential plastics, the most popular method for identifying microplastics is polymeric biopsy, which frequently involves the use of spectroscopic, optical or thermo-analytical techniques. It comprises a compositional chemical analysis (Yang et al., 2018).

The easiest and most popular method for recognizing microplastics is visual identification, which can be done using an optical microscope or by using your unaided eyes. The likelihood of a false positive using optical techniques grows significantly as the size of the particles under examination decreases. Therefore, it is advised to validate the identity of microplastics, especially in small items, using spectroscopic instruments or other analytical procedures.

By directing a strong electron beam onto a sample's surface, a scanning electron microscope (SEM) may produce high-resolution photographs of the material. Electrons image the sample's surface details at extremely high magnifications. By analyzing high-resolution photographs of their surface shape under SEM, microplastics can be identified from other organic or inorganic foreign components.

A specific chemical bond's distinctive infrared spectra can be obtained via Fourier transform infrared spectroscopy (FTIR). An unknown substance can be identified by comparing its spectrum to that of recognized compounds since various materials have distinct bond compositions. FTIR is quickly becoming one of the most used methods for analyzing microplastics extracted from environmental materials because of its great dependability.

A popular and very trustworthy method for identifying the polymers in microplastics that are found in a variety of environmental matrices is Raman spectroscopy. Raman spectroscopy is used to identify microplastics by shining a monochromatic laser beam onto a suspect sample. This causes the sample's unique molecular structure and atomic composition to absorb, scatter, or reflect light at a different frequency, which is then backscattered back onto the sample. Every polymer might have its own distinct spectra thanks to this well-known Raman shift.

By examining the results of heat breakdown, pyrolysis gas chromatography spectrometry, or Pyr-GC-MS, is a destructive approach that has also been effectively applied to the chemical detection of environmental microplastics. By contrasting the distinctive pyrograms of microplastics with reference pyrograms made by recognized pure polymers, the polymer types of the microplastics can be identified. Compared to ATR, FTIR, and microscopy spectroscopy, It has the significant benefit of being able to simultaneously offer extensive information about the chemical makeup of the polymer and

the organic additives it contains. Moreover, Pyr-GC-MS is insensitive to the size, shape, and accompanying inorganic or organic impurities of the particles under study (Esmeray and Armutcu, 2020).

The ways by which MPs degrade have been documented in a number of research conducted recently. Generally speaking, chemical, mechanical, and biological mechanisms lead to the breakdown of microplastics in the environment. Additionally, the breakdown of microplastics is also significantly influenced by abiotic variables, including ambient additives, pH, temperature, light, and oxygen bioturbation requirements (Liu et al., 2022). Because they are resistant to deterioration, conventional plastics may remain in the environment for extended periods of time (Andrady et al., 2023). Many different recycling techniques are currently available, but mechanical recycling is the most commonly used because it is inexpensive, produces little pollution, and can process a wide range of different materials. However, doses that are repeatedly subjected to mechanical recycling deteriorate the structures of the polymers and cause the product to become unusable. The four main physical methods are sol-gel, adsorption, coagulation, and filtration. Structural composite silica gel is created by the sol-gel process, and it then interacts and polymerizes with MPs (Li et al., 2023). Separation technology is then employed to remove these agglomerates and the MPs. In order to produce the separation effect, coagulation filtration leads MPs to form bigger agglomerates through coagulation. Since the sol–gel method reacts with pH, it is more suited for use with liquids (Herbort et al., 2018). Overuse of coagulants will damage organisms and result in secondary pollution. Various adsorbent materials have the ability to adsorbe MPs through mechanisms such as hydrogen bonding, π-π interactions, and electrostatic interactions. Though both magnetic and composite adsorbents have perfect removal efficiencies, their material synthesis is challenging and costly, and more study is needed to comprehend the adsorption mechanism of MPs, so the development of MPs adsorbents will remain the center of attention (Sharma et al., 2021).

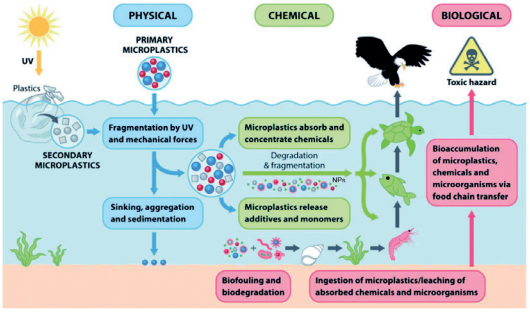

Plastics usually degrade chemically through oxidative and hydrolytic processes. Advanced Oxidation Processes (AOPs) are an effective chemical elimination technique and It may result in cross-linking, chemical chain

scission, or a range of reactive oxygen species (ROS). They also perform very well in the degradation of microplastics (MPs), according to certain recent research (Chen et al., 2022). Three main AOP processes are direct photodegradation, photocatalytic oxidation, and electrochemical oxidation. Nevertheless, because a significant amount of secondary waste debris is produced during the employment of chemical agents during degradation, this degradation strategy is only used on a modest scale (Arpia et al., 2021).

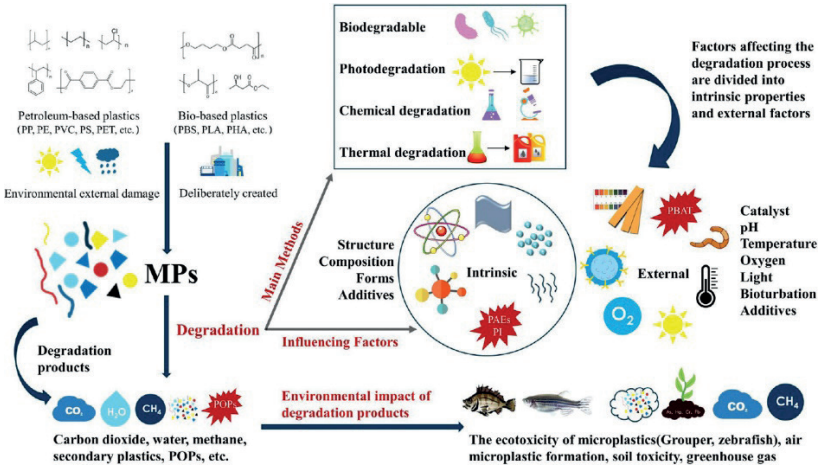

The process of eliminating microplastics using a variety of microorganisms, including bacteria, fungi and plants, is known as bioremediation or biodegradation. It is the most noteworthy kind of approach because of its high effectiveness, sustainability, and kindness to the environment. While MPs are chemically robust and may tolerate some degree of environmental degradation, research has shown that specific bacteria and fungi can accelerate the breakdown of MPs (Krueger et al., 2015). The physicochemical and microbiological degradation components of MPs are coupled in an integrated process that occurs in a variety of conditions (Ammala et al., 2011). MP transformation has been significantly impacted by microbial degradation, despite MPs being less susceptible to microbial attack than other degradable materials (Rujnic-Sokele and Pilipovic, 2017). Microbes have a specific ecological niche because MPs offer them both a carbon supply and assistance for colonization and growth. Numerous kinds of bacteria that are capable of breaking down MPs have been isolated from a range of environmental samples in order to study the degradation behavior of MPs. Biological degradation mechanisms allow microplastics to completely break down into carbon dioxide and water, releasing no secondary contaminants. Biologically based remediation is less harmful to the environment than other processes and detoxifies potentially toxic compounds instead of just shifting toxins from one environmental medium to another. Numerous studies have documented the function of microbial communities in the degradation of microplastics in both

terrestrial and marine environments (Goveas et al., 2023). Microorganisms have the ability to create enzymes that can destroy or change the chemical structure of microplastics. (Miloloža et al., 2022). The capacity of some plastic waste fractions to be degraded by microbial enzymes has been demonstrated by groundbreaking research conducted by many academics (Chellasamy et al., 2022). Sometimes two or more microorganisms are used together to eliminate the negative effects of toxic metabolites produced in MP degradation. (Yuan et al., 2020). Because toxic metabolite produced by one can be used as substrates by another (Singh and Wahid, 2015) It is thought that the best bacteria to use for the biodegradation of plastics are those that produce biofilms. Fungi are thought to be excellent natural candidates for the breakdown of plastic due to their extracellular complexes and multienzyme capabilities (Matavulj and Molitoris, 2009). The enzymatic system found inside the cells of fungi acts as an internal detoxifying mechanism and is a major role in their adaptability. The enzymes that drive the system are members of the cytochrome P450 family, which includes transferases and epoxidases. These enzymes engage in the processes of conjugation and oxidation, respectively, and catalyze them (Olicón-Hernández et al., 2017).

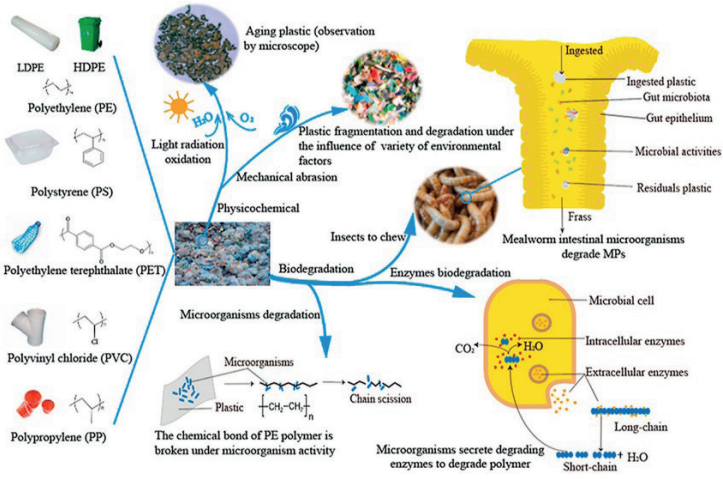

REFERENCES

Akçay, S., Törnük, F. & Yetim, H. (2020). Mikroplastikler: Gıdalarda Bulunuşu ve Sağlık Üzerine Etkileri. *Avrupa Bilim ve Teknoloji Dergisi*, (20), 530-538. DOI: 10.31590/ejosat.725259.

Anand, U., Dey, S., Bontempi, E., Ducoli, S., Vethaak, A.D., Dey, A., Federic, S. (2023). Biotechnological methods to remove microplastics: a review. Environmental Chemistry Letters https://doi.org/10.1007/s10311-022-01552-4

Andrady, A. L., Heikkilä, A. M., Pandey, K. K., Bruckman, L. S., White, C. C., Zhu, M.(2023).Effects of UV radiation on natural and synthetic materials. Photochem. Photobiol. Sci. 22, 1177–1202.

Ammala, A., Bateman, S., Dean, K., Petinakis, E., Sangwan, P., Wong, S., Yuan, Q., Yu, L., Patrick, C., Leong, K.H. (2011). An overview of degradable and biodegradable polyolefins. Prog. Polym. Sci. 36, 1015–1049.

Arı, M., Öğüt,S. (2021). Mikroplastikler ve Çevresel Etkileri, Düzce Üniversitesi Bilim ve Teknoloji Dergisi, 9, 864-877. DOI: 10.29130/dubited.757698

Arpia, A. A.;Chen,W.H.;Ubando, A.T.;Naqvi, S. R.;Culaba, A. B. (2021). Microplastic degradation as a sustainable concurrent approach for producing biofuel and obliterating hazardous environmental effects: a state-of-the-art review. J. Hazard. Mater. 418, 126381.

Bulat, F.N., Kılınç, B., (2020). Effects of plastics and microplastics on aquatic organisms and human health. *Ege Journal of Fisheries and Aquatic Sciences,* 37(4), 437-443. DOI: 10.12714/egejfas.37.4.16

Carr, S.A., Liu, J., Tesoro, A.G. (2016). Transport and fate of microplastic particles in wastewater treatment plants. Water Res. 91, 174–182.

Chellasamy, G., Kiriyanthan, R. M., Maharajan, T., Radha, A., Yun, K. (2022). Remediation of microplastics using bionanomaterials: A review. Environ. Res. 208, 112724.

Chen, J.L., Wu, J., Sherrell, P.C., Chen, J., Wang, H.P., Zhang, W.X., Yang, J.P. (2022). How to Build a Microplastics-Free Environment: Strategies for Microplastics Degradation and Plastics Recycling. Adv. Sci. 9, 2103764

Cho, Y., Shim, W.J., Jang, M., Han, G.M., Hong, S.H. (2019). Abundance and characteristics of microplastics in market bivalves from South Korea. Environ. Pollut. 245, 1107–1116.

Du, H., Xie, Y.Q., Wang, J. (2021). Microplastic degradation methods and corresponding degradation mechanism: Research status and future perspectives. J. Hazard. Mater. 418, 126377.

Ergin, A., Ergin, M.F. (2021a). The Role of Antifouling Coating in the Marine Industry. İstanbul: Gece Kitaplığı, 53-75.

Ergin, A., Ergin, M.F. (2021b). Nano Antifouling Coating Approaches in the Marine Industry. İstanbul: Gece Kitaplığı, 179-198.

Esmeray, E., Armutcu, C. (2020). Mikroplastikler, Çevre-İnsan Sağlığı Üzerine Etkileri ve Analiz Yöntemleri, Düzce Üniversitesi Bilim ve Teknoloji Dergisi, 8, 839-868. DOI: 10.29130/dubited.586453.

Frias, J. P. G. L. and Nash, R. (2019). Microplastics: Finding a consensus on the definition. Marine Pollution Bulletin, 138, 145-147.

Gaylarde, C.C., Neto, J.A.B., da Fonseca, E.M. (2021). Nanoplastics in aquatic systems—Are they more hazardous than microplastics? Environ. Pollut. 272, 115950.

Ge, J.H., Li, H., Liu, P., Zhang, Z.P., Ouyang, Z.Z., Guo, X.T. (2021). Review of the toxic effect of microplastics on terrestrial and aquatic plants. Sci. Total Environ. 791, 148333.

Gesamp. (2016). Sources, fate and effects of microplastics in the marine environment: part two of a global assessment. IMO/FAO/UNESCO-IOC/UNIDO/WMO/IAEA/UN/UNEP/UNDP Joint Group of Experts on the Scientific Aspects of Marine Environmental Protection, 220.

Goveas, L. C., Nayak, S., Kumar, P. S., Rangasamy, G., Vidya, S. M., Vinayagam, R. (2023). Microplastics occurrence, detection and removal with emphasis on insect larvae gut microbiota.Mar. Pollut. Bull. 188, 114580.

He, D., Luo, Y., Lu, S., Liu, M., Song, Y., Lei, L. (2018). Microplastics in soils: Analytical methods, pollution characteristics and ecological risks. Trends in Analytical Chemistry, 109, 163-172, 2018.

Herbort, A.F., Sturm, M.T., Schuhen, K. (2018). A new approach for the agglomeration and subsequent removal of polyethylene, polypropylene, and mixtures of both from freshwater systems—A case study. Environ. Sci. Pollut. Res. 25, 15226–15234.

Kirstein, I.V., Kirmizi, S., Wichels, A., Garin-Fernandez, A., Erler, R., Löder, M., Gerdts,G. (2016). Dangerous hitchhikers? Evidence for potentially pathogenic vibrio microplastic particles. Marine Environmental Research. 120, 1-8.

Koelmans, A.A., Nor, N.H.M., Hermsen, E., Kooi, M., Mintenig, S.M., De France, J. (2019). Microplastics in freshwaters and drinking water: critical review and assessment of data quality. Water Research. 155, 410-422.

Krueger, M.C., Harms, H., Schlosser, D. (2015). Prospects for microbiological solutions to environmental pollution with plastics. Appl. Microbiol. Biotechnol. 99, 8857–8874.

Li, L., Gu, Z., Xu, W., Tan, Y., Fan, X., Tan, D. (2023). Mixing mass transfer mechanism and dynamic control of gas-liquid-solid multiphase flow based on VOF-DEM coupling. Energy 272, 127015

Liu, L., Xu, M., Ye, Y., Zhang, B. (2022). On the degradation of (micro) plastics: Degradation methods, influencing factors, environmental impacts. Sci. Total

Environ. 806, 151312.

Lu, L., Luo, T., Zhao, Y., Cai, C., Fu, Z., Jin, Y. (2019). Interaction between microplastics and microorganism as well as gut microbiota: A consideration on environmental animal and human health", Science of the Total Environment. 667, 94-100.

Matavulj, M.,Molitoris, H. P. (2009). Marine fungi: degraders of poly-3-hydroxyalkanoate based plastic materials. Zb. Matice Srp. Za. Prir. Nauk. 253–65

Mateos-Cardenas, A., Scott, D.T., Seitmaganbetova, G., van Pelt, F., O'Halloran, J., Jansen, M.A.K. (2019). Polyethylene microplastics adhere to Lemna minor (L.), yet have no effects on plant growth or feeding by Gammarus duebeni (Lillj.). Sci. Total Environ. 689, 413–421.

Miloloža, M., Cvetnić, M., Kučić, G. D., Ocelić, B. V., Ukić, Š., Rogošić, M. (2022). Biotreatment strategies for the removal of microplastics from freshwater systems. A review. Environ. Chem. Lett. 20, 1377–1402.

Mishra, S., Rath, C.C., Das, A.P. (2019). Marine microfiber pollution: a review on present status and future challenges. Mar Pollut Bull 140, 188–197.

Oberbeckmann, S., Labrenz, M. (2020). Marine Microbial Assemblages on Microplastics: Diversity, Adaptation, and Role in Degradation. Annu. Rev. Mar. Sci. 12, 209–232.

Olicón-Hernández, D. R., González-López, J., Aranda, E. (2017). Overview on the biochemical potential of filamentous fungi to degrade pharmaceutical compounds. Front. Microbiol. 8, 1792.

Rodrigues, J.P., Duarte, A.C., Santos-Echeandia, J., Rocha-Santos, T. (2019). Significance of interactions between microplastics and POPs in the marine environment: A critical overview. Trac-Trends Anal. Chem. 111, 252–260.

Rujnic-Sokele, M., Pilipovic, A., (2017). Challenges and opportunities of biodegradable plastics: a mini review. Waste Manag. Res. 35, 132–140.

Qiao, R.X., Deng, Y.F., Zhang, S.H., Wolosker, M.B., Zhu, Q.D., Ren, H.Q., Zhang, Y. (2019). Accumulation of different shapes of microplastics initiates intestinal injury and gut microbiota dysbiosis in the gut of zebrafish. Chemosphere. 236, 124334.

Qu, H., Ma, R.X., Barrett, H., Wang, B., Han, J.J., Wang, F., Chen, P., Wang, W., Peng, G.L., Yu, G. (2020). How microplastics affect chiral illicit drug methamphetamine in aquatic food chain? From green alga (Chlorella pyrenoidosa) to freshwater snail (Cipangopaludian cathayensis). Environ. Int. 136, 105480.

Santana, M.F., Ascer, L.G., Custodio, M.R., Moreira, F.T., Turra, A. (2016). Microplastic contamination in natural mussel beds from a Brazilian urbanized coastal region: rapid evaluation through bioassessment. Mar. Pollut. Bull. 106, 183–189.

Sathicq, M.B., Sabatino, R., Corno, G., Di Cesare, A. (2021). Are microplastic particles a hotspot for the spread and the persistence of antibiotic resistance in aquatic systems? Environ. Pollut. 279, 116896.

Sharma, M.D., Elanjickal, A.I., Mankar, J.S., Krupadam, R.J. (2020). Assessment of cancer risk of microplastics enriched with polycyclic aromatic hydrocarbons. J. Hazard. Mater. 398, 122994.

Sharma, S., Basu, S., Shetti, N.P., Nadagouda, M.N., Aminabhavi, T.M. (2021). Microplastics in the environment: Occurrence, perils, and eradication. Chem. Eng. J. 408, 127317

Singh, L., Wahid, Z. A. (2015). Methods for enhancing bio-hydrogen production from biological process: A review. J. Ind. Eng. Chem. 21, 70–80.

Stabnikova, O., Stabnikov, V., Marinin, A., Klavins, M., Klavins, L., Vaseashta, A. (2021). Microbial Life on the Surface of Microplastics in Natural Waters. Appl. Sci. 11, 11692.

Tanaka, K., Watanuki, Y., Takada, H., Ishizuka, M., Yamashita, R., Kazama, M., Hiki, N., Kashiwada, F., Mizukawa, K., Mizukawa,H., et al. (2020). In Vivo Accumulation of Plastic-Derived Chemicals into Seabird Tissues. Curr. Biol. 30, 723–728.e3

Tang, Y.Q., Liu, Y.G., Chen, Y., Zhang, W., Zhao, J.M., He, S.Y., Yang, C.P., Zhang, T.,

Tang, C.F., Zhang, C., et al. (2021). A review: Research progress on microplastic pollutants in aquatic environments. Sci. Total Environ. 766, 142572

Toussaint, B., Raffael, B., Angers-Loustau, A., Gilliland, D., Kestens, V., Petrillo, M., Rio-Echevarria, I. M., Van den Eede, G. (2019). Review of micro-and nanoplastic contamination in the food chain. Food Additives & Contaminants: Part A, 36(5), 639-673.

Tsiropoulos, I., Faaij, A. P., Lundquist, L., Schenker, U., Briois, J. F., Patel, M. K. (2015). Life cycle impact assessment of bio-based plastics from sugarcane ethanol. Journal of Cleaner Production, 90, 114-127.

Van Raamsdonk, L.W., van der Zande, M., Koelmans, A. A., Hoogenboom, R. L., Peters, R. J., Groot, M. J., Peijnenburg., A. C. M., Weesepoel, Y. J. (2020). Current Insights into Monitoring, Bioaccumulation, and Potential Health Effects of Microplastics Present in the Food Chain. Foods, 9(1), 72.

Valeria, H.R,, Gutow, L., Thompson, R.C., Thiel, M. (2012). Microplastics in the marine environment: a review of the methods used for identification and quantification. Environmental Science&Technology. 46: 3060-3075.

Yang, X., Bento, C.P., Chen, H., Zhang, H., Xue, S., Lwanga, E.H., Zomer, P., Ritsema, C.J., Geissen, V. (2018). Influence of microplastic addition on glyphosate decay and soil microbial activities in Chinese loess soil. Environmental Pollution, 242, 338-347.

Yuan, J., Ma, J., Sun, Y., Zhou, T., Zhao, Y., Yu, F. (2020). Microbial degradation and other environmental aspects of microplastics/plastics. Sci. Total Environ. 715, 136968.

Yurtsever, M. (2015). Mikroplastikler'e Genel Bir Bakış", Dokuz Eylül Üniversitesi Mühendislik Fakültesi Fen Ve Mühendislik Dergisi, 17: 50, 68-83.

Yurtsever, M., Yurtsever, U. (2019). Use of a convolutional neural network for the classification of microbeads in urban wastewater, Chemosphere, 216, 271-280.

CHAPTER 2

QUASARS

E. Nihal ERCAN[1]

1 Prof. Dr. Boğaziçi University, Physics Department

INTRODUCTION

A quasar is a sub-class of active galactic nuclei (AGN) that are extremely luminous. The term quasar originates from "quasi-stellar object" or "QSO". This is because when first discovered in the 1950s, quasars were misunderstood as stellar objects because of their relatively small size. Scientists attributed their small angular size to them being stellar objects and linked their strong emissions to being proximity to Earth. Later these misconceptions were fixed as the observational capabilities advanced. This extremely luminous emission is generated by a supermassive black hole (SMBH) with a mass of 10^6-101^0 times solar mass. Around the SMBH, there is an accretion disc made up of gas. As the gravity of the black hole pulls the gas from the disc, falling matter releases huge amounts of energy because of friction and released gravitational potential energy. Since SMBH has a mind-blowing gravitational force falling matter reaches relativistic speeds. Then when this energy is released, the resulting emission is so powerful, that the quasar is more luminous than the whole galaxy it is located at. The radiant energy of quasars is enormous; the most powerful quasars have luminosities thousands of times greater than that of a galaxy such as the Milky Way[1]. High-definition images from the Hubble Space Telescope displayed quasars located in the centers of the galaxies that are hosting them. Some of these quasar-hosting galaxies seem to be strongly merging or interacting galaxies[2]. Detected features of a quasar are dependent on some factors such as the mass of its SMBH, accreting rate of gas, the relative orientation of the accretion disk to the observer, and whether it has a jet or not.

Number of quasars that have been found up to date is more than a million. The nearest observed quasar is 600 million light years away from us. However, in the most distant quasar category, competition is very tough. As years pass, new distant quasars have been found on and on. The discovery of the quasar ULAS J1342+0928 occurred in 2017 and it was determined to have a redshift of z=7.54. This particular quasar has a mass equivalent to 800 million suns and the light currently being observed from it was emitted when the universe was a mere 690 million years old. [3] [4]. The quasar Pōniuāʻena was detected in 2020, having emitted light only 700 million years after the Big Bang. This quasar is estimated to have a mass of 1.5 billion solar masses[5]. The quasar J0313–1806 was identified in 2021 and it was found to have a supermassive black hole with a mass of 1.6 billion solar masses. The redshift of this quasar, z=7.64, reveals that the light currently being observed from it was emitted around 670 million years after the Big Bang[6]. Searching of quasars has shown that quasar activity was more prevalent in the past, with a peak occurrence around 10 billion years ago[7] when the universe was still relatively young. When several quasars, gravitationally attracted to one another, are found nearby, they are referred to as a large quasar group (LQG) and are believed to be located within galaxy filaments, Largest structures in the universe.

OBSERVATIONAL ASPECTS

The first confirmed quasar discoveries were in the 1970's. At that time quasars were the brightest radiation sources observed by radio and optical range telescopes. Their emission was distributed a broad range of wavelengths, starting from the radio waves up to X-rays and even gamma-rays. Their appearance was point-like or as commonly stated quasi-stellar. The emission was so strong that it was 10^5-10^8 times more luminous than the standard galaxies. As opposed to galaxies that have been observed up to date, their emission is more focused in a small area known as the nuclear region of the galaxy. There are also less luminous active galaxies than quasars and they are named Seyfert galaxies, discovered by Carl Seyfert

Observing the quasar-hosting galaxies is quite hard because quasars are so bright that their "glare" makes it very hard to detect the host galaxy. Quasars are more luminous than their host galaxy. Thanks to the advanced imaging technologies of the Hubble Space Telescope, we have detected the host galaxies in some cases [8]. With regular or smaller telescopes, it is impossible to see the quasars. Their apparent magnitude is too low because of the huge distance between quasars and Earth. There is an exception for this case, quasar 3C 273. It is the most bright known quasar up to date with an apparent magnitude of 12.9. One can reach its photos using the link below:

https://www.google.com/search?sca_esv=fcb6e-7084a098e95&rlz=1C1CHBD_trTR966TR966&sxsrf=ACQVn0_pFvg-fRj1bgEeR2iTtho22jJG72A:1707712317000&q=3+c+273+photo+-nasan&tbm=isch&chips=q:3+c+273+photo+nasan,online_chips:273+quasar:I9PxLU_ngHg%3D&usg=AI4_-kRQv8DFTeSYiIjESweCnmWS-fT-3YA&sa=X&ved=2ahUKEwjj3aGQ_KSEAxUqh_0HHSwkAqwQgIoDKAB6BAgIEBA&biw=1536&bih=695&dpr=1.25

X-ray emissions from quasars were first discovered with Aerobee rocket flights in the 1960's. They seem to have a high X-ray luminosity. With immense luminosity but relatively small size, the source of the power must have been accretion, a process that is much more efficient than stellar nuclear fusion. Observed and calculated masses were about a million to billion times the solar mass. This indicated there is a supermassive black hole in the centers of quasars, accreting matter and producing intense levels of energy. Due to these processes, quasars are amongst the most energetic and luminous objects in the observable universe

Active galactic nuclei are all over the sky when looked at from an X-ray perspective. Up to almost %75 of the X-ray sources detected in X-ray surveys are active galactic nuclei. With this considered they make a huge contribution to cosmic X-ray background radiation. Strong AGNs also have a huge impact on processes like galaxy formation since they create strong winds of ionized

matter. Jets from the AGN can burst matter millions of light years away, into intergalactic space.

Pioneer AGN X-ray detections were published by Friedman et. al in 1967[9]. These detections were from 3C 273 and M87 galaxies. They suggested that these small extragalactic X-ray emissions may be responsible for the cosmic X-ray background radiation. Following these observations, astronomers detected a few Seyfert class galaxies with Uhuru X-ray satellite[10]. NASA High Energy Astronomy Observatory (HEAO-1) mission started in 1977. It was equipped with advanced scintillation detectors alongside previously used proportional counters, providing a chance of a complete X-ray survey of the X-ray universe[11]. HEAO-1 became useful with the spectral characterization of the diffuse X-ray background over the energy range 3-50 keV[12]. Einstein Observatory was a remarkable milestone in X-ray astronomy with its X-ray telescope with focusing optics necessary to produce images was launched in 1978[13]. It captured images of extended and diffused sources and hundreds of points like XRS's outside our galaxy with great resolution. Observations made with EXOSAT approved the occurrence of soft bumps in the X-ray spectrum[14].

ASCA and BeppoSAX were responsible for studies of continued AGN emission lines[15] [16]. ASCA was equipped with the first ever CCD X-ray camera in the focus of a telescope, and found evidence for a broad emission line from Fe in an AGN observation[17], offering that broadening of infra-red range caused by gravitation of the supermassive black hole. The unprecedented high resolution of Chandra gave us the resolution of CXB up to 8keV[18]. It is now understood that most of the CXB is the total emission from AGN's redshifted distribution. The Nuclear Spectroscopic Telescope Array (NuSTAR), launched in 2012, is the most recent addition to the collection of X-ray observatories[19]. In its first published result, the ability of NuSTAR to accurately determine the high-energy, 3-80 keV, X-ray spectrum of NGC 1365 was demonstrated. The data showed a clearer measurement of the broadening of the Fe fluorescence line, which is thought to be caused by the spin of the SMBH in NGC 1365[20]. X-ray observations by Chandra revealed a list of quasars which can be found in the link:

https://chandra.harvard.edu/photo/category/quasars.html

Also, the Hubble Space Telescope (HST) observed the brightest quasar in the early Universe which can be found in the link below.

https://science.nasa.gov/missions/hubble/nasas-hubble-helps-astronomers-uncover-the-brightest-quasar-in-the-early-universe/.

Infrared and optical observations of the hydrogen lines in quasars were published earlier and can be seen in **Astrophysical Journal, Vol. 243, p. 369-380 (1981).**

One can find the Swift UV, Optical, and X-ray observed quasar Catalog in the link below

https://heasarc.gsfc.nasa.gov/W3Browse/all/swsdssqso.html

THEORETICAL ASPECTS

In the 1970s, new advancements such as early X-ray space telescopes, understanding the black holes and newly developed cosmological models showed that redshifts of the quasars are rooted in the expansion of the universe, the quasar is very powerful and very distant and their source of energy is an accreting supermassive black hole[21]. Besides all of this finding and approving of controversial theories, optical and X-ray observations of the quasars explained the previously observed spectral anomalies. Quasars are located in the centres of active galaxies and are one of the most luminous, energetic, and powerful objects in the universe. They can emit up to 1000 times the total energy output of the Milky Way, which consists of hundreds of billions of stars. The electromagnetic emission of the quasars spans the whole electromagnetic spectrum, from X-rays to far infrared, with a peak in the ultraviolet and optical bands. Some quasars are also strong radio sources (radio-loud) and gamma-rays. Redshifts of the quasars are generally calculated from their visible and UV emission lines in their spectra. These wavelengths are more dominant than the continuous spectrum. They show the Doppler effect compatible with a few per cent of the speed of light.

In the 1960s Salpeter and Zeldovich proposed the idea of quasars being powered by supermassive black holes in the center of the galaxies that are accreting matter. At first, most astronomers did not accept this theory but as time went on this theory has been confirmed in many cases. Even the radiation or light can not escape the event horizon of the SMBH. All the emission, radiation and energy production occur outside of the event horizon of the black hole via releasing potential energy in the blackhole's potential well or friction of the accreting matter. The accretion discs of the quasars are very efficient in terms of energy conversion. Accretion discs of SMBH can convert %5-%31 of the accreting material's rest mass energy to free energy. For comparison, in the main sequence stars like the Sun powered by p-p chain reactions this energy conversion ratio is only %0.7.

Masses of the black holes in the quasars in the range between 10^5 - 10^9 solar mass.

Many nearby galaxies and the Milky Way have a supermassive black hole in their center. Due lack of matter to accrete, these galactic nuclei are not even nearly as active as quasars. This is why it is believed that quasars were more common in the past, earlier phases of our universe. Quasar's incredible emission requires immense matter flow from their surrounding space. As

time goes on, all the matter drains away accretion slows down and the galactic nuclei lose their activity. Only a small fraction of galaxies have enough matter around their nuclei to feed active nuclei such as quasars[22]. Quasars may also be reignited or ignited when two galaxies collide and their corresponding black holes feed with a new source of matter. Interestingly, scientists suggest that a new quasar could be formed when Andromeda and Milky Way collide in 3-5 billion years[23].

CONCLUSIONS

Quasars are extremely luminous due to the presence of a supermassive black hole (SMBH) with a mass of 10^6-10^10 times the mass of the sun. The SMBH is surrounded by an accretion disc made up of gas, which releases energy as it is pulled in by the black hole's gravity. Quasars are located in the centres of their host galaxies and are often found in merging or interacting galaxies. They can be detected in various parts of the electromagnetic spectrum and have characteristics that depend on factors such as the mass of the SMBH, the accretion rate of gas, the orientation of the accretion disk relative to the observer, and whether or not they have a jet. There are over a million known quasars, with the nearest one located 600 million light-years away. In recent years, particularly distant quasars have been discovered, including ULAS J1342+0928 and the quasar J0313-1806. Surveys have shown that quasar activity was more common in the past, with a peak epoch around 10 billion years ago. When several gravitationally attracted quasars are found nearby, they are known as a large quasar group (LQG). X-ray observatories, including NuSTAR, have been used to study quasars and other celestial objects.

Quasars are extremely luminous celestial objects that are located at the centres of galaxies and are powered by supermassive black holes. They were first detected in the 1970s and are known for their strong emission across a broad range of wavelengths, including radio, optical, X-ray, and gamma-ray. Quasars are much brighter than standard galaxies and are observed to have small, point-like appearances. It is difficult to observe the host galaxies of quasars because their bright emission makes them appear to "glare." X-ray emissions from quasars were first detected in the 1960s and it was discovered that they have high X-ray luminosity and relatively small size, leading scientists to conclude that the source of their power must be the accretion of matter onto a supermassive black hole. Active galactic nuclei, of which quasars are a type, make up a large portion of X-ray sources detected in surveys and contribute significantly to cosmic X-ray background radiation. They can also have a strong impact on processes such as galaxy formation through the creation of strong winds and jets of ionized matter.

Quasars are some of the brightest and most energetic objects in the universe. They are thought to have supermassive black holes at their centres,

which release huge amounts of energy through the process of accretion, or the falling of matter into the black hole. X-ray emissions from AGN were first detected in the 1960s and have been studied extensively since then using a variety of telescopes and satellites. These observations have helped astronomers understand the role AGN plays in the cosmic X-ray background radiation and the formation of galaxies. The most recent addition to the collection of X-ray observatories is the Nuclear Spectroscopic Telescope Array (NuSTAR), launched in 2012, which has provided detailed measurements of AGN emission spectra.

Quasars are bright objects that are powered by accreting supermassive black holes at the centres of active galaxies. They emit energy across the entire electromagnetic spectrum and have redshifts caused by the expansion of the universe. Their high luminosity and energy output are due to the efficient conversion of matter's rest mass energy into free energy in the accretion disks around the black holes. Quasars were more common in the past, but their activity has slowed as the matter around their nuclei is depleted. They may be reignited through galaxy collisions and mergers.

I want to thank Berkay Tümkaya, one of my undergraduate students, for helping me in preparation of the manuscript

REFERENCES

1-Wu, Xue-Bing; et al. (2015). "An ultraluminous quasar with a twelve-billion-solar-mass black hole at redshift 6.30". *Nature*. **518** (7540): 512–515.

2-*Bahcall, J. N.; et al. (1997). "Hubble Space Telescope Images of a Sample of 20 Nearby Luminous Quasars". The Astrophysical Journal.* **479** *(2): 642–658.*

3-*Bañados, Eduardo; et al. (6 March 2018). "An 800-million-solar-mass black hole in a significantly neutral Universe at a redshift of 7.5". Nature.* **553** *(7689): 473–476.*

4-Choi, Charles Q. (6 December 2017). "Oldest Monster Black Hole Ever Found Is 800 Million Times More Massive Than the Sun". *Space.com*. Retrieved 6 December 2017.

5-"Monster Black Hole Found in the Early Universe". *Gemini Observatory*. 2020-06-24. Retrieved 2020-08-31

6-*Maria Temming (January 18, 2021),* "The most ancient supermassive black hole is bafflingly big", *Science News*.

7- *Schmidt, Maarten; Schneider, Donald; Gunn, James (1995). "Spectroscopic CCD Surveys for Quasars at Large Redshift. IV. Evolution of the Luminosity Function from Quasars Detected by Their Lyman-Alpha Emission". The Astronomical Journal.*

8-Hubble Surveys the "Homes" of Quasars. Hubblesite News Archive, Release ID 1996–35.

9- Friedman H., Byram E. T., 1967, Science, 158, 257

10- Gursky H., Kellogg E. M., Leong C., Tananbaum H., Giacconi R., 1971, ApJ. Letters, 165, L43

11- Piccinotti G. et al., 1982, ApJ, 253, 485

12-Marshall F. E. et al., 1980, ApJ., 235, 4

13-Aschenbach B., 1985, Rep. Prog. Phys., 48, 579

14-Turner T. J., Pounds K. A., 1989, MNRAS, 240, 833

15-Tanaka Y., Inoue H., Holt, S. S., 1994, Pub. Astron. Soc. Japan, 46, L37

16-Boella G., Butler R. C., Perola G. C., Piro L., Scarsi L., Bleeker J.A.M., 1997, A&AS, 122, 299

17-Tanaka Y., Nandra K., Fabian A. C., et al., 1995, Nature, 375, 659

18-Mushotzky R. F., Cowie L. L., Barger A. J., Arnaud K. A., 2000, Nature, 404, 459

19-Harrison F., et al., 2013, ApJ, in press astro-ph arXiv;1301.7307v1

20-Risaliti G. et al., 2013, Nature, 494, 449

21- Keel, William C. (October 2009). "Alternate Approaches and the Redshift Controversy". The 22-University of Alabama. Retrieved 2010-09-27.

22-Tiziana Di Matteo; et al. (10 February 2005). "Energy input from quasars regulates the growth and activity of black holes and their host galaxies". *Nature*. **433** (7026): 604–607.

23- "Quasars in interacting galaxies". *ESA/Hubble*. Retrieved 19 June 2015.

CHAPTER 3

THE MICROBIAL LEVAN AND POTENTIAL FOR ANTIMICROBIAL APPLICATIONS IN TEXTILES*

Furkan ÖZTÜRK[1]
Nurcihan HACIOĞLU DOĞRU[2]

* This investigation is a part of Master thesis (Bazı Biyoteknolojik Uygulamalar için Bakteriyal Levan Üretimi ve Optimizasyonu; Danışman: Prof. Dr. Nurcihan Hacıoğlu Doğru) of Furkan ÖZTÜRK. This study was financially supported by the Çanakkale Onsekiz Mart University Scientific Research Projects Coordination Unit, Turkey (FYL-2022-4205)
1 Senior Biologist; Çanakkale Onsekiz Mart University School of Graduate Studies Department of Biology. bio.furkan.oztrk@gmail.com,
ORCID No: 0000-0002-9752-0584
2 Prof. Dr.; Çanakkale Onsekiz Mart Faculty of Science Department of Biology. nhacioglu@comu.edu.tr ORCID No:0000-0002-5812-9398.

1. INTRODUCTION

Polymers touch nearly every aspect of modern life, ensuring a high quality of life across various domains. From everyday consumer goods to highly advanced materials used in industries such as electronics, machinery, communication, transportation, pharmacy, and medicine, polymers are indispensable. The usage and industrial production of petroleum-derived polymers, which form the foundation of significant industrial products, continue to expand with each passing day. However, the broad spectrum of applications and increasing industrial production of these polymers pose environmental concerns due to their durable nature, which allows them to persist in the environment for many years without degradation. In recent years, the global polymer market has seen a rise due to increased demand from various end-use industries. However, the accumulation of waste in storage areas due to polymer usage, coupled with the energy requirements for recycling waste materials worldwide, raises concerns about both economic and environmental impacts of waste disposal.

In recent years, the high price of petroleum and society's increasing demand for greener and cleaner products have led to a growing interest in biologically renewable, biodegradable polymers, and the use of sustainable technologies to produce them. From this perspective, the production of EPS (Expanded Polystyrene) and research on biopolymers have gained importance as strategies for economically feasible materials (Sarilmiser et al., 2015).

Microbial production offers various advantages over plant or macroalgae-derived products in terms of overcoming environmental impacts and obtaining high-quality final products with defined and reproducible production parameters. Additionally, they exhibit higher efficiency compared to polysaccharides derived from plant preparations. Therefore, emphasis should be placed on microbial polysaccharides or biopolymer production, which serve important biological activities and have superior structural properties, serving as potential industrial products.

Microorganisms secrete high molecular weight compounds in the extracellular environment, known as exopolysaccharides (EPS). EPS are defined as high molecular weight (10-30 kDa), highly sugar-based polymers secreted by microorganisms into the environmental surroundings. These natural, non-toxic, and biologically degradable polymers not only protect microorganisms from environmental extremes such as Antarctic ecosystems, saline lakes, geothermal sources, or deep-sea hydrothermal vents but also play important roles in various biological mechanisms such as immune response, adhesion, infection, signal transduction, biofilm formation, biological pollution, nutrient storage, and microbial motility (Cruz et al., 2020).

Biopolymers constitute the structural components highly present in the chemical composition of EPS. There are various materials that can be defined using the term "biopolymer," but it generally refers to materials derived from or produced by biological sources such as microorganisms, plants, algae, etc. It can also refer to materials synthesized by synthetic chemistry from biological sources such as vegetable oils, sugars, resins, proteins, amino acids, etc. Furthermore, composite products produced by mixing two or more biopolymers are also categorized as biopolymers.

Compared to traditional products, biopolymers are known to possess various biological activities such as antimicrobial, anticancer, antibiofilm, anti-inflammatory, antioxidant, and immunomodulatory properties. Additionally, due to their cold water solubility, pH stability, storage stability, compatibility with ionic salts, sensitivity to metals, surface particles, and other polymers' chemical reactions, water vapor and oxygen permeability, and high thermostability, they find applications as emulsifiers, stabilizers, binders, gelling agents, coagulants, lubricants, film formers, thickeners, and suspending agents, holding potential for various biotechnological applications. This necessitates the identification of the chemical structure superiority and biological activities of biopolymers to increase their usage in various industrial, pharmaceutical, and medical applications (Domzał-Kedzia et al., 2023).

Levan is a biopolymer composed of repeating fructose units. The main chain structure of levan makes it a unique biopolymer. Levan biopolymer possesses the characteristic of being one of the few natural polymers where carbohydrates are found in the furanose form (Srikanth et al., 2015).

Numerous studies have demonstrated the biological activities of levan, such as antifungal, antitumor, anti-inflammatory, antioxidant, and antibiofilm properties. However, due to its high cost and limited availability of raw materials, levan has not found extensive use. Despite the high cost, the increasing demand for environmentally friendly products in sectors such as biomedical, pharmaceuticals, food, and feed (e.g., aquaculture) is creating a new commercial market encompassing bio-products, including levan (Domzał-Kedzia et al., 2023).

Antimicrobial agents, the main agents in infection control, also have various applications in production facilities, including food, pharmaceutical, and cosmetic industries, as protective agents in various products, waste control, biofilm control in sewage systems, and maintaining standard hygiene conditions. The wide range of applications has led to widespread use, contributing to the development of chemical antimicrobial resistance in bacteria. Additionally, chemicals used in the production of antimicrobial products, which are now mandatory for use, cause serious environmental

harm and bioaccumulation. To limit chemical production and usage, green production strategies should be adopted.

Chemical antimicrobial agents are also extensively used in the textile sector. The use of antimicrobial textiles can help control the growth or kill pathogens and limit the spread of infections through textiles. The high risk of infection transmission in communal living spaces such as accommodation centers, schools, and nurseries necessitates the use of antimicrobial agents, especially in textile products in such areas. Antibacterial fabrics prevent the growth and spread of such bacteria, ensuring safety against infections in hospitals where sterilization is essential for both doctors and patients. Synthetic, organic, and polymer-based antimicrobial agents are used in the final production of antimicrobial textiles. Commonly used antimicrobial agents in the textile sector include quaternary ammonium compounds (QACs), compounds containing halogens (fluorine or chlorine, molecules containing N-halamines or triclosan), guanidine-containing polymers (polyhexamethylene biguanide), phospho- and sulfo- derivatives containing polymers, and phenol polymers. Despite the advantages of chemical materials in textile production processes, such as durability and not altering the tactile and mechanical properties of the fabric, they also have disadvantages such as being toxic to humans and the environment due to their rapid biodegradation, causing skin irritation and sensitivity (Zhang, 2016). Levan polymer finds application in textile products due to its properties such as thermal stability, elasticity, high biological activity, and low toxicity. However, while there are numerous studies on the potential use of gelatin, chitosan, and alginate in textile products, literature knowledge regarding the use of levan is quite limited. In this study, we examined the literature data regarding the antimicrobial activity of levan and evaluated its potential use in textiles.

2. BIOPOLYMERS AND LEVAN

2.1. Microbial Exopolysaccharides (EPS)

Many microorganisms produce polysaccharides surrounding the cell composed of repeating sugar units. In microorganisms, these are generally found as intracellular storage polysaccharides (such as glycogen), lipopolysaccharides (LPS) mainly determining immunogenic properties in the outer membrane, and capsular polysaccharides (CPS) secreted as a separate surface layer forming capsule according to their biological functions. Loose extracellular polysaccharides, such as levan, xanthan, sphingan, alginate, cellulose, etc., are observed as EPS, loosely bound to the cell surface (Schmid et al., 2015).

EPSs are reported to have various industrial, pharmaceutical, and medical applications. Especially in recent years, pathogenic microorganisms have developed resistance in response to the indiscriminate use of commercial

antimicrobial drugs widely used in the treatment of infectious diseases. This has led to increased frequency of undesirable side effects of some antibiotics and previously rare infections, necessitating scientists to undertake research into new antimicrobial agents. In this context, it has been demonstrated in many studies that polysaccharides obtained from various organisms exhibit significant biological activities against important pathogens, such as antimicrobial, antifungal, antitumor, anti-inflammatory, antioxidant, antibiofilm, etc., and they have been reported to have significant potential as natural bioactive drugs (Elsakhawy et al., 2017).

The extracellular polymer matrix is crucial for maintaining hydration and structural integrity of the biofilm. In the case of the EPS isolated from Lactobacillus plantarum WLPL04, significant activity against biofilm formation of bacteria such as Pseudomonas aeruginosa CMCC 10104 could not be achieved. However, researchers have concluded that L. plantarum strains isolated from different sources may have specific EPS with varying activity against pathogens (Liu et al., 2017).

2.2. Biopolymer

Biopolymers are polymers produced from natural sources. They can be synthesized chemically from biological materials or biosynthesized by living organisms. All biopolymers are synthesized enzymatically in the cytoplasm, various compartments or organelles of cells, cytoplasmic membranes, or cell wall components, on the surface of cells, or even extracellularly. The synthesis of a biopolymer can be initiated as a single entity or continued in another part of a cell. There are various materials that can be defined using the term "biopolymer." Microbial and plant sources as well as biological materials such as oils, sugars, and proteins can be used for this purpose. Additionally, composite products produced by mixing two or more biopolymers are also categorized as biopolymers.

Biopolymers have a self-repeating configuration and are sensitive to chemical reactions with metals, surface particles, and other polymers (Etemadi et al., 2003). Moreover, they acquire complex structural diversity by folding spontaneously, gaining various biological functions. Many biopolymers, especially proteins, are monodisperse, meaning they are single-distributed. In other words, they are uniform polymers in which all molecules have the same degree of polymerization or relative molecular weight and have a polydispersity index (PDI, a measure of the width of a polymer's molecular weight distribution) equal to 1. Natural biopolymers with important physical properties such as cold water solubility, pH stability, storage stability, and compatibility with ionic salts are available. Additionally, biopolymers that undergo degradation are used as natural fertilizers in the agricultural sector, thus reducing chemical agricultural practices.

Throughout history, biopolymers have been used in various fields; however, their usage has been less compared to petroleum-derived materials due to the low cost of petrochemical raw materials and the rapid diversification of materials produced from these raw materials to meet societal needs. In recent years, concerns about adopting greener and cleaner products, driven by high petroleum prices, have led to increased interest in biologically renewable polymers and the use of sustainable technologies to produce them. From this perspective, the importance of research on biopolymers for their economic feasibility has increased (Hernández et al., 2014). Research indicates that the number of biopolymer enterprises, which was 500 in 2018, is expected to rise to 5000 by 2020, encompassing 25-30% of the plastic production industry, reflecting the growing significance of biopolymers. Biopolymers are divided into natural (polysaccharides, alginates, chitosan, etc., produced from natural materials under controlled conditions) and synthetic (having repeated physical and mechanical properties) categories (Hamamcı and Aktaş, 2018). According to their synthesis sources, natural polymers are categorized into biomass and agricultural as well as microorganism-derived, while synthetic biopolymers are divided into biotechnology-derived and petroleum-derived sources. Additionally, new studies have accelerated, combining natural biopolymer and synthetic biopolymer applications, with the use of microorganisms in production. Particularly, targeted template biopolymer production methods have been developed using molecular techniques with microorganisms. The aim is to achieve more controlled polymerization compared to chemical production strategies (Schultz, 2017). Furthermore, recent developments in synthetic biopolymer synthesis involve the use of combinatorial strategies that mimic natural polymers such as polypeptides, oligosaccharides, and nucleic acids, which play key roles in cellular and molecular recognition, signal transduction, immune response, and are central to the life processes of all organisms. These synthetic biopolymers are synthesized using techniques employing combinatorial strategies, allowing the structure of these biopolymers to be defined and compound libraries to be generated. These libraries, containing millions of compounds, are then screened, and the biological functions of these molecules are tested to develop potential methods for drug discovery and design (Cho et al., 1993).

The development of these methods, which are of interest in drug discovery, relies on environmentally friendly production methods for biopolymer synthesis, determination of the production efficiency conditions of the synthesized biopolymer, characterization of the target biopolymer, and determination of the low-cost industrial usage potential. Thus, by increasing the known abundance of the target biopolymer in nature, limitations posed by natural biopolymer scarcity will be addressed, reducing the necessity for chemical polymerization techniques and enabling the application of

new techniques for drug design. As time and technology progress, it is anticipated that with suitable synthesis strategies, biopolymers will replace their petroleum-based counterparts, leading to additional opportunities with acceptable levels of biopolymer synthesis efficiency and product purity (Hernández et al., 2014). Furthermore, biopolymer composite materials, despite their low mechanical properties as dental implants, are being tested in vivo and in vitro due to their processing flexibility, optimal porosity, lighter weight compared to metals, biocompatibility, and biodegradability. Positive strategies are being developed for them to become ideal implant materials.

Research is underway to explore exceptional and innovative ways of using biopolymers in various biotechnological product derivations for sustainable biotechnology and bioeconomy. There is a particular focus on the high-volume production of microbial biopolymers. Microbial biopolymer production is emphasized due to the ability of microorganisms to enable low-cost and rapid production compared to other organisms. Microbial biopolymers exhibit high biological activity and various physicochemical properties compared to those produced from plants and algae, leading to the adoption of microbial bioproduction strategies (Jing et al., 2011).

2.3. Biopolymer Levan

The history of levan dates back to its discovery by Lipmann in 1870-1881, followed by reports of levan polymers produced by microorganisms isolated from eucalyptus sap by Greig-Smith and Steel in 1902. Subsequently, research in this field, particularly in Germany, England, and France, focused on the biosynthesis, production, and harvesting of levan from 1870 to 1940. Starting from the 1930s, microbial levan production and polymer applications opened up new horizons, leading to the development of a commercial market for polysaccharides, especially in the United States (Srikanth et al., 2015).

Levan biosynthesis occurs through the activity of levansucrase (EC 2.4.1.10, sucrose: 2,6-β-D-fructan 6-β-D-fructosyltransferase). Levansucrase catalyzes the transfer of fructosyl groups to a polyfructose (fructan) chain from sucrose, leading to the formation of microbial exopolysaccharide known as levan. This enzyme belongs to the glycosyltransferase family, particularly fructosyltransferases. Glycosyltransferases (EC 2.4) catalyze the transfer of activated glycosyl groups from donor carbohydrates to acceptor molecules. They play a significant role in the biosynthesis or modification of polysaccharides and in the production of oligosaccharide derivatives of many organic compounds (Koşarsoy Ağçeli ve Yucel, 2023).

Levansucrases are reported to be found in both gram-negative and gram-positive bacteria, with widespread distribution especially among Gram-positive bacteria (Khandekar et al., 2014).

In plants, levan exists in a mixed FOS (fructooligosaccharide) structure with both β-(2→6) and β-(2→1) fructofuranosidic bonds between fructosyl units. Bacterial levan, on the other hand, typically exhibits β-(2→6) linkage, with higher molecular weight compared to plant levans. Consequently, structural differences in levan, such as molecular weight, degree of polymerization, and branching of repeating units, are source-dependent. Levans obtained from plants are much smaller than those produced by microorganisms, typically ranging in molecular weight from 2000 to 33000 Daltons (Da) (Srikanth et al., 2015a). On the other hand, microbial levans have molecular weights ranging from 2 to 100 million Da, with bacterial levans having much higher molecular weights due to multiple branching (Srikanth et al., 2015a).

Levan Biosynthesis

Due to its wide range of functional properties, levan is considered a homopolysaccharide with a broad potential for industrial applications. In recent years, there has been an increasing interest in the commercial production of levan (Sarilmiser et al., 2015).

In the medical and pharmaceutical sectors, levan finds applications in many areas, particularly due to its biodegradability, biocompatibility, and film-forming ability (Silbir et al., 2014). Levan polymers have potential industrial applications as thickeners, encapsulating agents, for medical uses, and as substitutes for some petrochemicals. Additionally, levan has the potential to be used as edible coating materials for foods and pharmaceuticals due to its low oxygen permeability properties (Kaplan et al., 1993).

In cosmetic products, levan has been reported to act as a formulation aid, exhibiting excellent cell proliferation and moisturizing effects on the skin. Furthermore, levan derivatives can also be used in hair care products (Divya and Sugumaran, 2015).

In general, the carbon source plays a significant role in the production of levansucrase via microbial fermentation. For example, increased sucrose concentration usually leads to increased levan formation, and sucrose concentration often plays a crucial role in controlling the targeted molecular weight of the produced levan molecule (Zhang et al., 2014). Among the factors tested to control the molecular weight of levan produced as a result of levansucrase activity from *B. subtilis* NRC 33a, sucrose concentration was shown to be the most important factor. Various studies conducted with *Bacillus circulans*, *Bacillus amyloliquefaciens*, *Bacillus* sp., and *Geobacillus stearothermophilus* (Inthanavong et al., 2013) bacteria have reported that sucrose is required as an inducer to enhance levansucrase production, and levansucrase production ceases at very low sucrose concentrations or in the absence of sucrose. Levansucrase is the key enzyme for producing microbial levan from sucrose, and sucrose supplementation generally induces

levansucrase expression during fermentation (Srikanth et al., 2015a). It has been shown that sucrose supplementation alone has no significant effect on levansucrase production in B. subtilis NRC 33a (Abdel-Fattah et al., 2005).

The production of levansucrase is also influenced by the nitrogen source. While bacteria such as *B. amyloliquefaciens* (Tian et al., 2011), *B. subtilis* NRC 33a (Abdel-Fattah et al., 2005), and *Bacillus* sp. (Belghith et al., 2012) require yeast extract for levansucrase production, it has been reported that *Geobacillus stearothermophilus* requires an environment containing peptone or tryptone instead of yeast extract for high-level levansucrase production.

It is known that other factors such as culture temperature and metal ions also have significant effects on levansucrase production, and species-specific production efficiency may vary depending on the applied metal ion and incubation temperature. While the optimum temperature and supplemented metal for levansucrase production from *B. subtilis* NRC 33a were determined to be 30°C and Mg2+, respectively (Abdel-Fattah et al., 2005), the optimum temperature and metal requirement for Bacillus sp. bacteria were reported to be 50°C and Fe2+ (Belghith et al., 2012).

The properties of levan obtained from the cultivation of *Azotobacter vinelandii* D-08 in environments provided with molasses and distillation waste were investigated for its potential use as a hydrogel component capable of adsorbing highly toxic heavy metals and radionuclides. It was reported that a culture medium containing 5% molasses and 2-15% distillation waste was the most suitable condition for the efficient synthesis of levansucrase and levan. Particularly, levan synthesized depending on levansucrase activity from bacteria cultured using molasses and 10% distillation waste was characterized by High-Performance Liquid Chromatography (HPLC) and Infrared Spectroscopy (IR). Two different levan structures with high and low molecular weights were identified (Shutova et al., 2021).

As a result of these studies, it is suggested that levan can be used for the production and enrichment of uranium ores known to contain heavy metals and radionuclides, as well as for the treatment of industrial, multi-component wastewater from atomic power plants and facilities. It is observed that levan has the potential to be used for the removal of heavy metal ions from wastewater and for the remediation of soils contaminated with toxic metals, which is a significant environmental issue resulting from industrial activities (Shutova et al., 2021).

Levansucrase generally exhibits different temperature optima for polymerization and sucrose hydrolysis reactions, where low temperatures typically support the polymerization reaction, while high temperature conditions support sucrose hydrolysis. The optimum temperature for levan synthesis in *Pseudomonas syringae* pv. is approximately 18 °C, while it is 60 °C

for sucrose hydrolysis (Hettwer et al., 1995).

The molecular weight of the produced levan is usually controlled by the reaction temperature. It has been found that *Bacillus licheniformis* RN-01 produces high molecular weight levan (612 kDa) as the main product at 50 °C, while it produces low molecular weight levan (11 kDa) at 30 °C (Nakapong et al., 2013).

Levan isolated from *B. licheniformis* has been shown to significantly stimulate the proliferation of spleen lymphocytes. It has been determined that EPS is directly mitogenic for mouse splenocytes (Liu et al., 2010).

The optimization of levan obtained from *Acetobacter xylinum* has been studied, and it was found that the highest levan production conditions were 10 g/L nitrogen, pH 6.8, levan concentration between 0.1-0.4 g/L, and sucrose concentration between 50-60 g/L. The antioxidant activity of the extracted levan was observed to be 81.26% at a concentration of 1 mg/mL (w/v) and 100% at a concentration of 1.25 mg/mL. These results suggest that the isolated levan can be used as a potent antioxidant for pharmaceutical and biomedical applications. Furthermore, an inhibitory effect of 71.18% was observed at a concentration of 0.25 mg/mL in the in vitro anti-inflammatory assay performed using protein (BSA) extracted from *A. xylinum* NCIM 2526, indicating a high anti-inflammatory activity compared to standard drugs (Srikahnt et al., 2015).

Levans are not produced on a commercial scale, and there is limited data available on their physiological or health effects. However, research conducted on rats has shown that a diet supplemented with levan increased superoxide dismutase (SOD) and catalase (CAT) enzyme levels by 40% and 28%, respectively, and positively altered plasma antioxidant enzyme activities. Additionally, rat groups fed with levan exhibited significantly reduced total cholesterol, triglyceride, and LDL-cholesterol levels. Due to these potential antioxidant effects, levan may hold promise for the treatment of metabolic diseases related to oxidative stress (Dahech et al., 2013). However, human clinical trials evaluating the physiological effects of levan type fructans are very limited to date.

Marx et al. (2000) investigated levan as a novel carbohydrate source for the growth of *Bifidobacteria* and reported that certain Bifidobacterium sp. strains showed good growth on levan oligosaccharides. In contrast, Niv et al. (2012) examined the effects of consuming 500 mL of natural orange juice enriched with 11.25 g of levan daily for 8 weeks compared to natural orange juice without levan on the weight, gastrointestinal symptoms, and metabolic profiles of 48 individuals. They found no significant difference in the studied parameters between the two types of fruit juices. It was stated that levan consumption had no effect on intestinal habits, serum lipid levels, gastrointestinal symptoms,

or blood pressure. Dal Bello et al. (2001) demonstrated that levan-type exopolysaccharides obtained from *Lactobacillus sanfranciscensis* exhibited bifidogenic properties in in vitro experiments.

3. POTENTIAL BIOTECHNOLOGICAL APPLICATIONS OF LEVAN

Antimicrobial Activity of Levan

Three different levan compounds, namely high molecular weight, low molecular weight, and difructose dianhydride, have been tested for their antibacterial activity against pathogens commonly responsible for food spoilage and foodborne diseases worldwide. Low molecular weight levan effectively inhibited the growth of *Bacillus cereus, Staphylococcus aureus*, *Escherichia coli* O157:H7, and *P. aeruginosa* at a concentration of 1%. At concentrations above 3%, low molecular weight levan strongly inhibited the growth of *B. subtilis*, *B. cereus*, *S. aureus*, *Listeria monocytogenes*, *E. coli* O157:H7, *S. typhimurium*, *P. aeruginosa*, and *Enterobacter aerogenes*. On the other hand, the 5% concentration of high molecular weight levan did not exhibit effective antimicrobial activity against *B. subtilis*, *S. typhimurium*, and *E. aerogenes*, but showed high antimicrobial activity against *B. cereus*, *S. aureus*, *L. monocytogenes*, *E. coli* O157:H7, and *P. aeruginosa*. Difructose dianhydride at concentrations above 3% strongly inhibited the growth of most tested pathogenic bacteria except *E. aerogenes* (Byun et al., 2014).

The antimicrobial efficacy of levan-coated silver nanoparticles (AgLeNP) has been investigated as a drug delivery system and bactericidal agent. The bacteriostatic activity against Gram-positive bacterium *B. subtilis* ATCC 6051 and Gram-negative bacterium *E. coli* K12 strain was tested and antagonistic activity was observed against both groups. When examining the concentration of activity, it was found that AgLeNPs were less effective against Gram-positive due to the peptidoglycan wall (González-Garcinuño et al., 2019).

The antimicrobial activity of commercial levan produced by *Zymomonas mobilis* NRRL B-1402 and levan produced by *B. subtilis* against bacterial strains and fungal species isolated from food products has been tested. Since none of the tested microorganisms showed inhibition effects even at the highest levan concentration of 40 mg/mL, no minimum inhibitory concentration (MIC) value could be determined for both levan products (Gökmen et al., 2020).

The antibacterial activity of levan was evaluated against *S. aureus* ATCC 33592 and *E. coli* ATCC 25922. They respectively formed inhibition zones of 1 cm and 0.8 cm. Additionally, both strains exhibited an MIC value of >256 μg/mL (Bouallegue et al., 2020).

In another study, levan produced by *Pseudomonas mandelii* was evaluated for its antibacterial activity against test cultures of *S. aureus*, *E.*

coli, *C. albicans*, and *A. niger*. It was observed that levan at a concentration of 100 µg/mL formed an inhibition zone against E. coli and S. aureus but did not show antifungal effects against *C. albicans* and *A. niger*. However, levan at a concentration of 200 µg/mL exhibited both antibacterial and antifungal activity (Koşarsoy and Cihangir, 2020).

The composition of the culture medium containing carbon, nitrogen, and micro- and macro-elements is crucial for bacterial polysaccharide synthesis. The addition of pre-formed levan to the levan production medium can accelerate levan formation and increase the final yield of levan; however, the presence of pre-formed levan is not necessary for bacterial levan production. Additionally, the initial levan concentration affects the production of homogeneous, high-molecular-weight levan (Han, 1990).

The antibiofilm activity of levan produced by *P. mandelii* has been tested, and all concentrations of levan, namely 100, 200, 500, and 1000 µg/mL, exhibited antibiofilm activity against test microorganisms including *S. aureus*, *E. coli*, *C. albicans*, and *K. pneumoniae* (Koşarsoy and Cihangir, 2020).

Levan-based antimicrobial film composites have become an important research topic in recent years. It has been found that a film composite formed with levan produced by *Paenibacillus polymyxa*, bentonite, and essential oils exhibits antimicrobial activity (Koşarsoy Ağçeli et al., 2022). In another study, nanocomposites of levan and chia seed mucilages were investigated for their antimicrobial film properties, and although they exhibited antibacterial properties, they did not show antifungal activity (Koşarsoy Ağçeli, 2022a). Additionally, film samples prepared using ostrich eggshell powder and levan showed antibacterial and antibiofilm activities (Koşarsoy Ağçeli, 2022b).

The antibiofilm and antimicrobial activities of levan produced by *Halomonas elongata* 153B at concentrations of 250, 500, 750, and 1000 µg/mL have been tested, and all applied concentrations showed antibiofilm and antimicrobial activities against test cultures including *E. coli* ATCC 25922, *S. aureus* ATCC 6538, *P. aeruginosa* ATCC 11778, and *C. albicans* ATCC 10231 (Altıntaş et al., 2023).

P. polymyxa HCT33-3 (at concentrations of 0.50, 0.25, and 0.10 g/mL) and commercial levan produced by *Erwinia herbicola* (at a concentration of 0.50 g/mL) have been tested for their antimicrobial activities against various microbial cultures including *E. coli* ATCC 35218, *S. aureus* ATCC 2921, *K. pneumoniae* ATCC 1705, *P. aeruginosa* ATCC 27853, *C. albicans* ATCC 90029, and *A. niger*. It was observed that levan derived from *P. polymyxa* exhibited antibacterial activity against all bacteria, while pure levan obtained from *E. herbicola* showed antimicrobial activity only against *A. niger* (Koşarsoy Ağçeli and Günan, 2023).

Antimicrobial Textile Applications

In recent years, the application of antimicrobial finishing processes to textiles has become extremely important in the production of protective, decorative, and technical textile products, leading to increased consumer demand in this direction. The use of such textiles has provided opportunities to expand into various applications in industries such as medicine, engineering, agriculture, and food. Antimicrobial textile products offer advantages in preventing biological degradation due to their sensitivity to microorganisms such as bacteria and fungi that accumulate on textiles depending on moisture, nutrients, and temperature. Biological degradation occurring in textile materials leads to unpleasant odors, fading of fiber colors, and deterioration of the material. The extent of biological degradation in textile materials depends on the type of microorganism, the chemical composition of the textile material, molecular structure, and degree of polymerization. Generally, cellulose fibers are most susceptible to attack by microorganisms. It is known that bacteria of the genera *Cytophaga*, *Bacillus*, *Cellulomonas*, *Clostridium*, *Cellvibrio*, and *Sporocytophaga* often degrade cellulose-containing fabrics. The degradation of wool products, whose main polymer substance is keratin, is mainly attributed to bacteria belonging to the genera *Bacillus*, *Pseudomonas*, and Actinomycetes. In this context, hydrophilic natural and regenerated textile fibers are more vulnerable to microbial growth, while synthetic fibers have a lower risk of microbial colonization (Harmsen et al., 2021).

A significant portion of the sectoral objectives in the textile industry regarding antimicrobial finishing processes target medical applications. Medical textiles are used in medical sciences and applications such as wound dressings, bandages, wound care products, hygiene products, surgical garments, and the production of implant materials. Antimicrobial textiles have the potential to reduce the transmission of infections in hospital and care environments. Additionally, antimicrobial properties can enhance the performance and lifespan of products, while also reducing the formation of unpleasant odors in these fabrics.

With the widespread use of antimicrobial textiles in the medical field, confusion has arisen in the purpose of use and classification of textile products, leading to regulatory interventions. The US Food and Drug Administration (FDA) and the US Environmental Protection Agency (EPA) have engaged in discussions to regulate antimicrobial textile products, defining the sole purpose of antimicrobial textile products as exclusively protecting articles or substances. The ability of antimicrobial textile products to serve a therapeutic purpose has been limited by the requirement for antimicrobial textile products to be registered with the FDA as medical devices.

Antimicrobial applications in textile products protect users from pathogenic or odor-causing microorganisms and unwanted aesthetic changes or damage caused by decay, which can lead to medical and hygiene issues.

In the current textile sector, the amount of suitable antimicrobial agents applied to textile products has significantly increased. These antimicrobial agents vary in chemical structure, efficacy, application methods, as well as their effects on humans and the environment, and also in terms of cost (Gao and Cranston, 2008).

The demand for antimicrobial textiles has not only increased for medical textiles but also for sports apparel, food packaging, home furnishings, automotive textiles, air filters, water purification systems, and others.

Various chemical substances are used as antimicrobial agents in textile applications. Generally, antibacterial agents are classified into two groups: bactericidal or bacteriostatic. Almost all commercial antimicrobial agents used in textiles are bactericides. The mechanism of action of general bactericides aims to damage the cell wall, hinder cell membrane permeability, and inhibit enzyme activity or lipid synthesis—all essential functions for the survival of microorganisms. Common chemicals encountered as antimicrobial agents include metal salts (e.g., silver), quaternary ammonium compounds (QACs), halogenated phenols (e.g., triclosan), polybiguanides (e.g., Polyhexamethylene biguanide (PHMB)), chitosan, and N-based chemicals. In the current industry, many antibacterial products and chemicals are available and under development using different technologies (Akarslan and Altınay, 2017).

Despite their traditionally high antimicrobial efficacy, synthetic materials are harmful to human health. As a result, natural or safe adjuncts are seen as alternatives to synthetic ones for the functionalization of textile materials. Chitosan is a polysaccharide with anticancer, nontoxic, biodegradable, and biocompatible properties. Initially used as a dye fixative in textiles, chitosan improves surface properties by forming a homogeneous coating film on the fiber surface, reducing the repellency between the fabric and dyes, and significantly increasing the dye absorption rate. Moreover, chitosan has the potential to be widely used as an antimicrobial agent in the textile industry, particularly due to its strong availability and low cost advantages, especially its antibacterial properties. Compared to chitosan, chitosan oligosaccharide (COS) has relatively lower molecular weight and stronger water solubility advantages, along with antibacterial and antiviral activity (Lan et al., 2023).

In the antimicrobial textile sector, there is a focus on chitosan biopolymer and nanoparticle (NP) applications as antimicrobial agents, and the combination of metal and metal oxide nanoparticles with biopolymers is an important research topic. However, there is no research available on the use of levan biopolymer as an antimicrobial agent in the textile sector.

Studies in the literature that demonstrate the high antimicrobial and particularly antibiofilm efficacy of levan suggest its potential to serve as an alternative to polymers such as chitosan. Furthermore, these studies indicate that levan has the potential to increase the use of eco-friendly biopolymers in textiles.

REFERENCES

Abdel-Fattah, A. F., Mahmoud, D. A. ve Esawy, M. A. (2005). "Production of levansucrase from Bacillus subtilis NRC 33a and enzymic synthesis of levan and fructo-oligosaccharides". Current Microbiology, 51, 402-407.

Akarslan, F. ve Altınay, Ö. (2017). "Doğal Antimikrobiyal Maddeler İle İşlem Görmüş Kumaşların Fiziksel ve Antimikrobiyal Özelliklerin İncelenmesi". Anka E-Dergi, 2 (2), 35-47. https://dergipark.org.tr/en/pub/anka/issue/33406/358084.

Altıntaş, Ö.E., Toksoy Öner, E., Çabuk, A. ve Aytar Çelik, P. (2023). "Biosynthesis of levan by Halomonas elongata 153B: Optimization for enhanced production and potential biological activities for pharmaceutical field". Journal of Polymers and the Environment, 31 (4), 1440-1455. https://doi.org/10.1007/s10924-022-02681-1.

Belghith, K. S., Dahech, I., Belghith, H. ve Mejdoub, H. (2012). "Microbial production of levansucrase for synthesis of fructooligosaccharides and levan". International Journal of Biological Macromolecules, 50 (2), 451-458.

Bouallegue, A., Casillo, A., Chaari, F., La Gatta, A., Lanzetta, R., Corsaro, M. M. ve Ellouz-Chaabouni, S. (2020). "Levan from a new isolated Bacillus subtilis AF17: Purification, structural analysis and antioxidant activities". International Journal of Biological Macromolecules, 144, 316-324

Byun, B. Y., Lee, S. J. ve Mah, J. H. (2014). "Antipathogenic activity and preservative effect of levan (β-2, 6-fructan), a multifunctional polysaccharide". International Journal of Food Science & Technology, 49 (1), 238-245. https://doi.org/10.1111/ijfs.12304.

Cho, C., Moran, E., Cherry, Stephans, J., Fodor, S., Adams, C., … Schultz, P. (1993). "An unnatural biopolymer". Science, 261 (5126), 1303–1305. https://doi.org/10.1126/science.7689747.

Cruz, D., Vasconcelos, V., Pierre, G., Michaud, P. ve Delattre, C. (2020). "Exopolysaccharides from cyanobacteria: Strategies for bioprocess development". Applied Sciences, 10 (11), 3763. https://doi.org/10.3390/app10113763.

Dahech, I., Harrabi, B., Hamden, K., Feki, A., Mejdoub, H., Belghith, H. ve Belghith, K. S. (2013). "Antioxidant effect of nondigestible levan and its impact on cardiovascular disease and atherosclerosis". International Journal of Biological Macromolecules, 58, 281–286. https://doi.org/10.1016/j.ijbiomac.2013.04.058.

Dal Bello, F., Walter, J., Hertel, C. ve Hammes, W. P. (2001). "In vitro study of prebiotic properties of levan-type exopolysaccharides from lactobacilli and non-digestible carbohydrates using denaturing gradient gel electrophoresis". Systematic and Applied Microbiology, 24 (2), 232-237. https://doi.org/10.1078/0723-2020-00033.

Divya, J. M. ve Sugumaran, K. R. (2015). "Fermentation parameters and condition affecting levan production and its applications". Journal of Chemical and Pharmaceutical Research, 7 (2), 861-865.

Domzał-Kedzia, M., Ostrowska, M., Lewi´nska, A., Łukaszewicz, M. (2023). "Recent Developments and Applications of Microbial Levan, A Versatile PolysaccharideBased Biopolymer". Molecules, 28, 5407. https:// doi.org/10.3390/molecules28145407

Elsakhawy, T.A., Sherief, F. A. ve Abd-EL-Kodoos, R. Y. (2017). "Marine microbial polysaccharides environmental role and applications: an overview Environ". Biodiver. Soil Sec., 1, 61-70.

Etemadi, O., Petrisor, I. G., Kim, D., Wan, M. W. ve Yen, T. F. (2003). "Stabilization of metals in subsurface by biopolymers: Laboratory drainage flow studies", Soil and Sediment Contamination: An International Journal, 12 (5), 647-661.

González-Garcinuño, Á., Masa, R., Hernández, M., Domínguez, Á., Tabernero, A. ve Del Valle, E. M. (2019). "Levan-capped silver nanoparticles for bactericidal formulations: Release and activity modelling". International Journal of Molecular Sciences, 20 (6), 1502. https://doi.org/10.3390/ijms20061502.

Gökmen, G. G., Silbir, S., Goksungur, Y. ve Kisla, D. (2020). "The effect of microbial levan on the growth of microorganisms: Inhibitory or stimulatory?". Fresenius Environmental Bulletin, 29, 1648-54.

Hamamcı, B., Çiftçi, M. ve Aktaş, T. (2018). "Yeşil kompozitlerde biyopolimerlerin kullanımının önemi". Karadeniz Fen Bilimleri Dergisi, 8 (1), 12-24.

Harmsen, P., Slottje, C., Baggerman, M., & Sillekens, E. (2021). Biological degradation of textiles: And the relevance to textile recycling. Wageningen Food & Biobased Research. https://doi.org/10.18174/557073.

Hernández, N., Williams, R. C. ve Cochran, E. W. (2014). "The battle for the "green" polymer. Different approaches for biopolymer synthesis: Bioadvantaged vs. bioreplacement". Org. Biomol. Chem., 12 (18), 2834–2849. https://doi.org/10.1039/c3ob42339e.

Hettwer, U., Gross, M. ve Rudolph, K. (1995). "Purification and characterization of an extracellular levansucrase from Pseudomonas syringae pv. Phaseolicola". Journal of Bacteriology, 177 (10), 2834-2839.

Inthanavong, L., Tian, F., Khodadadi, M. ve Karboune, S. (2013). "Properties of Geobacillus stearothermophilus levansucrase as potential biocatalyst for the synthesis of levan and fructooligosaccharides". Biotechnology Progress, 29 (6), 1405-1415.

Jing D., Zengyi S. ve Huimin Z. (2011). Engineering microbial factories for synthesis of value-added products, 38(8), 873–890. https://doi.org/10.1007/s10295-011-0970-3.

Khandekar, S., Srivastava, A., Pletzer, D., Stahl, A. ve Ullrich, M. S. (2014). "The conserved upstream region of lscB/C determines expression of different levansucrase genes in plant pathogen Pseudomonas syringae". BMC Microbiology, 14 (1), 1-11.

Koşarsoy Ağçeli, G. (2022a). "A new approach to nanocomposite carbohydrate polymer

films: Levan and chia seed mucilage". International Journal of Biological Macromolecules, 218, 751-759.

https://doi.org/10.1016/j.ijbiomac.2022.07.157 72 Koşarsoy Ağçeli, G. (2022b). "Devekuşu yumurta kabuğu ve nano-levan bazlı yenilebilir biyopolimer kompozit filmlerin geliştirilmesi: Karakterizasyon ve biyoaktivite". Polim. Boğa. 79 (12) 11201–11215. https://doi.org/10.1007/s00289- 021-04069-y.

Koşarsoy Ağçeli, G. ve Günan Yücel, H. (2023). "Levan production by Paenibacillus polymyxa immobilized on Fe3O4@ SiO2 nanoparticles using molasses medium with emphasis on the bioactivity". Journal of Polymers and the Environment, 1-16. https://doi.org/10.1007/s10924-023-02960-5

Liu, C., Lu, J., Lu, L., Liu, Y., Wang, F. ve Xiao, M. (2010). "Isolation, structural characterization and immunological activity of an exopolysaccharide produced by Bacillus licheniformis 8-37-0-1". Bioresource Technology, 101 (14), 5528–5533. https://doi.org/10.1016/j.biortech.2010.01.151.

Marx, S. P., Winkler, S. ve Hartmeier, W. (2000). "Metabolization of β-(2, 6)-linked fructose-oligosaccharides by different bifidobacteria". FEMS Microbiology Letters, 182 (1), 163-169. https://doi.org/10.1111/j.1574-6968.2000.tb08891.x.

Nakapong, S., Pichyangkura, R., Ito, K., Iizuka, M. ve Pongsawasdi, P. (2013). "High expression level of levansucrase from Bacillus licheniformis RN-01 and synthesis of levan nanoparticles". International Journal of Biological Macromolecules, 54, 30-36.

Sarilmiser, K., Ateş, O., Özdemir, G., Arga, K. Y. ve Őner, E. T. (2015). "Effective stimulating factors for microbial levan production by Halomonas smyrnensis AAD6T". Journal of Bioscience and Bioengineering, 119 (4), 455-463.

Schmid, J., Sieber, V. ve Rehm, B. (2015). "Bacterial exopolysaccharides: Biosynthesis pathways and engineering strategies". Frontiers in Microbiology, 6. https://doi.org/10.3389/fmicb.2015.00496.

Schultz, P. (2017). Biopolymers Containing Unnatural Amino Acids. United States

Shutova, V. V., Revin, V. V. ve Kalinkina, E. A. (2021). "Azotobacter vinelandii'den, ağır metaller ve radyonüklidler için biyosorbentlerin bir bileşeni olarak Levan". Appl Biochem Microbiol, 57, 102–109. https://doi.org/10.1134/S0003683821010178.

Silbir, S., Dagbagli, S., Yegin, S., Baysal, T. ve Goksungur Y. (2014). "Levan production by Zymomonas mobilis in batch and continuous fermentation systems". Carbohydrate Polymers, 99, 454-461.

Srikanth, R., Reddy, C. H. S. S., Siddartha, G., Ramaiah, M. J. ve Uppuluri, K. B. (2015a). "Review on production, characterization and applications of levan". Carbohydrate Polymers, 120, 102-114.

Tian, F., Inthanavong, L. ve Karboune, S. (2011). "Purification and characterization of levansucrases from Bacillus amyloliquefaciens in intra- and extracellular forms useful for the sythesis of levan and fructooligosaccharides". Biosci Biotechnol Biochem, 75 (10), 1929- 1938.

Zhang, T., Li, R., Qian, H., Mu, W., Miao, M. ve Jiang, B. (2014). "Biosynthesis of levan by levansucrase from Bacillus methylotrophicus SK 21.002". Carbohydrate Polymers, 101, 975-981.

Zhang, Y., Xu, Q., Fu, F. ve Liu, X. (2016). "Durable antimicrobial cotton textiles modified with inorganic nanoparticles". Cellulose, 23, 2791-2808.

CHAPTER 4

PARTIAL DERIVATIVES AND GRADIENT OPERATOR OF SPLIT QUATERNIONIC FUNCTIONS*

Ali ATASOY[1]

* Note: This study is derived from a section of the doctoral thesis titled "Quaternions and Some Applications of Quaternionic Functions" by the author Ali ATASOY (YÖK thesis no: 337862; Dumlupınar University-2013, https://acikbilim.yok.gov.tr/handle/20.500.12812/609977, Süpervisor: Doç. Dr. Erhan Ata).

1 Dr. Asst. Prof., Kırıkkale University, Keskin Vocational School, Kırıkkale, Türkiye, https://orcid.org/0000-0002-1894-7695

1. Introduction

Split quaternionic functions involve a mathematical framework that extends beyond the conventional real and complex numbers, incorporating quaternions with components that may also take on values from a split-complex number system. The partial derivatives and gradient operator within this context demand a nuanced understanding due to the non-commutative nature of quaternions (Mandic et al., 2011; Brenner, 1951) and the unique properties of split quaternions (Masrouri et al., 2011).

Split quaternionic functions introduce an advanced mathematical framework that significantly extends the traditional realms of real and complex numbers by incorporating elements of quaternions, where the components are allowed to adopt values from a split-complex number system. This extension necessitates a deeper exploration and understanding of mathematical operations, especially in the context of partial derivatives and the gradient operator, due to the inherent non-commutative properties of quaternions (Mandic et al., 2011; Zhang, 1997). Moreover, the introduction of split quaternions adds another layer of complexity because of their unique algebraic properties, which differ markedly from those of both real numbers and standard complex numbers. This sophisticated structure demands a nuanced approach to mathematical analysis, particularly when dealing with differential operations and understanding the geometric interpretations in higher dimensions that this framework facilitates. The study of split quaternionic functions thus opens up new avenues for research and application in fields requiring advanced mathematical modeling and analysis, pushing the boundaries of what is achievable with conventional numerical systems.

Split quaternions, also known as hyperbolic quaternions, extend the concept of quaternions by introducing a different type of multiplication rule. Quaternions themselves are a system of numbers that extend complex numbers (Hamilton, 1843; Atasoy and Yaylı, 2021). While complex numbers

can be thought of as points in a two-dimensional plane, quaternions exist in four dimensions, adding an extra layer of complexity. The real quaternion algebra defined over the real numbers with basis $\{1, i, j, k\}$, where

$$i^2 = j^2 = k^2 = -1, ij = k, jk = i, ki = j.$$

For information detailed, see (Dickson, 1919; Hacısalihoğlu, 1983).

Split quaternions modify this structure. They still form a four-dimensional algebra over the real numbers, but with a crucial difference in the multiplication rules of the basis elements. Specifically, in the split quaternion algebra, the basis elements still satisfy $i^2 = -1$, but $j^2 = k^2 = 1$ and

$$ijk = -1, ij = k, jk = -i, ki = j.$$

This change alters the properties of the algebra significantly. For instance, unlike the real quaternions, the norm of a split quaternion can be zero without the quaternion itself being zero. This is because the norm of a split quaternion $q = t + ix + jy + kz$ is given by

$$N(q) = t^2 + x^2 - y^2 - z^2$$

which can be positive, negative, or zero. This property introduces the possibility of zero divisors in the algebra of split quaternions (Kula and Yaylı, 2007).

Split quaternions have applications in various fields such as theoretical physics, where they can be used to model certain spacetime geometries, and in computer graphics and robotics for performing transformations and rotations in a non-Euclidean space. Their structure and properties provide a rich field of study, bridging mathematics and physics, and offering intriguing possibilities for modeling and analysis in spaces that behave differently from our usual Euclidean perspective.

2. Preliminaries

Split-quaternionic functions, also known as hyperbolic quaternionic functions, can be represented through matrices, extending the complex analysis into four dimensions. This extension allows for a richer structure and applications in physics and engineering, particularly in special relativity and signal processing.

To understand the matrix representation of split-quaternionic functions, it's essential to map the components of a split quaternion to a $2x2$ matrix form. This representation leverages the algebraic properties of matrices to simulate the behavior of split quaternions, facilitating their manipulation and application in various domains.

2.1. Matrix Representation of Split Quaternions

The matrix representation of a split quaternion

$$q = t + ix + jy + kz = (t + ix) + j(y - iz)$$

is given by:

$$T_q = \begin{pmatrix} t + ix & y + iz \\ y - iz & t - ix \end{pmatrix}$$

where t, x, y and z are real numbers, and the matrix elements mirror the components of the split quaternion (Alagöz et al, 2012).

This representation is powerful because it allows for the application of linear algebra techniques to study and manipulate split-quaternionic functions. For example, matrix operations such as addition, multiplication, and inversion correspond to similar operations in the split-quaternionic algebra, providing a bridge between abstract algebra and more tangible matrix calculations.

In the algebra of split quaternions, denoted as Q, with a natural basis $\{1, i, j, k\}$, we define an operator, T_q, acting on any element p of Q through the operation $T_q(\mathrm{p}) = \mathrm{qp}$. This operation leads to a matrix representation of the operator T_q. Specifically, the matrix representation of T_q is given by the

following $4x4$ matrix:

$$T_q \equiv \begin{bmatrix} t & x & y & z \\ -x & t & z & -y \\ y & z & t & x \\ z & -y & -x & t \end{bmatrix}$$

where the elements of the matrix are arranged in such a manner that they correspond to the coefficients of the split quaternion $q = t + xi + yj + zk$. This matrix form provides a concrete way to visualize and compute the action of T_q on any split quaternion p in Q, facilitating operations such as multiplication and analysis of split quaternion properties within the algebraic structure defined by Q (Pereira and Rocha, 2008; Atasoy, 2013).

Similarly, let us define the operator F_q on Q such that $F_q(p) = pq$, where p and q are quaternions. In this context, the matrix representation of the F_q operator can be expressed as follows:

$$F_q \equiv \begin{bmatrix} t & x & y & z \\ -x & t & -z & y \\ y & -z & t & -x \\ z & y & x & t \end{bmatrix}$$

where t, x, y and z are the components of the quaternion q (Ata & Yaylı, 2009).

2.1. Matrix Representation of Split Quaternionic Functions

Considering the split quaternionic function $f = f_1 + if_2 + jf_3 + kf_4$, where f_1, f_2, f_3 and $f_4$are real-valued functions, we can introduce a matrix representation (Hacısalihoğlu, 1983) of f, denoted as T_f. This representation is particularly insightful for understanding the structure and transformation properties of split quaternions. The matrix T_f is explicitly given by:

$$T_f \equiv \begin{bmatrix} f_1 & f_2 & f_3 & f_4 \\ -f_2 & f_1 & f_4 & -f_3 \\ f_3 & f_4 & f_1 & f_2 \\ f_4 & -f_3 & -f_2 & f_1 \end{bmatrix}$$

This matrix form offers a convenient way to analyze and manipulate split

quaternionic functions, facilitating operations such as addition, multiplication, and inversion in the context of split quaternion algebra. It embodies the essence of split quaternionic behavior, capturing both the algebraic and geometric interpretations of these entities. The representation underscores the interplay between the real and imaginary components of the split quaternion, reflecting the rich structure that these mathematical constructs encapsulate.

3. Partial Derivatives of Split Quaternionic Functions

Given a split quaternion represented as $q = t + ix + jy + kz$, we can define the derivative of a function f with respect to q, denoted $f'(q) = \frac{df}{dq}$, using the limit definition:

$$f'(q) = \lim_{\Delta q \to 0} \left[\frac{f(q + \Delta q) - f(q)}{\Delta q} \right].$$

Considering that a function $f(q)$ of a split quaternion can be expressed as

$$f(q) = f_1(q) + if_2(q) + jf_3(q) + kf_4(q)$$

drawing a parallel to the algebra of complex numbers where a complex number $z = x + iy$ and a function $f(z) = f_1(z) + if_2(z)$, we can write the derivative with respect to z as:

$$\frac{df}{dz} = \begin{bmatrix} \frac{\partial f_1}{\partial x} & \frac{\partial f_2}{\partial x} \\ \frac{\partial f_1}{\partial y} & \frac{\partial f_2}{\partial y} \end{bmatrix}$$

Furthermore, the Cauchy-Riemann conditions in the context of complex analysis state that:

$$\frac{\partial f_1}{\partial x} = \frac{\partial f_2}{\partial y} \quad \text{and} \quad \frac{\partial f_2}{\partial x} = -\frac{\partial f_1}{\partial y}$$

These conditions also imply that the Jacobian of the transformation, given

by

$$J = \left(\frac{\partial f_1}{\partial x}\right)^2 + \left(\frac{\partial f_2}{\partial x}\right)^2$$

, plays a crucial role in understanding the properties of $f(z)$ (Weisz, 1991).

In the field of advanced mathematics, particularly when examining the properties and differentiation of functions within the realm of split quaternionic analysis, the work by (Masrouri et al., 2011) presents a noteworthy theorem (Teorem 3.1), which elucidates the derivative of a split quaternionic function with respect to a split quaternion.

Theorem 3.1, Let $f = f_1 + if_2 + jf_3 + kf_4$ represent a split quaternionic function, where each component f_n is a real-valued function, and let $q = t + ix + jy + kz$ denote a split quaternion. According to this theorem, the derivative of f with respect to q, denoted as $\frac{\partial f}{\partial q}$, can be expressed through a matrix formulation as follows:

$$\frac{df}{dq} = \begin{bmatrix} \frac{\partial f_1}{\partial t} & \frac{\partial f_2}{\partial t} & \frac{\partial f_3}{\partial t} & \frac{\partial f_4}{\partial t} \\ \frac{\partial f_1}{\partial x} & \frac{\partial f_2}{\partial x} & \frac{\partial f_3}{\partial x} & \frac{\partial f_4}{\partial x} \\ \frac{\partial f_1}{\partial y} & \frac{\partial f_2}{\partial y} & \frac{\partial f_3}{\partial y} & \frac{\partial f_4}{\partial y} \\ \frac{\partial f_1}{\partial z} & \frac{\partial f_2}{\partial z} & \frac{\partial f_3}{\partial z} & \frac{\partial f_4}{\partial z} \end{bmatrix}$$

Proof: The proof of this theorem unfolds by considering the partial derivatives of f with respect to each of the components of q (i.e., (t, x, y, z)). It demonstrates how these partial derivatives relate to the components of the split quaternion and their interaction under differentiation. For instance, the derivative of f with respect to t yields

$$\frac{\partial f}{\partial t} = \frac{df}{dq}\frac{\partial q}{\partial t} = \frac{df}{dq}.1 = f'(q)$$

which simplifies to $f'(q)$ where $f'(q)$ encompasses

$$f'(q) = \frac{\partial f_1}{\partial t} + i\frac{\partial f_2}{\partial t} + j\frac{\partial f_3}{\partial t} + k\frac{\partial f_4}{\partial t}.$$

Similar relations are derived for derivatives with respect to x, y and z, each revealing the interplay between the split quaternionic function's components and the underlying quaternionic structure. Namely,

$$\frac{\partial f}{\partial x} = \frac{df}{dq}\frac{\partial q}{\partial x} = \frac{df}{dq}.i$$

$$= f'(q)i \Rightarrow f'(q) = \frac{-\partial f}{\partial x}i = \frac{\partial f_2}{\partial x} - i\frac{\partial f_1}{\partial x} - j\frac{\partial f_4}{\partial x} + k\frac{\partial f_3}{\partial x}$$

$$\frac{\partial f}{\partial y} = \frac{df}{dq}\frac{\partial q}{\partial y} = \frac{df}{dq}.j$$

$$= f'(q)j \Rightarrow f'(q) = \frac{\partial f}{\partial y}j = \frac{\partial f_3}{\partial y} + i\frac{\partial f_4}{\partial y} + j\frac{\partial f_1}{\partial y} + k\frac{\partial f_2}{\partial y}$$

$$\frac{\partial f}{\partial z} = \frac{df}{dq}\frac{\partial q}{\partial z} = \frac{df}{dq}.k$$

$$= f'(q)k \Rightarrow f'(q) = \frac{\partial f}{\partial z}k = \frac{\partial f_4}{\partial z} - i\frac{\partial f_3}{\partial z} - j\frac{\partial f_2}{\partial z} + k\frac{\partial f_1}{\partial z}$$

Through careful analysis, this theorem enables one to construct the split derivative quaternion, $T_{f'}$, represented as a matrix that captures the essence of differentiation in the split quaternionic domain. Since the coefficients of 1, i, j and k are equal and considering the matrix

$$T_q \equiv \begin{bmatrix} t & x & y & z \\ -x & t & z & -y \\ y & z & t & x \\ z & -y & -x & t \end{bmatrix}$$

which is the matrix representation of a split quaternion, the split derivative quaternion

$$\frac{\partial f}{\partial t} = \frac{\partial f_1}{\partial t} + i\frac{\partial f_2}{\partial t} + j\frac{\partial f_3}{\partial t} + k\frac{\partial f_4}{\partial t}$$

can be written in matrix form as

$$T_{f'} \equiv \begin{bmatrix} \frac{\partial f_1}{\partial t} & \frac{\partial f_2}{\partial t} & \frac{\partial f_3}{\partial t} & \frac{\partial f_4}{\partial t} \\ \frac{-\partial f_2}{\partial t} & \frac{\partial f_1}{\partial t} & \frac{\partial f_4}{\partial t} & \frac{-\partial f_3}{\partial t} \\ \frac{\partial f_3}{\partial t} & \frac{\partial f_4}{\partial t} & \frac{\partial f_1}{\partial t} & \frac{\partial f_2}{\partial t} \\ \frac{\partial f_4}{\partial t} & \frac{-\partial f_3}{\partial t} & \frac{-\partial f_2}{\partial t} & \frac{\partial f_1}{\partial t} \end{bmatrix} \equiv \begin{bmatrix} \frac{\partial f_1}{\partial t} & \frac{\partial f_2}{\partial t} & \frac{\partial f_3}{\partial t} & \frac{\partial f_4}{\partial t} \\ \frac{\partial f_1}{\partial x} & \frac{\partial f_2}{\partial x} & \frac{\partial f_3}{\partial x} & \frac{\partial f_4}{\partial x} \\ \frac{\partial f_1}{\partial y} & \frac{\partial f_2}{\partial y} & \frac{\partial f_3}{\partial y} & \frac{\partial f_4}{\partial y} \\ \frac{\partial f_1}{\partial z} & \frac{\partial f_2}{\partial z} & \frac{\partial f_3}{\partial z} & \frac{\partial f_4}{\partial z} \end{bmatrix}$$

Thus the proof is completed.

Moreover, the significance of this theorem extends to the computation of the determinant or the Jacobian of the matrix representation, which, as elucidated by (Mandic et al., 2011).

4. Gradient of Split Quaternionic Functions

Given the split quaternions $q_1$and q_2, let's consider the condition that they are similar if there exists at least one split quaternion μ such that

$$q_1 = \mu q_2 \mu^{-1}.$$

Based on this premise, we explore the concept of involutions of a split quaternion q, denoted as q^i, q^j, and q^k, which are essentially forms of q that are similar to it under certain transformations (Bekar and Yaylı, 2013). Specifically, these involutions can be derived through the application of quaternionic conjugation operations involving the quaternion units i, j and k.

The involutions can be calculated as follows:

$$\begin{aligned} q^i = -iqi = -i(t + ix + jy + kz)i = -i(ti - x - ky + jz) \\ = t + ix - jy - kz \end{aligned}$$

$$\begin{aligned} q^j = -jqj = -j(t + ix + jy + kz)j = -j(tj + kx + y + iz) \\ = -t + ix - jy + kz \end{aligned}$$

$$\begin{aligned} q^k = -kqk = -k(t + ix + jy + kz)k = -k(tk - jx - iy + z) \\ = -t + ix + jy - kz. \end{aligned}$$

In the equation system

$$\left.\begin{aligned} q &= t + ix + jy + kz \\ q^i &= t + ix - jy - kz \\ q^j &= -t + ix - jy + kz \\ q^k &= -t + ix + jy - kz \end{aligned}\right\}$$

the real values of t, x, y ve z are

$$\left.\begin{aligned} t &= \frac{1}{4}\left(q + q^i - q^j - q^k\right) \\ x &= \frac{1}{4i}\left(q + q^i + q^j + q^k\right) \\ y &= \frac{1}{4j}\left(q - q^i - q^j + q^k\right) \\ z &= \frac{1}{4k}\left(q - q^i + q^j - q^k\right) \end{aligned}\right\}$$

and written as

$$\left.\begin{aligned} dt &= \tfrac{1}{4}\left(dq + dq^i - dq^j - dq^k\right) \\ dx &= \tfrac{-i}{4}\left(dq + dq^i + dq^j + dq^k\right) \\ dy &= \tfrac{j}{4}\left(dq - dq^i - dq^j + dq^k\right) \\ dz &= \tfrac{k}{4}\left(dq - dq^i + dq^j - dq^k\right) \end{aligned}\right\}.$$

If these values are replaced in the partial derivatives of the function f, the equations

$$\frac{\partial f}{\partial q} = \frac{\partial f}{\partial t}\frac{\partial t}{\partial q} + \frac{\partial f}{\partial x}\frac{\partial x}{\partial q} + \frac{\partial f}{\partial y}\frac{\partial y}{\partial q} + \frac{\partial f}{\partial z}\frac{\partial z}{\partial q} = \frac{\partial f}{\partial t}\frac{1}{4} + \frac{\partial f}{\partial x}\frac{(-i)}{4} + \frac{\partial f}{\partial y}\frac{j}{4} + \frac{\partial f}{\partial z}\frac{k}{4}$$

$$= \frac{1}{4}\left(\frac{\partial f}{\partial t} - i\frac{\partial f}{\partial x} + j\frac{\partial f}{\partial y} + k\frac{\partial f}{\partial z}\right)$$

$$\frac{\partial f}{\partial q^i} = \frac{\partial f}{\partial t}\frac{\partial t}{\partial q^i} + \frac{\partial f}{\partial x}\frac{\partial x}{\partial q^i} + \frac{\partial f}{\partial y}\frac{\partial y}{\partial q^i} + \frac{\partial f}{\partial z}\frac{\partial z}{\partial q^i}$$

$$= \frac{\partial f}{\partial t}\frac{1}{4} + \frac{\partial f}{\partial x}\frac{1}{4i} + \frac{\partial f}{\partial y}\frac{(-1)}{4j} + \frac{\partial f}{\partial z}\frac{(-1)}{4k}$$

$$= \frac{1}{4}\left(\frac{\partial f}{\partial t} - i\frac{\partial f}{\partial x} - j\frac{\partial f}{\partial y} - k\frac{\partial f}{\partial z}\right)$$

$$\frac{\partial f}{\partial q^j}=\frac{\partial f}{\partial t}\frac{\partial t}{\partial q^j}+\frac{\partial f}{\partial x}\frac{\partial x}{\partial q^j}+\frac{\partial f}{\partial y}\frac{\partial y}{\partial q^j}+\frac{\partial f}{\partial z}\frac{\partial z}{\partial q^j}$$
$$=\frac{\partial f}{\partial t}\frac{1}{4}+\frac{\partial f}{\partial x}\frac{1}{4i}+\frac{\partial f}{\partial y}\frac{(-1)}{4j}+\frac{\partial f}{\partial z}\frac{1}{4k}$$
$$=\frac{1}{4}\left(-\frac{\partial f}{\partial t}-i\frac{\partial f}{\partial x}-j\frac{\partial f}{\partial y}+k\frac{\partial f}{\partial z}\right)$$
$$\frac{\partial f}{\partial q^k}=\frac{\partial f}{\partial t}\frac{\partial t}{\partial q^k}+\frac{\partial f}{\partial x}\frac{\partial x}{\partial q^k}+\frac{\partial f}{\partial y}\frac{\partial y}{\partial q^k}+\frac{\partial f}{\partial z}\frac{\partial z}{\partial q^k}$$
$$=\frac{\partial f}{\partial t}\frac{(-1)}{4}+\frac{\partial f}{\partial x}\frac{1}{4i}+\frac{\partial f}{\partial y}\frac{1}{4j}+\frac{\partial f}{\partial z}\frac{(-1)}{4k}$$
$$=\frac{1}{4}\left(-\frac{\partial f}{\partial t}-i\frac{\partial f}{\partial x}+j\frac{\partial f}{\partial y}-k\frac{\partial f}{\partial z}\right)$$

are obtained. These partial derivatives can be written in matrix form

$$\begin{bmatrix}\frac{\partial f(q,q^i,q^j,q^k)}{\partial q}\\ \frac{\partial f(q,q^i,q^j,q^k)}{\partial q^i}\\ \frac{\partial f(q,q^i,q^j,q^k)}{\partial q^j}\\ \frac{\partial f(q,q^i,q^j,q^k)}{\partial q^k}\end{bmatrix}=\frac{1}{4}\begin{bmatrix}1&-i&j&k\\1&-i&-j&-k\\-1&-i&-j&k\\-1&-i&j&-k\end{bmatrix}\begin{bmatrix}\frac{\partial f}{\partial t}\\ \frac{\partial f}{\partial x}\\ \frac{\partial f}{\partial y}\\ \frac{\partial f}{\partial z}\end{bmatrix}.$$

Its conjugate is written as,

$$\begin{bmatrix}\frac{\partial f(q,q^i,q^j,q^k)}{\partial q^*}\\ \frac{\partial f(q,q^i,q^j,q^k)}{\partial q^{i^*}}\\ \frac{\partial f(q,q^i,q^j,q^k)}{\partial q^{j^*}}\\ \frac{\partial f(q,q^i,q^j,q^k)}{\partial q^{k^*}}\end{bmatrix}=\frac{1}{4}\begin{bmatrix}1&i&-j&-k\\1&i&j&k\\-1&i&j&-k\\-1&i&-j&k\end{bmatrix}\begin{bmatrix}\frac{\partial f}{\partial t}\\ \frac{\partial f}{\partial x}\\ \frac{\partial f}{\partial y}\\ \frac{\partial f}{\partial z}\end{bmatrix}.$$

Here,

$$\nabla f = \begin{bmatrix} \frac{\partial f}{\partial t} \\ \frac{\partial f}{\partial x} \\ \frac{\partial f}{\partial y} \\ \frac{\partial f}{\partial z} \end{bmatrix}$$

is the gradient of the function f (Mandic et al., 2011).

The gradient of the function f, denoted by ∇f, is a vector comprising the partial derivatives of f with respect to t, x, y, and z. This gradient plays a crucial role in understanding the direction and magnitude of the steepest ascent of f, offering insights into the geometric and analytic properties of f in the context of split quaternions and their involutions.

In the context of quaternion calculus, an intriguing relationship emerges when we consider the conjugate of a split quaternion, denoted as $q^* = \mathrm{t} - \mathrm{ix} - \mathrm{jy} - \mathrm{kz}$. This conjugate can be expressed in terms of the quaternion and its components as follows:

$$q^* = \frac{1}{4}(q + q^i - q^j - q^k) - i\frac{1}{4i}(q + q^i + q^j + q^k) - j\frac{1}{4j}(q - q^i - q^j + q^k)$$
$$-k\frac{1}{4k}(q - q^i + q^j - q^k) = \frac{1}{2}(-q + q^i - q^j - q^k)$$

This formulation leads to a fascinating insight when we consider a function f defined on the conjugate of the quaternion, $f(q^*)$, resulting in the equality:

$$f(q^*) = f(\frac{1}{2}(-q + q^i - q^j - q^k))$$

By differentiating this equation, we obtain a relationship between the differentials of f with respect to q^* and the components of the quaternion q, as follows:

$$\frac{\partial f}{\partial q^*}dq^* = -\frac{1}{2}\frac{\partial f}{\partial q}dq + \frac{1}{2}\frac{\partial f}{\partial q^i}q^i - \frac{1}{2}\frac{\partial f}{\partial q^j}q^j - \frac{1}{2}\frac{\partial f}{\partial q^k}q^k$$

Upon rearranging this equation, we can derive an interesting form that reveals a connection between the differential of f and the quaternionic components:

$$-2\frac{\partial f}{\partial q^*}dq^* + \frac{\partial f}{\partial q^i}q^i = \frac{\partial f}{\partial q}dq + \frac{\partial f}{\partial q^j}q^j + \frac{\partial f}{\partial q^k}q^k$$

When this equation is utilized within the differential df, defined as

$$df = \frac{\partial f}{\partial q}dq + \frac{\partial f}{\partial q^i}q^i + \frac{\partial f}{\partial q^j}q^j + \frac{\partial f}{\partial q^k}q^k$$

an intriguing result emerges:

$$df = \frac{\partial f}{\partial q^i}q^i - 2\frac{\partial f}{\partial q^*}dq^* + \frac{\partial f}{\partial q^i}q^i = 2\frac{\partial f}{\partial q^i}q^i - 2\frac{\partial f}{\partial q^*}dq^*$$

$$= 2\frac{\partial f}{\partial q^i}q^i - 2\left(\frac{\partial f}{\partial q}dq\right)^* = 2\left[\frac{\partial f}{\partial q^i}q^i - \left(\frac{\partial f}{\partial q}dq\right)^*\right]$$

$$= 2\left[(\tfrac{\partial f}{\partial q}dq)^i - (\tfrac{\partial f}{\partial q}dq)^*\right].$$

Conclusion

The implications of our research are far-reaching, offering a new lens through which to view the dynamics of split quaternionic functions. This work not only enriches the theoretical framework of quaternionic analysis but also opens up new avenues for practical applications. From the design of complex systems in engineering to advancements in theoretical physics, the insights gained from this study have the potential to influence a wide array of disciplines.

The exploration of partial derivatives and the gradient operator within the realm of split quaternionic functions has yielded a comprehensive understanding of their mathematical properties and potential applications. This research marks a significant step forward in the field of quaternionic analysis, paving the way for future investigations and developments.

REFERENCES

Alagöz, Y., Oral, K. H., & Yüce, S. (2012). Split quaternion matrices, Miskolc Mathematical Notes, 13(2), 223-232.

Ata, E., & Yaylı, Y. (2009). Split quaternions and semi-Euclidean projective spaces, Chaos Solitons Fractals, 41(4), 1910–1915.

Atasoy, A. (2013). Quaternions and Some Applications of Quaternionic Functions, Dumlupınar University Institute of Science, Doctoral Thesis, Kütahya, Türkiye.

Atasoy, A., & Yaylı, Y. (2021). Obtaining triplet from quaternions, International Journal of Optimization and Control: Theories and Applications , (11)1, 109-113.

Bekar, M., & Yaylı, Y. (2013). Involutions of complexified quaternions and split quaternions, Advances in Applied Clifford Algebras, 23, 283-299.

Brenner, J. L. (1951). Matrices of quaternions, Pacific J. Math., 1, 329-335.

Dickson, L. E. (1919). On Quaternions and Their Generalization and the History of the Eight Square Theorem, Annals of Mathematics, Second Series, 20(3), 155–171.

Hacısalihoğlu, H. H. (1983). Hareket Geometrisi ve Kuaterniyonlar Teorisi, Gazi Üniversitesi Fen Edebiyat Fak. Yayınları, Math. No.2, Ankara, Türkiye.

Hamilton, W. R. (1843). On A New Spaces of Imaginary Quantities Connected with A Theory of Quaternions, Duplin Proc., 2(13), 424-434.

Kula, L., & Yaylı, Y., (2007). Split Quaternions and Rotations in Semi-Euclidean Space R_2^4, J. Korean Math. Soc. 44(6), 1313-1327.

Mandic, D. P., Jahanchahi, C., & Took, C. C. (2011). A Quaternion Gradient Operator and Its Aplications, IEEE Signal Processing Letters, 18(1), 47-50.

Masrouri, N., Yayli, Y. (2011). Comments On Differentiable Over Function of Split Quaternions, Revista Notas de Matemática, 7, 128-134.

Pereira, R., & Rocha, P. (2008). On the Determinant of Quaternionic Polynomial Matrices and its Application to System Stability, Mathematical Methods in the Applied Sciences, 31, 99-122.

Weisz, J. F. (1991). Comments on mathematical analysis over quaternions, Int. J. Math. Educ. Sci. Technol., 22(4), 499-506.

Zhang, F. (1997). Quaternions and Matrices of Quaternions, Linear Algebra and Its Applications, 251, 21-57.

CHAPTER 5

LACUNARY UNIFORMLY STATISTICAL NEUTROSOPHIC CONVERGENCE ON A KIND OF NORMED SPACES

Nazmiye GONUL BILGIN[1]

Gurel BOZMA[2]

1 Associate Professor Nazmiye GONUL BILGIN, Zonguldak Bulent Ecevit University, Faculty of Sciences, Department of Mathematics, Zonguldak Turkey. ORCID: 0000-0001-6300-6889
2 PhD student Gurel BOZMA, (in Zonguldak Bulent Ecevit University), Zonguldak Governorship, Zonguldak Turkey. ORCID: 0000-0002-0916-5894

1. INTRODUCTION

After Azerbaijani scientist Lotfi Aliasker Zadeh introduced the concept of fuzzy sets in 1965, important studies on fuzzy set theory have been carried out in almost every branch of mathematics. The concept of fuzzy sets arose from the need to mathematically model uncertainties. Since very few fuzzy number sequences and series are convergent, it was necessary to investigate the addition methods for divergent fuzzy number sequences and series and to determine the conditions for these methods. Later, Atanassov (1983), based on the concept of fuzzy set, gived intuitionistic fuzzy set as a generalization of fuzzy set. After the introduction of the concept, generalizations of the definitions and concepts in various fields of mathematics in intuitionistic fuzzy set theory were made. Intuitionistic fuzzy sets are developed by membership and non-membership functions. Using these two functions, it can be said that each element in the set has membership and non-membership values, and the sum of these two values cannot be greater than one. In 1999, Smarandache, introduced the idea of a neutrosophic set with three distinct components: membership, uncertainty and non-membership. In the transition to the Neutrosophic approach, firstly, in addition to the membership and non-membership values, the degree of uncertainty of each element was taken into account and it was accepted that the sum of these three values would be equal to one. Here, if the sum of the membership and non-membership values is one, it is considered that the element examined is not in uncertainty. However, later this situation was relaxed and the sum of the three functions could take the value of 2 or 3 depending on whether they were dependent on each other or independent. Brief information about all three cases is given in Figure 1.

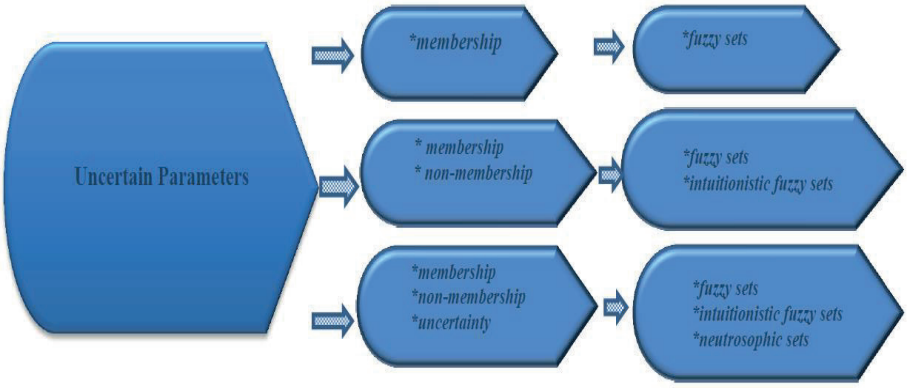

Figure 1: Uncertain Parameters

Although sets are more understandable by using these three functions, the studies still seem to need improvement due to authors with different perspectives. In fact, the main purpose of all these approaches is to eliminate inadequacy, uncertainty and confusion in data analysis. While analyzing the data, in order to increase the reliability of the findings, the classical approach should be abandoned and fuzzy, intuitionistic fuzzy and neutrosophic approaches should be taken into consideration, respectively. By taking into account the classification and correct processing of information, the neutrosophic approach has been applicable to many fields. Examples of these include decision-making processes related to daily life, medical diagnosis, drug production, studies in engineering, education and theoretical science.

Since classical logic recommends evaluation within precise and certain limits, it is very difficult to express the available data in a structure close to ideal for the uncertainty problems encountered in areas where personal opinions are effective. Therefore, it is not easy to classify data correctly and eliminate uncertainty.

If we return to the neutrosophic studies in the field of mathematics, many applications have been made in terms of the decision-making process by defining the concepts of set, sequences, number and then basic topological concepts. For example (Gonul Bilgin et al, 2022). In the field of mathematical analysis, the theory has made great progress with the help of special series whose neutrosophic versions have been defined, and important studies have

been carried out in different spaces with many series in hybrid structure. Rough and lacunary sequences are some of them. Lacunary sequences have been evaluated with many different concepts due to their ease of study. For example, (Aytar, 2008; Aktuğlu, 2009, Gönül, 2013; Dundar and Cakan, 2014) can be given.

Another area where the convergence of special sequences is investigated is statistical convergence. The notion of statistical convergence was given with (Fast, 1951; Steinhaus, 1951). Later, this concept was developed by Salt (1980), Fridy (1985), Connor (1988), Fridy and Miller (1991), Fridy and Orhan (1993). The specially defined array we will use in our study is the lacunary sequences. The statistical convergence of this sequences was first defined by Fridy and Orhan in 1993. Statistical convergence was examined to intuitionistic fuzzy normed spaces by Karakus and Demirci in 2008. Statistical convergence on neutrosophic normed space is applied by (Kirisci and Simsek, 2020). Later, many mathematicians evaluated the definition of statistical convergence together with many different types of convergence, established hybrid definitions, and presented the relationships between them. Some of these can be given as: (Sözbir et. al, 2020; Gonul Bilgin and Bozma, 2020; 2021,Bilgin, 2022), The concept of lacunary statistical convergence is worked in neutrosophic normed spaces by Khan et. al. in 2021. After those studies, statistical convergence were carried out in the neutrosophic normed space with the help of different types of convergence. For example (Kisi, 2021a; Kisi, 2021b; Gonul Bilgin, 2022; Bilgin, 2023a; 2023b).

The studies gained a new dimension by transferring the concept of statistical convergence of sequences on neutrosophic normed spaces to functions. The concept of statistical convergence of function sequences in this space was defined by Khan et al in 2023.

Considering the studies summarized above, the statistical convergence of function sequences on neutrosophic normed spaces will be combined with lacunary sequences and their important properties will be examined. The structure of the research is as following: First of all, the basic background needed for the paper will be presented. In the first of the main sections, the

concept of lacunar statistical convergence of a function to neutrosophic normed spaces will be defined. Important theoretical characteristics such as uniqueness and Cauchy sequence will be introduced for this concept. For sequences of functions, the evolution of the notion of statistical convergence in the literature will be described. Lastly, results and suggestions will be presented.

2. PRELIMINARIES

After summarizing the relevant literature on the concepts necessary for our study, we shall present the basic definitions to be used.

Definition 2.1 (Neutrosophic Set) Assume $Б(u), þ(u)$ and $đ(u)$ are the degrees of membership, indeterminacy and non-membership. A neutrosophic set $\mathfrak{N}$ is in the following form: for each u in Ц, $Б(u), đ(u), þ(u) \in [0,1]$, $0 \leq Б(u) + đ(u) + þ(u) \leq 2$,

$\mathfrak{N} = \{(u, Б(u), đ(u) \text{ and } þ(u)) : u \in Ц\}$.

Here, $þ(u)$ is an independent component, $Б(u)$ and $đ(u)$ are dependent components.

(Kirisci and Simsek, 2020) gave the definition of Neutrosophic normed space with the concept of statistical convergence in this space, while (Khan et al.2021) gave the definition of lacunary type statistical convergence in Neutrosophic normed space.

Definition 2.2 Let Ц be a linear spaces, $\boxdot$ and $\oplus$ show the continuous t-norm and t-conorm. A Neutrosophic normed is denoted with next form $\{((u, v), Б(u, v), đ(u, v), þ(u, v)) : (u, v) \in Ц \times (0, \infty)\}$ where $Б(u, v), þ(u, v), đ(u, v)$ are demonstrated the degree of membership, indeterminacy and non-membership of (u, v) on $Ц \times (0, \infty)$ satisfies following conditions:

For each $u, \tilde{u} \in Ц$,

i. $Б(u, v), đ(u, v), þ(u, v) \in [0,1]$,

ii. For all $u \in (0,\infty)$, $Б(u,v) + đ(u,v) + þ(u,v) \leq 2$,

iii. For every $c \neq 0$,

$$Б(cu,v) = Б\left(u,\frac{v}{|c|}\right),\ þ(cu,v) = þ\left(u,\frac{v}{|c|}\right),\ đ(cu,v) = đ\left(u,\frac{v}{|c|}\right),$$

iv. For every $v \in (0,\infty)$,

$Б(u,v) = 1 \iff u = 0,\ þ(u,v) = 0 \iff u = 0,\ đ(u,v) = 0 \iff u = 0$,

v. For every $w, v \in \mathbb{R}^+$ and $u, \tilde{u} \in Ц$,

$Б(u,v) \boxdot Б(\tilde{u},v) \leq Б(u+\tilde{u}, w+v)$,

$þ(u,v) \oplus þ(\tilde{u},v) \geq þ(u+\tilde{u}, w+v)$,

$đ(u,v) \oplus đ(\tilde{u},v) \geq đ(u+\tilde{u}, w+v)$.

vi. $Б(u,.)$ is continuous non-decreasing function, $þ(u,.)$, $đ(u,.)$ are continuous non-increasing function,

vii. $\lim_{t\to\infty} Б(u,v) = 1$, $\lim_{t\to\infty} þ(u,v) = 0$, $\lim_{t\to\infty} đ(u,v) = 0$,

viii. For $v \leq 0$, $Б(u,v) = 0$, $þ(u,v) = 1$ and $đ(u,v) = 1$.

So, $(Ц, Б, đ, þ, \boxdot, \oplus)$ is called Neutrosophic normed spaces. Here $Б$ and $đ$ are dependent and $þ$ is an independent components.

Now, in this section where we will remind the definition of various types of statistical convergence in neutrosophic normed spaces, let us first give the definition of statistical convergence defined by (Fast, 1951; Steinhaus, 1951).

Definition 2.3 Let for every $\varepsilon > 0$, $u = (u_n)$ satisfying the next condition,

$$\delta(\{j: |u_j - ł| \geq \varepsilon\}) = 0.$$

In this case, $u = (u_n)$ is called statistically convergent to $ł$, is denoted with $st - limu = ł$.

Let us give the concepts of lacunary sequences and lacunary statistical convergence presented by (Fridy and Orhan, 1993).

Definition 2.4 Let $\theta = \{j_i\}$, $j_0 = 0$ and $\hbar_i := j_i - j_{i-1}$. If $\lim_{r\to\infty} \hbar_i := \lim_{i\to\infty} j_i - j_{i-1}$ then, θ is called to be a lacunary sequences. In this paper, $I_i := (j_{i-1}, j_i], q_i := \frac{j_i}{j_{i-1}}$ will be used.

Based on the statistical convergence definition of Fast and Steinhaus, the definition of lacunary statistical convergence is given as follows:

Definition 2.5 Let $\theta = \{j_i\}$ be a lacunary sequence. For every $\varepsilon > 0$, if $\mathcal{u} = (\mathcal{u}_n)$ satisfying

$$lim_i \frac{1}{\hbar_i} \left|\{j \in I_i : |\mathcal{u}_j - \mathfrak{l}| \geq \varepsilon\}\right| = 0,$$

then $\mathcal{u}$ is called lacunary statistical convergent and it's denoted by $\mathcal{st}^{\theta} - lim\, \mathcal{u} = \mathfrak{l}$. The set of all these sequences is demonstrated with $\mathcal{St}_{\theta}$. Here, $|\mathcal{M}|$ is represents the cardinality of $\mathcal{M}$.

Definition 2.6 Let $(Ц, Б, \text{д}, ƀ, \boxdot, \oplus)$ and $(\tilde{Ц}, Б, \text{д}, ƀ, \boxdot, \oplus)$ be two neutrosophic normed spaces, $\psi_n : (Ц, Б, \text{д}, ƀ, \boxdot, \oplus) \to (\tilde{Ц}, Б, \text{д}, ƀ, \boxdot, \oplus)$ be a sequences of functions. Then, ψ_n is called pointwise neutrosophic convergent on $Ц$ to a function ψ, if for every $ц \in Ц$, the sequence $(\psi_n(ц))$ is convergent to $\psi(ц)$.

Now let us remind you of the definition of uniform neutrosophic convergence of function sequences for neutrosophic normed spaces, which was previously established by (Kirişci and Simsek, 2020), inspired by the definition given for neutrosophic metric spaces.

Definition 2.7 Let $(Ц, Б, \text{д}, ƀ, \boxdot, \oplus)$ and $(\tilde{Ц}, Б, \text{д}, ƀ, \boxdot, \oplus)$ be two neutrosophic normed spaces, $\psi_n : (Ц, Б, \text{д}, ƀ, \boxdot, \oplus) \to (\tilde{Ц}, Б, \text{д}, ƀ, \boxdot, \oplus)$ be a sequences of functions. Then, ψ_n is called uniformly neutrosophic convergent on $Ц$ to a function ψ, if given $n \in (0,1)$, then there exists positive integer $n_0 \in \mathbb{N}$ such that every $ц \in Ц$ and $n \geq n_0$: $Б(\psi_n(ц), \psi(ц)) > 1 - \varepsilon, \text{д}(\psi_n(ц), \psi(ц)) < \varepsilon$ and

$\text{ƥ}\left(\psi_n(\text{ц}), \psi(\text{ц})\right) < \varepsilon$.

Based on the definition of pointwise neutrosophic convergent function sequence, the definition of pointwise statistically neutrosophic convergence was given by Khan et al in 2023. Now let's remind this definition.

Definition 2.8 Let $(\text{Ц}, \text{Б}, \text{đ}, \text{ƥ}, \boxdot, \oplus)$ and $\left(\tilde{\text{Ц}}, \text{Б}, \text{đ}, \text{ƥ}, \boxdot, \oplus\right)$ be two neutrosophic normed spaces, ψ_n: $(\text{Ц}, \text{Б}, \text{đ}, \text{ƥ}, \boxdot, \oplus) \to \left(\tilde{\text{Ц}}, \text{Б}, \text{đ}, \text{ƥ}, \boxdot, \oplus\right)$ be a sequences of functions. Then, ψ_n is called pointwise statistically neutrosophic convergent to a function ψ on Ц, if for every ц ∈ Ц, the sequence $\left(\psi_n(\text{ц})\right)$ is statistically convergent to $\psi(\text{ц})$.

In this case we show it with $\text{ѕ}t(\text{Б}, \text{đ}, \text{ƥ}) - \psi_n \to \psi$.

Having presented the statistical version of the uniformly neutrosophic convergence of function sequences, we can proceed to the description of its modification, which is constructed with the help of a special sequences and for which we will give important properties.

Definition 2.9 Let $(\text{Ц}, \text{Б}, \text{đ}, \text{ƥ}, \boxdot, \oplus)$ and $\left(\tilde{\text{Ц}}, \text{Б}, \text{đ}, \text{ƥ}, \boxdot, \oplus\right)$ be two neutrosophic normed spaces, ψ_n: $(\text{Ц}, \text{Б}, \text{đ}, \text{ƥ}, \boxdot, \oplus) \to \left(\tilde{\text{Ц}}, \text{Б}, \text{đ}, \text{ƥ}, \boxdot, \oplus\right)$ be a sequences of functions. Then, ψ_n is called uniformly statistical neutrosophic convergent on Ц to a function ψ, if given $\varepsilon \in (0,1)$, then there exists positive integer $n_0 \in \mathbb{N}$ such that every ц ∈ Ц and $n \geq n_0$: $\text{Б}\left(\psi_n(\text{ц}), \psi(\text{ц})\right) > 1 - \varepsilon, \text{đ}(\psi_n(\text{ц}), \psi(\text{ц})) < \varepsilon$ and $\text{ƥ}\left(\psi_n(\text{ц}), \psi(\text{ц})\right) < \varepsilon$.

3. MAIN RESULTS

In this section, we introduce lacunary pointwise statistically convergent sequences of functions in neutrosophic normed spaces and also we give uniform statistically convergent versions of these definitions. Now, let's review the history of this concept in the literature. The concept of lacunary statistical pointwise convergence and its uniformly convergent version of a function sequence were defined by Aktuğlu and Gezer in 2009. The concept The version of this concept on intuitionistic fuzzy normed space was defined by Karakaya et al in 2014. We established this definition by taking into account

the study by Khan et al in 2023, in which only the statistical similarity of a function sequence in neutrosophic normed spaces was examined, and this literature summary.

Definition 3.1 Let $(Ц, Б, đ, þ, \boxdot, \oplus)$ and $(\tilde{Ц}, Б, đ, þ, \boxdot, \oplus)$ be two neutrosophic normed spaces, $\psi_i: (Ц, Б, đ, þ, \boxdot, \oplus) \to (\tilde{Ц}, Б, đ, þ, \boxdot, \oplus)$ be a sequences of functions. Then, ψ_i is called lacunary pointwise statistically neutrosophic convergent to a function ψ on Ц, if for every ц ∈ Ц,

$$\lim_i \frac{1}{ħ_i} \left|\left\{j \in I_i: Б\left(\psi_j(ц), \psi(ц)\right) < 1-\varepsilon \; or \; đ\left(\psi_j(ц), \psi(ц)\right) > \varepsilon, þ\left(\psi_j(ц), \psi(ц)\right) > \varepsilon\right\}\right| = 0.$$

This situation can also be expressed as: ψ_i is called lacunary pointwise statistically neutrosophic convergent to a function ψ on Ц, if for every ц ∈ Ц, the sequence $(\psi_i(ц))$ is lacunary statistically convergent to $\psi(ц)$ on neutrosophic normed spaces.

In this case we show with $(\psi_i(ц)) \overset{st(\theta)}{\to} \psi(ц)$.

Definition 3.2 Let $(Ц, Б, đ, þ, \boxdot, \oplus)$ and $(\tilde{Ц}, Б, đ, þ, \boxdot, \oplus)$ be two neutrosophic normed spaces, $\psi_i: (Ц, Б, đ, þ, \boxdot, \oplus) \to (\tilde{Ц}, Б, đ, þ, \boxdot, \oplus)$ be a sequences of functions. Then, ψ_i is called lacunary pointwise statistically neutrosophic Cauchy sequences in $(\tilde{Ц}, Б, đ, þ, \boxdot, \oplus)$, if for every ц ∈ Ц and $\varepsilon \in (0,1)$, there exists a $\bar{\bar{j}}$ such that

$$\lim_i \frac{1}{ħ_i} \left|\left\{j \in I_i: Б\left(\psi_j(ц), \psi_{\bar{j}}(ц)\right) < 1-\varepsilon \; or \; đ\left(\psi_j(ц), \psi_{\bar{j}}(ц)\right) > \varepsilon, þ\left(\psi_j(ц), \psi_{\bar{j}}(ц)\right) > \varepsilon\right\}\right| = 0.$$

Definition 3.3 Let $(Ц, Б, đ, þ, \boxdot, \oplus)$ and $(\tilde{Ц}, Б, đ, þ, \boxdot, \oplus)$ be two neutrosophic normed spaces, $\psi_i: (Ц, Б, đ, þ, \boxdot, \oplus) \to (\tilde{Ц}, Б, đ, þ, \boxdot, \oplus)$ be a sequences of functions. Then, ψ_i is called lacunary uniformly statistical neutrosophic convergent on Ц to a function ψ, if given $\varepsilon \in (0,1)$, then there exists positive integer $i_0 \in \mathbb{N}$ such that every ц ∈ Ц and $i \geq i_0$:

$$\lim_{i}\frac{1}{\hbar_i}\left|\left\{j\in I_i: Б\left(\psi_j(ц),\psi(ц)\right)<1-\varepsilon \text{ or } д\left(\psi_j(ц),\psi(ц)\right)>\varepsilon, ƥ\left(\psi_j(ц),\psi(ц)\right)>\varepsilon\right\}\right|=0.$$

This definition can be expressed as: ψ_i is called lacunary uniformly statistically neutrosophic convergent to a function ψ on Ц, if for given $\varepsilon\in(0,1)$, then there exists positive integer $i_0\in\mathbb{N}$ such that every $ц\in Ц$ and $i\geq i_0$, the sequence $\left(\psi_i(ц)\right)$ is lacunary statistically convergent to $\psi(ц)$ on neutrosophic normed spaces.

In this case we show with $\left(\psi_i(ц)\right)\overset{st(\theta)}{\rightrightarrows}\psi(ц)$.

Lemma 3.1 and Lemma 3.2 whose proof is obvious will be given without proof.

Lemma 3.1 Let $(Ц,Б,д,ƥ,\boxdot,\oplus)$ and $(\widetilde{Ц},Б,д,ƥ,\boxdot,\oplus)$ be two neutrosophic normed spaces, $\psi_i:(Ц,Б,д,ƥ,\boxdot,\oplus)\to(\widetilde{Ц},Б,д,ƥ,\boxdot,\oplus)$ be a sequences of functions. If $\left(\psi_i(ц)\right)$ is lacunary uniformly statistically neutrosophic convergent on $(\widetilde{Ц},Б,д,ƥ,\boxdot,\oplus)$ then $\left(\psi_i(ц)\right)$ lacunary pointwise statistically neutrosophic convergent to $\psi(ц)$.

Lemma 3.2 Let $(Ц,Б,д,ƥ,\boxdot,\oplus)$ and $(\widetilde{Ц},Б,д,ƥ,\boxdot,\oplus)$ be two neutrosophic normed spaces, $\psi_i:(Ц,Б,д,ƥ,\boxdot,\oplus)\to(\widetilde{Ц},Б,д,ƥ,\boxdot,\oplus)$ be a sequences of functions. In this case, the following situations are equal.

i) $\left(\psi_i(ц)\right)\overset{st(\theta)}{\to}\psi(ц)$.

ii) $$\lim_{i}\frac{1}{\hbar_i}\left|\left\{j\in I_i: Б\left(\psi_j(ц),\psi(ц)\right)<1-\varepsilon \text{ or } д\left(\psi_j(ц),\psi(ц)\right)>\varepsilon, ƥ\left(\psi_j(ц),\psi(ц)\right)>\varepsilon\right\}\right|=0.$$

iii) $$\lim_{i}\frac{1}{\hbar_i}\left|\left\{j\in I_i: Б\left(\psi_j(ц),\psi(ц)\right)>1-\varepsilon \text{ or } д\left(\psi_j(ц),\psi(ц)\right)<\varepsilon, ƥ\left(\psi_j(ц),\psi(ц)\right)<\varepsilon\right\}\right|=0.$$

Lemma 3.3 Let $(Ц,Б,д,ƥ,\boxdot,\oplus)$ and $(\widetilde{Ц},Б,д,ƥ,\boxdot,\oplus)$ be two neutrosophic normed spaces, $\psi_i,\varphi_i:(Ц,Б,д,ƥ,\boxdot,\oplus)\to(\widetilde{Ц},Б,д,ƥ,\boxdot,\oplus)$

be a sequences of functions and ψ_i, φ_i be lacunary pointwise statistical neutrosophic convergent. Then for all $a, b \in \mathbb{R}$,

$\left((a\psi_i + b\varphi_i)(ц)\right) \overset{st(\theta)}{\to} (a\psi_i + b\varphi_i)(ц)$.

Proof: Without losing generality, let's take $a, b \neq 0$. For each $ц \in Ц$, using

$\left((\psi_i)(ц)\right) \overset{st}{\to} (\psi_i)(ц)$ and $\left((\varphi_i)(ц)\right) \overset{st(\theta)}{\to} (\varphi_i)(ц)$, we write following sets.

$$A_1 = \left\{\frac{1}{ћ_i}\left\{j \in I_i : Б\left(\psi_j(ц), \psi(ц)\right) > 1 - \varepsilon \; or \; ð\left(\psi_j(ц), \psi(ц)\right) < \varepsilon, þ\left(\psi_j(ц), \psi(ц)\right) < \varepsilon\right\}\right\},$$

$$A_2 = \left\{\frac{1}{ћ_i}\left\{j \in I_i : Б\left(\varphi_j(ц), \varphi(ц)\right) > 1 - \varepsilon \; or \; ð\left(\varphi_j(ц), \varphi(ц)\right) < \varepsilon, þ\left(\varphi_j(ц), \varphi(ц)\right) < \varepsilon\right\}\right\},$$

The density of both sets is 0, so the density of $K = A \cup B$ is also 0.

So, there exists a $j \in \mathbb{N}$: $Б\left(\psi_j(ц), \psi(ц)\right) > 1 - \varepsilon, Б\left(\varphi_j(ц), \varphi(ц)\right) > 1 - \varepsilon$;

$ð\left(\psi_j(ц), \psi(ц)\right) < \varepsilon, ð\left(\varphi_j(ц), \varphi(ц)\right) < \varepsilon$; $þ\left(\psi_j(ц), \psi(ц)\right) < \varepsilon, þ\left(\varphi_j(ц), \varphi(ц)\right) < \varepsilon$.

On the other hand,

$$L = \left\{\frac{1}{ћ_i}\left\{j \in I_i : Б\left(\left(a\psi_j + b\varphi_j\right)(ц), (a\psi + b\varphi)(ц)\right) > 1 - \varepsilon \; or \; ð\left(\left(a\psi_j + b\varphi_j\right)(ц), (a\psi + b\varphi)(ц)\right) < \varepsilon, þ\left(\left(a\psi_j + b\varphi_j\right)(ц), (a\psi + b\varphi)(ц)\right) < \varepsilon\right\}\right\}.$$

Now, we need to investigate whether $K^c \subset L$. Let we take $j \in K^c$. In this case,

$$Б\left(\psi_j(ц), \psi(ц)\right) > 1-\varepsilon, Б\left(\varphi_j(ц), \varphi(ц)\right) > 1-\varepsilon\,;$$

$$д\left(\psi_j(ц), \psi(ц)\right) < \varepsilon, д\left(\varphi_j(ц), \varphi(ц)\right) < \varepsilon; \qquad ƀ\left(\psi_j(ц), \psi(ц)\right) < \varepsilon, ƀ\left(\varphi_j(ц), \varphi(ц)\right) < \varepsilon.$$

Then,

$$Б\left((a\psi_j + b\varphi_j)(ц), (a\psi + b\varphi)(ц)\right) \geq Б\left(\psi_j(ц), \psi(ц)\right) \boxdot Б\left(\varphi_j(ц), \varphi(ц)\right) > 1-\varepsilon,$$

$$д\left((a\psi_j + b\varphi_j)(ц), (a\psi + b\varphi)(ц)\right) \leq д\left(\psi_j(ц), \psi(ц)\right) \oplus д\left(\varphi_j(ц), \varphi(ц)\right) < \varepsilon,$$

$$ƀ\left((a\psi_j + b\varphi_j)(ц), (a\psi + b\varphi)(ц)\right) \leq ƀ\left(\psi_j(ц), \psi(ц)\right) \oplus ƀ\left(\varphi_j(ц), \varphi(ц)\right) < \varepsilon.$$

So, $K^c \subset L$. Also, $L^c \subset K$ and the density of K is zero. Therefore, the density of K is zero. Then,

$$\lim_i \frac{1}{ħ_i}\left|\left\{j \in I_i : Б\left((a\psi_j + b\varphi_j)(ц), (a\psi + b\varphi)(ц)\right) > 1-\varepsilon \; or \; д\left((a\psi_j + b\varphi_j)(ц), (a\psi + b\varphi)(ц)\right) < \varepsilon, ƀ\left((a\psi_j + b\varphi_j)(ц), (a\psi + b\varphi)(ц)\right) < \varepsilon\right\}\right| = 0.$$

Thus, $\left((a\psi_i + b\varphi_i)(ц)\right) \overset{st(\theta)}{\rightarrow} (a\psi_i + b\varphi_i)(ц)$.

Lemma 3.4 Let $(Ц, Б, д, ƀ, \boxdot, \oplus)$ and $\left(\widetilde{Ц}, Б, д, ƀ, \boxdot, \oplus\right)$ be two neutrosophic normed spaces, $\psi_i : (Ц, Б, д, ƀ, \boxdot, \oplus) \to \left(\widetilde{Ц}, Б, д, ƀ, \boxdot, \oplus\right)$ be a sequences of functions. In this case, the following situations are equal.

i) $\left(\psi_i(ц)\right) \overset{st(\theta)}{\rightrightarrows} \psi(ц)$.

ii) $$\lim_i \frac{1}{ħ_i}\left|\left\{j \in I_i : Б\left(\psi_j(ц), \psi(ц)\right) < 1-\varepsilon \; or \; д\left(\psi_j(ц), \psi(ц)\right) > \varepsilon, ƀ\left(\psi_j(ц), \psi(ц)\right) > \varepsilon\right\}\right| = 0.$$

$$iii)\ \lim_i \frac{1}{\hbar_i}\left|\left\{j \in I_i : Б\left(\psi_j(ц), \psi(ц)\right) > 1-\varepsilon \ or\ д\left(\psi_j(ц), \psi(ц)\right) < \varepsilon, ƀ\left(\psi_j(ц), \psi(ц)\right) < \varepsilon\right\}\right| = 0.$$

Lemma 3.5 Let $(Ц, Б, д, ƀ, \boxdot, \oplus)$ and $(\tilde{Ц}, Б, д, ƀ, \boxdot, \oplus)$ be two neutrosophic normed spaces, $\psi_i : (Ц, Б, д, ƀ, \boxdot, \oplus) \to (\tilde{Ц}, Б, д, ƀ, \boxdot, \oplus)$ be a sequences of functions and ψ_i be lacunary pointwise statistical neutrosophic convergent. Then ψ_i is lacunary pointwise statistical neutrosophic Cauchy sequences.

Proof: Let for all $\varepsilon \in (0,1)$, $\left(\psi_i(ц)\right) \overset{st(\theta)}{\to} \psi(ц)$. In this case, if choose $\gamma > 0$ such that

$(1-\varepsilon) \boxdot (1-\varepsilon) > 1-\gamma$ and $\varepsilon \oplus \varepsilon < \gamma$. For all $ц \in Ц$, let

$$M := \left\{j \in I_i : Б\left(\psi_j(ц), \psi(ц)\right) < 1-\varepsilon \ or\ д\left(\psi_j(ц), \psi(ц)\right) > \varepsilon, ƀ\left(\psi_j(ц), \psi(ц)\right) > \varepsilon\right\},$$

$$M^c := \left\{j \in I_i : Б\left(\psi_j(ц), \psi(ц)\right) > 1-\varepsilon \ or\ д\left(\psi_j(ц), \psi(ц)\right) < \varepsilon, ƀ\left(\psi_j(ц), \psi(ц)\right) < \varepsilon\right\}.$$

Then, density of M is zero. So, density of M^c is one. Let $\ddot{j} \in M^c$. In this case,

$$Б\left(\psi_{\ddot{j}}(ц), \psi(ц)\right) > 1-\varepsilon \ or\ д\left(\psi_{\ddot{j}}(ц), \psi(ц)\right) < \varepsilon.$$

Now it must now be shown that a number $\ddot{j}$ exists such that

$$\lim_i \frac{1}{\hbar_i}\left|\left\{j \in I_i : Б\left(\psi_j(ц), \psi_{\ddot{j}}(ц)\right) < 1-\varepsilon \ or\ д\left(\psi_j(ц), \psi_{\ddot{j}}(ц)\right) > \varepsilon, ƀ\left(\psi_j(ц), \psi_{\ddot{j}}(ц)\right) > \varepsilon\right\}\right| = 0.$$

So, for all $ц \in Ц$,

$$R := \left\{j \in I_i : Б\left(\psi_j(ц), \psi_{\ddot{j}}(ц)\right) < 1-\gamma \ or\ д\left(\psi_j(ц), \psi_{\ddot{j}}(ц)\right) > \gamma, ƀ\left(\psi_j(ц), \psi_{\ddot{j}}(ц)\right) > \gamma\right\}.$$

Also it should be shown that $R \subset M$. Let assume that $R \not\subset M$. In this case, at least one j, it is an element of R but not an element of M. Then, $j \in R \setminus M$. On the other hand, we have

$$Б\left(\psi_j(ц), \psi_{j'}(ц)\right) < 1-\gamma, Б\left(\psi_j(ц), \psi(ц)\right) > 1-\varepsilon \quad \text{and}$$

$$Б\left(\psi_{j'}(ц), \psi(ц)\right) > 1-\varepsilon.$$

Then,

$$1-\gamma > Б\left(\psi_j(ц), \psi_{j'}(ц)\right) > Б\left(\psi_j(ц), \psi(ц)\right) \boxdot Б\left(\psi_{j'}(ц), \psi(ц)\right) > (1-\varepsilon) \boxdot (1-\varepsilon) > 1-\gamma,$$

this is not possible. Also, $д\left(\psi_j(ц), \psi_{j'}(ц)\right) > \gamma, д\left(\psi_j(ц), \psi(ц)\right) < \varepsilon, д\left(\psi_{j'}(ц), \psi(ц)\right) < \varepsilon.$

$$\gamma < д\left(\psi_j(ц), \psi_{j'}(ц)\right) < д\left(\psi_j(ц), \psi(ц)\right) \oplus д\left(\psi_{j'}(ц), \psi(ц)\right) < \gamma.$$

But, this is not possible. So, $R \subset M$. Then, the densities of R and M are zero. As a result, ψ_j is lacunary pointwise statistical neutrosophic Cauchy sequences.

Lemma 3.6 Let $(Ц, Б, д, ƀ, \boxdot, \oplus)$ and $\left(\widetilde{Ц}, Б, д, ƀ, \boxdot, \oplus\right)$ be two neutrosophic normed spaces, ψ_i: $(Ц, Б, д, ƀ, \boxdot, \oplus) \to \left(\widetilde{Ц}, Б, д, ƀ, \boxdot, \oplus\right)$ be a sequences of functions. If $\left(\psi_i(ц)\right)$ is lacunary uniformly neutrosophic convergent on $\left(\widetilde{Ц}, Б, д, ƀ, \boxdot, \oplus\right)$ then $\left(\psi_i(ц)\right)$ lacunary uniformly statistically neutrosophic convergent to $\psi(ц)$.

Proof: Let $\left(\psi_i(ц)\right)$ is lacunary uniformly neutrosophic convergent on $\left(\widetilde{Ц}, Б, д, ƀ, \boxdot, \oplus\right)$. Then, given $\varepsilon \in (0,1)$, there exists $i_0 \in \mathbb{N}$ such that every $ц \in Ц$ and $i \geq i_0$,

$$Б\left(\psi_j(ц), \psi(ц)\right) > 1-\varepsilon, д\left(\psi_j(ц), \psi(ц)\right) < \varepsilon, ƀ\left(\psi_j(ц), \psi(ц)\right) < \varepsilon.$$

So, for all $i < i_0$,

$$Б\left(\psi_j(ц), \psi(ц)\right) < 1-\varepsilon, д\left(\psi_j(ц), \psi(ц)\right) > \varepsilon, ƀ\left(\psi_j(ц), \psi(ц)\right) > \varepsilon$$

is ensured and the numbers of i satisfying this condition are finite. So, using that the density of the finite set is zero, we can say that the density of the complement of this set is 1. If the complement of this finite set is denoted with T, for all $\varepsilon \in (0,1)$, there exists $i_0 \in \mathbb{N}, T \subset \mathbb{N}$ and density of T is 1 such that for all ų ∈ Ц and $i \geq i_0$,

$$Б\left(\psi_j(ų), \psi(ų)\right) > 1 - \varepsilon\,, đ\left(\psi_j(ų), \psi(ų)\right) < \varepsilon, þ\left(\psi_j(ų), \psi(ų)\right) < \varepsilon.$$

Then, we have $\left(\psi_i(ų)\right) \overset{st(\theta)}{\rightrightarrows} \psi(ų)$.

Definition 3.4 Let $(Ц, Б, đ, þ, \boxdot, \oplus)$ and $\left(\widetilde{Ц}, Б, đ, þ, \boxdot, \oplus\right)$ be two neutrosophic normed spaces, $\psi_i: (Ц, Б, đ, þ, \boxdot, \oplus) \to \left(\widetilde{Ц}, Б, đ, þ, \boxdot, \oplus\right)$ be a sequences of functions. Then, ψ_i is called lacunary uniformly statistically neutrosophic Cauchy sequences in $\left(\widetilde{Ц}, Б, đ, þ, \boxdot, \oplus\right)$, if for $\varepsilon \in (0,1)$, there exists a $\bar{j}$ such that

$$\lim_i \frac{1}{ħ_i}\left|\left\{j \in I_i: Б\left(\psi_j(ų), \psi_{\bar{j}}(ų)\right) < 1 - \varepsilon \; or \; đ\left(\psi_j(ų), \psi_{\bar{j}}(ų)\right) > \varepsilon, þ\left(\psi_j(ų), \psi_{\bar{j}}(ų)\right) > \varepsilon\right\}\right| = 0.$$

Lemma 3.7 Let $(Ц, Б, đ, þ, \boxdot, \oplus)$ and $\left(\widetilde{Ц}, Б, đ, þ, \boxdot, \oplus\right)$ be two neutrosophic normed spaces, $\psi_i: (Ц, Б, đ, þ, \boxdot, \oplus) \to \left(\widetilde{Ц}, Б, đ, þ, \boxdot, \oplus\right)$ be a sequences of functions and ψ_i be lacunary uniformly statistical neutrosophic convergent. Then ψ_i is lacunary uniformly statistical neutrosophic Cauchy sequences.

Proof: Let, $\left(\psi_i(ų)\right) \overset{st(\theta)}{\rightrightarrows} \psi(ų)$. Let for all $\varepsilon \in (0,1)$, there exists positive integer $i_0 \in \mathbb{N}, T \subset \mathbb{N}$ and ų ∈ Ц and $\delta(T) = 1$such that $i \geq i_0, i \in T$,

such that

$$Б\left(\psi_j(ų), \psi(ų)\right) > 1 - \varepsilon\,, đ\left(\psi_j(ų), \psi(ų)\right) < \varepsilon, þ\left(\psi_j(ų), \psi(ų)\right) < \varepsilon.$$

If we choose $ǰ \in T, ǰ > i_0$. Then, $Б\left(\psi_j(ų), \psi(ų)\right) > 1 - \varepsilon\,, đ\left(\psi_j(ų), \psi(ų)\right) < \varepsilon$,

$þ\left(\psi_j(ų), \psi(ų)\right) < \varepsilon$. Then, if we take $ǰ$:

$$\lim_{i} \frac{1}{\hbar_i} \left| \left\{ j \in I_i : Б\left(\psi_j(ц), \psi_{j}(ц)\right) < 1 - \varepsilon \; or \; đ\left(\psi_j(ц), \psi_{j}(ц)\right) > \varepsilon, þ\left(\psi_j(ц), \psi_{j}(ц)\right) > \varepsilon \right\} \right| = 0.$$

For each $j \in T$, we get

$$Б\left(\psi_j(ц), \psi_{j}(ц)\right) > Б\left(\psi_j(ц), \psi(ц)\right) ⊡ Б\left(\psi(ц), \psi_{j}(ц)\right) > (1 - \varepsilon) ⊡ (1 - \varepsilon) = 1 - \varepsilon.$$

$$đ\left(\psi_j(ц), \psi_{j}(ц)\right) < đ\left(\psi_j(ц), \psi(ц)\right) ⊕ đ\left(\psi(ц), \psi_{j}(ц)\right) < \varepsilon.$$

Also, if we use $\delta(T) = 1$, ψ_i is lacunary uniformly statistical neutrosophic Cauchy sequences.

RESULTS

By using the neutrosophic version of the studies on intuitionistic normed spaces and lacunary sequences logic together, some important findings have been obtained for function sequences. A comparison was made with some concepts existing in the literature. It is planned to carry out such studies in neutrosophic normed spaces using different convergence types in the coming days.

REFERENCES

Aktuğlu, H., & Gezer, H. (2009). Lacunary equi-statistical convergence of positive linear operators. *Open Mathematics*, 7 (3), 558-567.

Atanassov, K. T. (1983). Intuitionistic fuzzy sets, VII ITKR's Session, Sofia deposed in Central Sci. *Technical Library of Bulg. Acad. of Sci*, *1697*, 84.

Aytar, S. (2008). Rough statistical convergence. *Numerical functional analysis and optimization*, *29*(3-4), 291-303.

Bilgin, N. G., & Bozma, G. (2020). On Fuzzy n-Normed Spaces Lacunary Statistical Convergence of Order alpha. *i-Manager's Journal on Mathematics*, 9ν(2), 1.

Bilgin, N. G., &Bozma, G. (2021). Fibonacci lacunary statistical convergence of order γ in IFNLS. *International Journal of Advances in Applied Mathematics and Mechanics*, 8 (4), 28-36.

Bilgin, N. G. (2022). Rough Statistical Convergence In Neutrosophic Normed Spaces. *Euroasia Journal of Mathematics, Engineering, Natural & Medical Sciences*, 9 (21), 47-55. doi:10.38065/euroasiaorg.958

Bilgin, N. G. (2023a). Arithmetic statistically convergent on neutrosophic normed spaces. *Gümüşhane Üniversitesi Fen Bilimleri Dergisi*, 13 (2), 270-280.

Bilgin, N. G. (2023b). Hilbert I-Statistical Convergence on Neutrosophic Normed Spaces. *Gazi University Journal of Science Part A: Engineering and Innovation*, 10 (1), 1-8.

Connor, J., (1988). The statistical and strong p-Ces‡ro sonvergence of sequences. *Analysis*, 8, 47-63.

Dundar, E., & Çakan, C. (2014). Rough I-convergence. *Demonstratio Mathematica*, 47 (3), 638-651.

Fast, H., (1951). Sur la convergence statistique, *Colloq. Math.*, 2, 241-244.

Fridy, J. A., &Miller, H. I. (1991). A matrix characterization of statistical convergence. *Analysis*, 11 (1), 59-66.

Fridy, J.A., &Orhan, C. (1993). Lacunary statistical convergence, *Pacific J. Math.*, 160 (1), 43-51.

Fridy, J.A., (1985). On statistical convergence, *Analysis*, 5, 301-313.

Gonul, N. (2013). Lacunary A-convergence. *Karaelmas Fen ve Mühendislik Dergisi*, 3 (1), 17-20.

Gonul Bilgin, N. (2022). Hibrid Δ-Statistical Convergence for Neutrosophic Normed Space. *Journal of Mathematics*, 2022, 3890308. doi:10.1155/2022/3890308

Gonul Bilgin, N., Pamučar, D., & Riaz, M. (2022). Fermatean neutrosophic topological spaces and an application of neutrosophic kano method. *Symmetry*, 14 (11), 2442.

Karakus, S., & Demirci, K. (2008). Statistical Convergence of Double Sequences on Intuitionistic Fuzzy Normed Spaces. *Journal of Computational Analysis & Applications*, *10*(1).

Khan, V. A., Khan, M. D., & Ahmad, M. (2021). Some new type of lacunary statistically convergent sequences in neutrosophic normed space. *Neutrosophic Sets and Systems*, 42 (1), 15.

Khan, V. A., Rahaman, S. K., Hazarika, B., & Alam, M. (2023). Rough lacunary statistical convergence in neutrosophic normed spaces. *Journal of Intelligent & Fuzzy Systems*, (Preprint), 1-17.

Kirisci M., & Simsek, N. (2020). Neutrosophic normed spaces and statistical convergence, *Journal of Analysis*, 28 (4), 1059-1073. doi:10.1007/s41478-020-00234-0

Kirişci, M., & Şimşek, N. (2020). Neutrosophic metric spaces. *Mathematical Sciences*, 14 (3), 241-248.

Kisi, O. (2021a). On Iθ-convergence in Neutrosophic Normed Spaces. *Fundamental Journal of Mathematics and Applications*, *4*(2), 67-76.

Kisi, O. (2021b). Ideal convergence of sequences in neutrosophic normed spaces. *Journal of Intelligent & Fuzzy Systems*, 41 (2), 2581-2590. doi:10.3233/JIFS-201568

Salt, T. (1980). On statistically convergent sequences of real numbers, *Math. Slovaca*, 30, 139-150.

Smarandache, F. (1999). A unifying field in Logics: Neutrosophic Logic. In *Philosophy* (pp. 1-141). American Research Press.

Sözbir, B., Altundağ, S., & Basarır, M. (2020). On The (Delta, F)-Lacunary Statistical Convergence Of The Functions. *Maltepe Journal Of Mathematics*, 2 (1), 1-8.

Steinhaus, H. (1951). Sur la convergence ordinaire et la convergence asymtotique, *Colloq. Math.*, 2, 73-74.

Karakaya, V., Simsek, N., Gürsoy, F., & Ertürk, M. (2014). Lacunary statistical convergence of sequences of functions in intuitionistic fuzzy normed space. *Journal of Intelligent & Fuzzy Systems*, 26 (3), 1289-1299.

Zadeh, L. A. (1965). Fuzzy sets. *Information and control*, 8 (3), 338-353.

CHAPTER 6

FIRST INVESTIGATION OF A W UMa TYPE ECLIPSING BINARY IN THE SUPERWASP ARCHIVE: NSVS 6283621

Burcu ÖZKARDEŞ[1]
Seda KAPTAN[2]

1 Doç. Dr. Burcu ÖZKARDEŞ, Department of Space Sciences and Technolo-gies, Faculty of Science, Çanakkale Onsekiz Mart University, Terzioğlu Kampüsü, TR-17020, Çanakkale, Türkiye. ORCID ID: 0000-0002-6764-9299
2 Seda KAPTAN, İstanbul University, Institute of Graduate Studies in Science, Programme of Astronomy and Space Science, 34116, Beyazıt, İstanbul, Türkiye. ORCID ID: 0000-0003-0873-0983

1. INTRODUCTION

Contact binary stars with late spectral type, that is, W UMa type binary systems, are a natural laboratory in terms of shedding light on some physical events that are not understood in astrophysics, such as the proximity effect, the matter transfer/loss, the chromospheric activity, and the stellar evolutionary. In this study, we focus on the photometric investigation of the eclipsing binary NSVS 6283621. Within the scope of this study, we aimed to obtain fundamental information about the nature of the system by analyzing SuperWASP[1] (hereafter WASP) data, for the first time.

NSVS 6283621 is the photometrically neglected binary star. Hoffmann et al. (2009) identified 4659 variable objects in NSVS survey. In their study, the variability classification for the system is given as W UMa. Also, the period of the system, J-H, H-K, K mag. and amplitude variation in magnitude are given as 0.39178 days, 0.334, 0.069, 11.408 and 0.598, respectively. Drake et al. (2014) presented the Catalina Surveys Periodic Variable Star Catalog (CRTS) containing approximately 47000 periodic variables. They gave the values of the orbital period and amplitude of the eclipsing binary as 0.3917660 days and 0.55 mag., respectively, and classified the system as EW. The first data catalog of variable stars qualified by the ATLAS (Asteroid Terrestial-impact Last Alert System) operations was presented by Heinze et al. (2018). The authors classified NSVS 6283621 as CBF (Close binary, full period).

The equatorial coordinates (α, δ), *V* mag., TIC No (Stassun et al., 2018; Stassun et al., 2019) and GAIA parallax (π) (Gaia Collaboration, 2022) of the eclipsing binary star according to the SIMBAD[2] database are given in Table 1.

[1] https://wasp.cerit-sc.cz/form
[2] https://simbad.u-strasbg.fr/simbad/

Table 1

Basic Information of NSVS 6283621 Based on SIMBAD Database

Star Name	**α (h:m:s)**	**δ (°:′:″)**	**TIC No**	***V* (mag.)**	**π (mas)**
NSVS 6283621	23:59:53	+29:06:38	407306748	13.10	1.4193

2. MINIMA TIMES AND NEW LIGHT ELEMENTS

There are no minimum light times of the neglected binary in the literature. Only the system's T_0 (2458328.9361) and P (0.3917628 days) are given in The International Variable Star Index (VSX)[3]. In this work, we obtained 5 primary minima times (Min I) and 5 secondary minima times (Min II) from WASP *V* light curve. These eclipsing times (HJD) are listed in Table 2.

Table 2

Eclipsing Times of NSVS 6283621

HJD (+2400000)	**Error**	**Min. Type**	**HJD (+2400000)**	**Error**	**Min. Type**	**Ref.**
53944.6873	0.0005	I	53943.7111	0.0005	II	1
53950.5618	0.0007	I	53945.6679	0.0013	II	1
53973.6766	0.0005	I	54003.6495	0.0007	II	1
54003.4514	0.0005	I	54064.3716	0.0013	II	1
54074.3602	0.0004	I	54075.3449	0.0013	II	1
58328.9361	--	I	--	--	--	2

(1) This study, (2) VSX database

Using all minimum light times the *O-C* diagram has been created to study the period variation of the eclipsing binary NSVS 6283621. Figure 1 shows the *O-C* diagram of the system.

[3] https://www.aavso.org/vsx/index.php?view=search.top

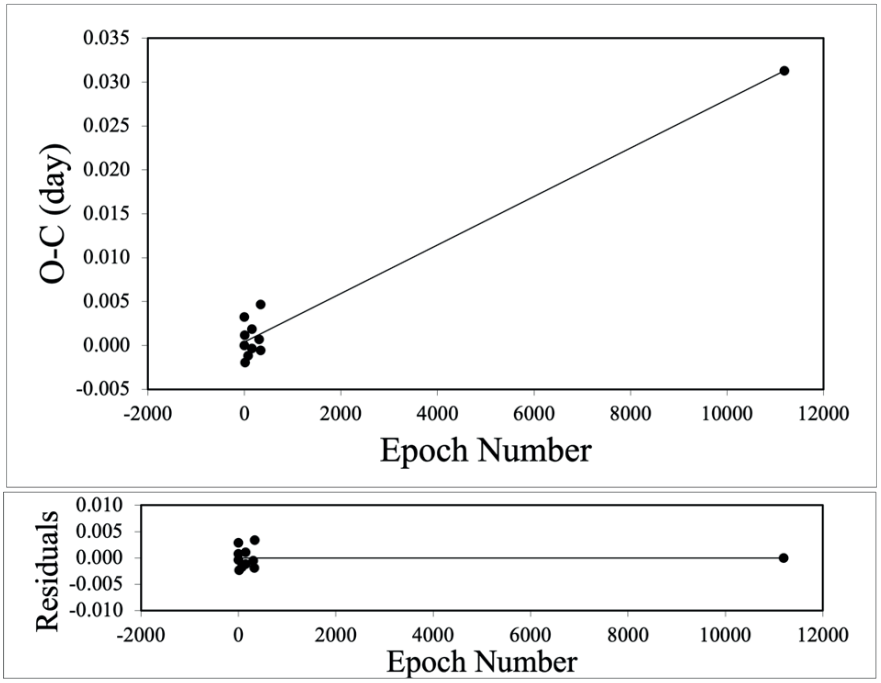

Figure 1. *O-C* diagram for NSVS 6283621 (top panel) and residuals (bottom panel)

Figure 1 clearly shows that there is no change in the orbital period of the system. We corrected the light elements by applying the linear regression fit to *O-C* values. Linear ephemerides (T_0 and P) are given in below. The WASP *V* light curve was phased using these elements (see Figure 3).

$$\text{Min. I} = \text{HJD } 2453944.6877(6)+0^{d}.3917656(2)\times E. \quad (1)$$

3. LIGHT CURVE SOLUTION

The phase folded *V* light curve was modelled with the Wilson-Devinney (W-D) method (Wilson & Devinney, 1971). The MC algorithm (Kreiner et al., 2003) was used in spite of DC code of W-D.

Following Eker et al. (2009), the $(B\text{-}V)_0$'s value was calculated to be 0.605. According to this values the primary component's temperature was determined as 5916±200 K using the calibration table of the empirical main sequence given by Budding and Demircan (2007), and kept constant in the analysis. g_{12} and A_{12} were fixed at 0.32 and 0.5, respectively (Lucy, 1967; Rucinski, 1969). Claret and Bloemen (2011) and Claret et al. (2013)'s calibration tables were used for limb-darkening coefficients' values by adopting the square-root limb-darkening law. It was assumed that the components were rotated synchronously and the shape of the system's orbit was circular. The light contribution of the third component (l_3) was adopted to be zero.

The adjustible parameters in the search were q (mass ratio), i (orbital inclination), φ (phase-shift), T_2 (the secondary component's temperature), $\Omega_1=\Omega_2$ (non-dimensional surface potential parameters of components), L_1 (the primary's luminosity).

The system's light curve shows the O'Connell effect, that is, the difference between the maximum light levels (see Figure 3). The spot model was applied in the MC solution. A cold spot on the surface of the massive component star was assumed. The spot parameters (ϕ: colatitude of spot, λ: longitude of spot, θ: angular radius of spot and temperature factor of spot) were adjusted during the iterations.

The spectroscopic mass ratio of the system has not been in the literature. The q-search method was used to detect a suitable mass ratio for an interval of values from zero to 2. While the minimum chi-square value was obtained at q=0.6 for $0<q<1$ the minimum chi-square value was obtained at q=1.6 for $1<q<2$ (see Figure 2). Therefore, the two solutions, $q<1$ (A type) and $q>1$ (W type), were performed in the MC search. Due to the χ^2 value obtained for $q<1$ being smaller than that obtained for $q>1$, the results of the A type model have been accepted to be the final solution. The final MC solution parameters are listed in Table 3. The best theoretical fit derived from the MC solution are compared with the WASP light curve in Figure 3. The location of the spot and the Roche geometry of the system are shown in Figure 4.

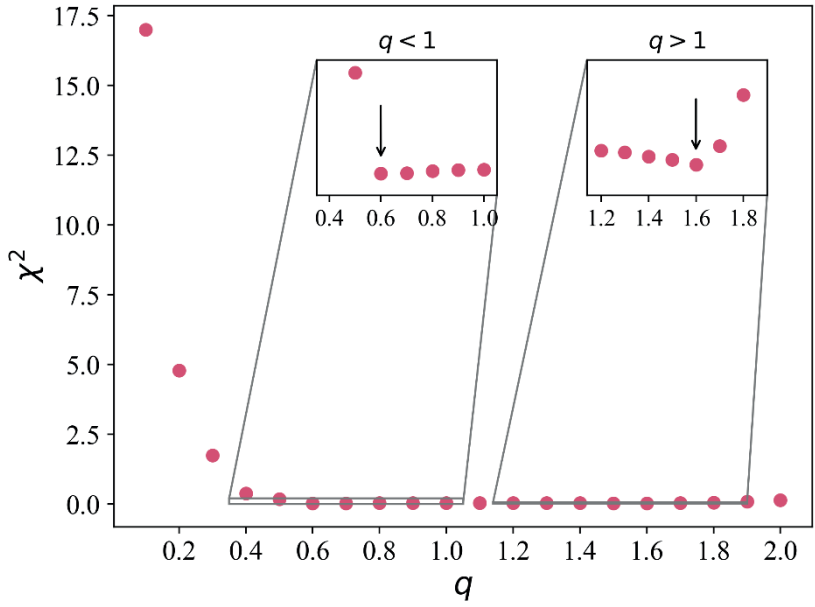

Figure 2. q-search diagram for NSVS 6283621.

Table 3

The MC Solution Parameters of NSVS 6283621

Parameters	**Value**	**Error**	**Parameters**	**Value**	**Error**
i (°)	78.8	0.2	q (M_2/M_1)	0.5645	0.0131
Phase shift (φ)	0.0009	0.0008	$\Omega_1 = \Omega_2$	2.9750	0.0241
T_1 (K)	5916	Fixed	r_1 (mean)	0.43	0.01
T_2 (K)	5799	50	r_2 (mean)	0.33	0.01
Fill out (%)	7	-	L_1/L_{total} (*V*)	0.61	0.01
Spot parameters					
ϕ (°)	15.2	0.9			
λ (°)	134.6	1.4			
θ (°)	27.7	1.5			
Temperature factor	0.707	0.071			
$\Sigma(O\text{-}C)^2$ (*V*)	4.739				

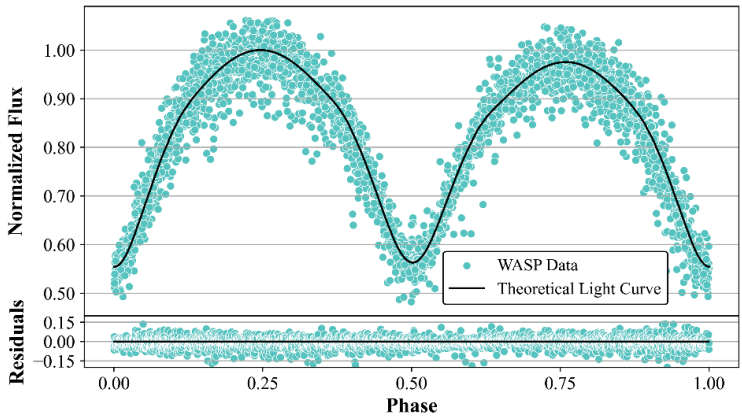

Figure 3. Top panel: Comparison between the WASP *V* light curve and the theoretical (solid line) light curve of NSVS 6283621; Lower panel: The residuals of the MC model fitting.

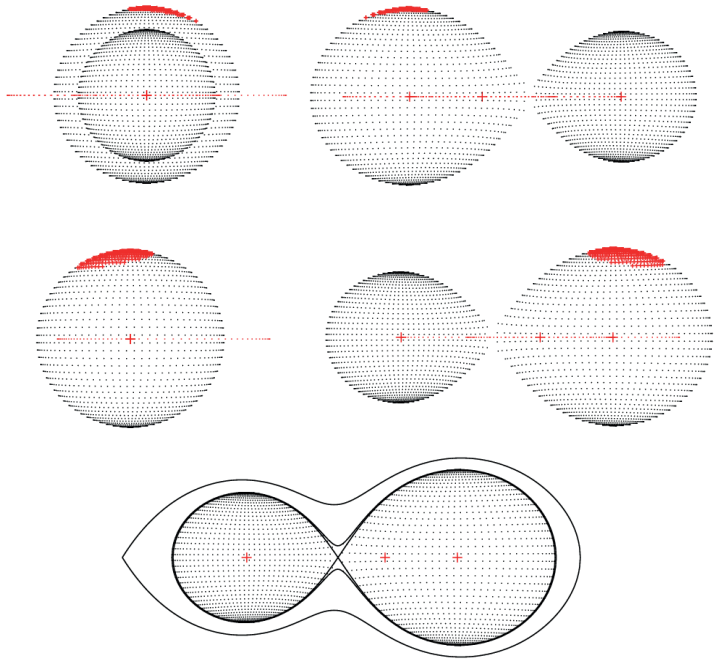

Figure 4. 3D-Roche geometry of the system and the spot location are shown at phases 0.0, 0.25, 0.5 and 0.75, respectively, from the upper left corner to the lower right corner. Bottom panel shows 2D-surface geometry of the system.

4. RESULTS

4.1. ESTIMATED ABSOLUTE PARAMETERS

Since there are no spectroscopic observations of the system, its absolute parameters were estimated. The mass of the primary was assumed to be 1.01±0.03 $M_\odot$, which corresponds to its temperature, using the calibration table of the empirical MS stars (Budding & Demircan, 2007). By means of the mass ratio, the mass of the secondary was determined as 0.57±0.03 $M_\odot$. The semi-major axis of the binary orbit was calculated as 2.62±0.01 $R_\odot$ using the Keplerian orbital equation. The radii of the components were calculated by the equation (2).

$$r_i = \frac{R_i}{a} \tag{2}$$

The surface gravity values and bolometric magnitudes of the component stars were calculated using Pecaut and Mamajek (2013)'s the values for the sun. In Table 4 the absolute parameters (mass, radius, luminocity) are listed. The distance of the system was calculated to be 712±46 pc considering the interstellar reddening (A_V = 0.138; E(*B*-*V*) = 0.045). The parallax of the system is given by Gaia DR3 (Gaia Collaboration, 2022) as 1.4193±0.0234 mas (=705±12 pc). Accordingly, it seems that the distance determined in this study is close to that of Gaia DR3.

Table 4

Absolute Parameters of The Eclipsing Binary NSVS 6283621

Parameters	Value	Error
a ($R_\odot$)	2.62	0.01
M_1 ($M_\odot$)	1.01	0.03
M_2 ($M_\odot$)	0.57	0.03
R_1 ($R_\odot$)	1.14	0.03
R_2 ($R_\odot$)	0.87	0.03
L_1 ($L_\odot$)	1.44	0.21
L_2 ($L_\odot$)	0.77	0.12

log g_1 (cgs)	4.33	0.03
log g_2 (cgs)	4.31	0.01
d (pc)	712	46

4.2. EVOLUTIONARY STATE

The positions of the components of NSVS 6283621 are plotted in the log (T_{eff}) – log ($L/L_{\odot}$) plane (see Figure 5). The theoretical lines of ZAMS, TAMS and the evolutionary tracks given by Girardi et al. (2000) for Z=0.019 were used. The A-subtype components shown in the diagram were taken from Latkovic et al. (2021) and Özkardeş and Kaptan (2022). While the secondary is located close to the ZAMS, the primary is located within the main-sequence band. The locations of the system components appear to be compatible with the archival A-subtype ones. Also, the evolutionary isochrones from Girardi et al. (2000) were used to estimate the age of the system, and the best fit was found at the age of 5.012 Gyr.

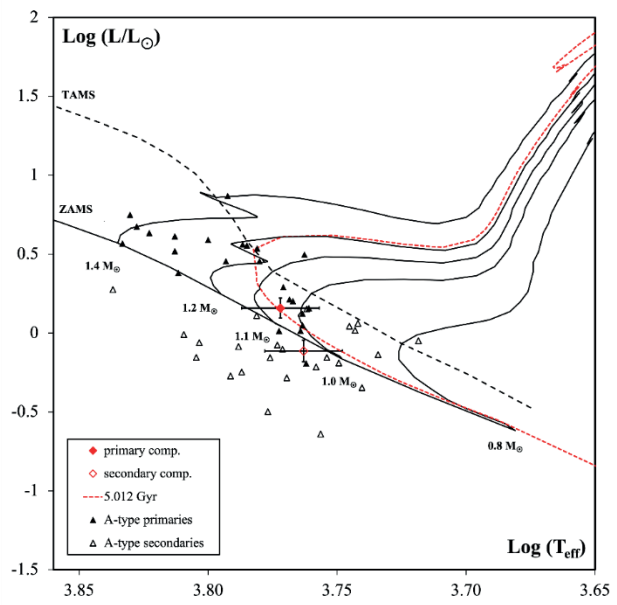

Figure 5. Position of the components of the eclipsing binary NSVS 6283621 in the log (T_{eff}) – log ($L/L_{\odot}$) diagram.

5. CONCLUSION

The eclipsing binary NSVS 6283621 was examined photometrically in this study for the first time. The photometric solution defined the binary star NSVS 6283621 as a new A sub-type shallow contact system ($f < 20\%$ (Liao et al. 2021)) with a fill-out parameter of $f = 7\%$. Investigating NSVS 6283621 and similar shallow contact binaries in detail play an important role in understanding the evolutionary states and structures of the contact binary systems. For this, multi-color photometric light curves, spectroscopic observations and the eclipsing times of the system are needed.

Acknowledgements: "This work was supported by Çanakkale Onsekiz Mart University The Scientific Research Coordination Unit, Project number: FBA-2019-2930".

REFERENCES

1. Budding, E. and Demircan, O. (2007). Introduction to Astronomical Photometry, second ed. Cambridge University Press.

2. Claret, A., Bloemen, S. (2011). Gravity and limb-darkening coefficients for the Kepler, CoRoT, Spitzer, uvby, UBVRIJHK, and Sloan photometric systems. *Astronomy and Astrophysics*, 529, 75, DOI: 10.1051/0004-6361/201116451.

3. Claret, A., Hauschildt, P.H., & Witte, S. (2013). New limb-darkening coefficients for Phoenix/1d model atmospheres. II. Calculations for 5000 K Teff 10 000 K Kepler, CoRot, Spitzer, uvby, UBVRIJHK, Sloan, and 2MASS photometric systems. *Astronomy and Astrophysics*, 552, 16, DOI: 10.1051/0004-6361/201220942.

4. Drake, A. J., Graham, M. J., & Djorgovski, S. G. et al. (2014). The Catalina Surveys Periodic Variable Star Catalog. *The Astronomical Journal Supplement Series* , 213(1), 9, 29 pp.

5. Eker, Z., Bilir, S., Yaz, E., Demircan, O., & Helvacı, M. (2009). New absolute magnitude calibrations for W Ursa Majoris type binaries. *Astronomische Nachrichten*, 330(1), 68.

6. Gaia Collaboration, (2022). VizieR Online Data Catalog: Gaia DR3 Part 1. Main source. VizieR On-line Data Catalog: I/355, DOI: 10.26093/cds/vizier.1355.

7. Girardi, L., Bressan, A., Bertelli, G., & Chiosi, C. (2000). Evolutionary tracks and isochrones for low- and intermediate-mass stars: From 0.15 to 7 Msun, and from Z=0.0004 to 0.03. *Astronomy and Astrophysics Supplement*, 141, 371-383.

8. Heinz, A. N., Tonry, J. L., & Denneau, L. et al. (2018). A First Catalog of Variable Stars Measured by the Asteroid Terrestrial-impact Last Alert System (ATLAS). *The Astronomical Journal*, 156(5), 241, 49 pp.

9. Hoffman, D. I., Harrison, T. E., & McNamara, B. J. (2009). Automated Variable Star Classification Using the Northern Sky Variability Survey. *The Astronomical Journal*, 138(2), 466-477.

10. Kreiner, J. M., Rucinski S. M., Zola S., Niarchos P., Ogloza W., Stachowski G., Baran A., Gazeas K., Drozdz M., Zakrzewski, B., Pokrzywka B., Kjurkchieva D. and Marchev D. (2003). Physical Parameters Of Components In Close Binary Systems. I. *Astronomy and Astrophysics*, 412: 465-471.

11. Latkovic, O., Ceki, A., & Lazarevic, S. (2021). Statistics of 700 Individually Studied W UMa Stars. *The Astrophysical Journal Supplement Series*, 254(1), id.10, 18 pp.

12. Liao, W-ping, Li, Lin-Jia, Zhou, X., Wang, Q-Shan. (2021). The First Photometric Investigations of The G-Type Shallow Contact Binary. Research in Astronomy and Astrophysics, 21, 2, 41-49 p.

13. Lucy, L. B. (1967). Gravity-Darkening for Stars with Convective Envelopes. *Zeitschrift für Astrophysik*, 65, p.89.

14. Özkardeş, B. and Kaptan, S. (2022). V1095 Her: TESS görüş alanındaki olası üçüncü bileşenli değen çift yıldız. A. Dayangaç, H. Akgül and M. Sevindik (Ed.), Fen Bilimleri & Matematikte Araştırma ve Değerlendirmeler (p. 1-19). Ankara: Gece Publishing.

15. Pecaut, M. J. and Mamajek, E. E. (2013). Intrinsic Colors, Temperatures, and Bolometric Corrections of Pre-main-sequence Stars. *The Astrophysical Journal Supplement*, 208(1), id. 9, 22 pp.

16. Rucinski, S. M. (1969). The Proximity Effects in Close Binary Systems. II. The Bolometric Reflection Effect for Stars with Deep Convective Envelopes. *Acta Astronomica*, 19, p. 245.

17. Stassun, K. G., Oelkers, R. J., Pepper, J., Paergert, M. et al. (2018). The TESS Input Catalog and Candidate Target List. *The Astronomical Journal*, 156(3), id. 102, 1-39.

18. Stassun, K. G., Oelkers, R. J., Pepper, J., Paergert, M. et al. (2019). The Revised TESS Input Catalog and Candidate Target List. *The Astronomical Journal*, 158(4), id. 138, 1-21.

19. Wilson, R. E. and Devinney, E. J. (1971). Realization of Accurate Close-Binary Light Curves: Application to MR Cygni. *Astrophysical Journal*, 166, 605-619.

CHAPTER 7

COUMARIN DERIVATIVES SYNTHESIZED AGAINST ALZHEIMER'S DISEASE IN 2023

Hülya Çelik ONAR[1]

1 Assoc.Prof. Hülya ÇELİK ONAR İstanbul University-Cerrahpaşa, Engineering Faculty, Chemistry Department, Organic Chemistry Devision Avcılar, İstanbul, Turkey ORCID: 0000-0003-2573-5751

Major depressive disorder (MDD) and other mental health issues affect millions of individuals worldwide. In 2019 (before to the pandemic), there were over 970 million cases of mental disorders worldwide, with 28.9% of cases being depressive disorders. Due to the drawbacks of current antidepressant medications, which include high cost, poor performance, safety concerns, delayed onset, adverse effects, and long-term consequences, scientists are now investigating natural products, such as plants [1-4].

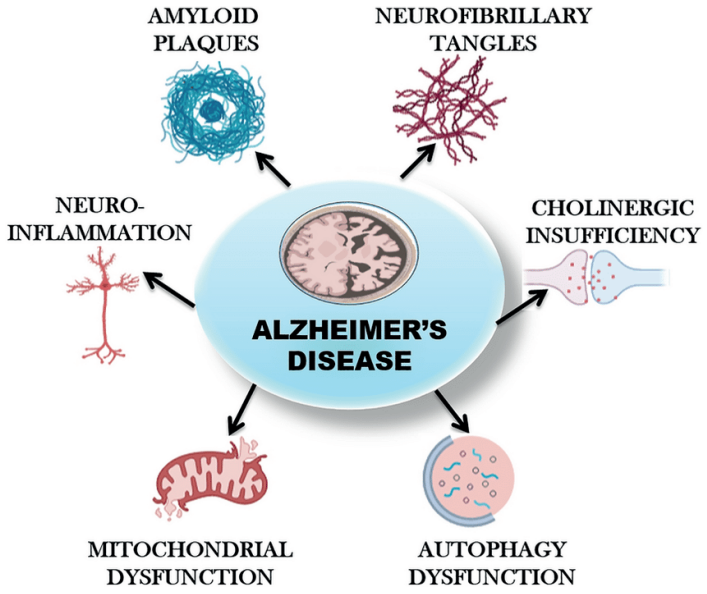

Sixty to seventy percent of dementia cases are caused by Alzheimer's disease, a brain disease that often begins slowly and gets worse over time [5]. Alzheimer's disease is typified by alterations that result in the buildup of specific proteins in the brain. It is primarily linked to the formation of amyloid plaques, neurofibrillary tangles, and the loss of neural connections within the brain. In the end, it results in brain cell death and shrinkage. Memory loss related to recent events is the most prevalent early symptom [6]. As the illness worsens, linguistic difficulties, mood fluctuations, motivation loss, self-neglect, and behavioral problems can all be signs. Disorientation can also involve difficulty getting lost easily. A person often withdraws from family and community as their health worsens. Body functions gradually decline and eventually end in death [7].

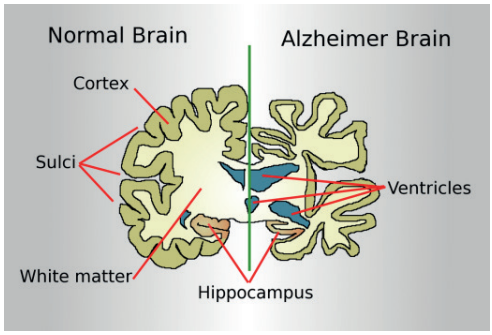

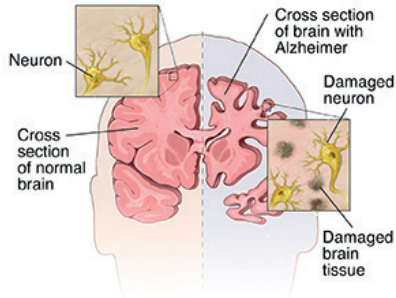

Based on approximations, AD impacts 13% of persons above 65 and 45% of adults over 85 [8]. Globally, there are already about 50 million Alzheimer's sufferers; and by 2050, that figure is expected to triple [9]. Most Alzheimer's cases still have an unidentified cause[10]. A number of rival theories endeavor to elucidate the fundamental reason; the most widely accepted theory is the amyloid beta (Aβ) hypothesis. According to the tau theory, aberrant tau protein starts the illness cascade [10]. According to this concept, hyperphosphorylated tau starts to form paired helical filaments with other tau threads. They eventually create neurofibrillary tangles within the cell bodies of nerves [11]. This results in the disintegration of the microtubules, which breaks down the cytoskeleton of the cell and collapses the transport system of the neuron. The cholinergic hypothesis, which contends that decreased synthesis of the neurotransmitter acetylcholine is the cause of Alzheimer's disease, is the oldest and the foundation for the majority of pharmacological treatments.

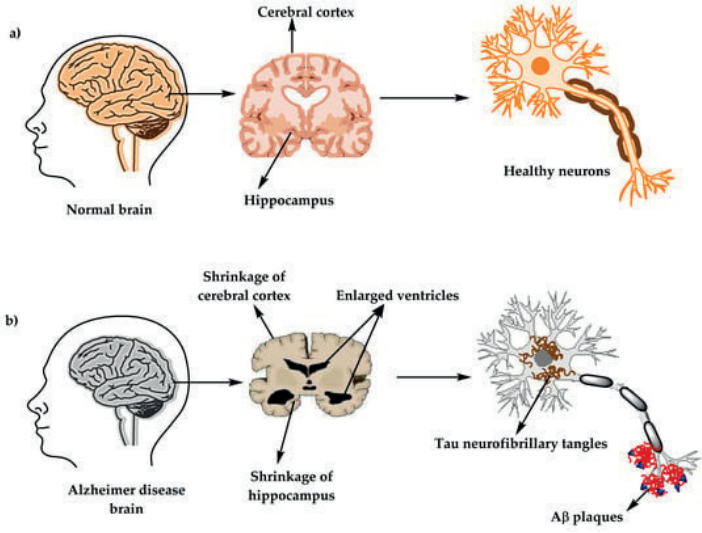

Four primary drugs have FDA approval in the United States for the treatment of AD: memantine is an NMDA glutamate receptor antagonist, and rivastigmine, galantamine, and donepezil are AChE inhibitors. Tacrine was outlawed despite having been permitted in the past because of its many negative effects [12].

Scientists are constantly researching to produce new active compounds [13-17]. Coumarin compounds are among the most important of these compounds. Coumarins are a class of heterocyclic compounds consisting of a benzene ring and a pyrone ring. Coumarin and its derivatives have numerous biological activities [18-23]. Many activities of coumarin compounds synthesized by our team have also been proven [24-26]. The effectiveness of coumarin and its derivatives on mental health has been proven in previous studies [4, 27, 28]. One of the reasons why coumarins have been studied so much is that they have many substituted centers in their structures.

New compounds of coumarin acetohydrazide (4a-d) were synthesized in this study. The capacity of the recently created substances to inhibit acetylcholinesterase (AChE) was examined and compound 4c in particular shown a promising inhibitory action with an IC50 value of 0.802 mM when compared to the reference medication donepezil [29].

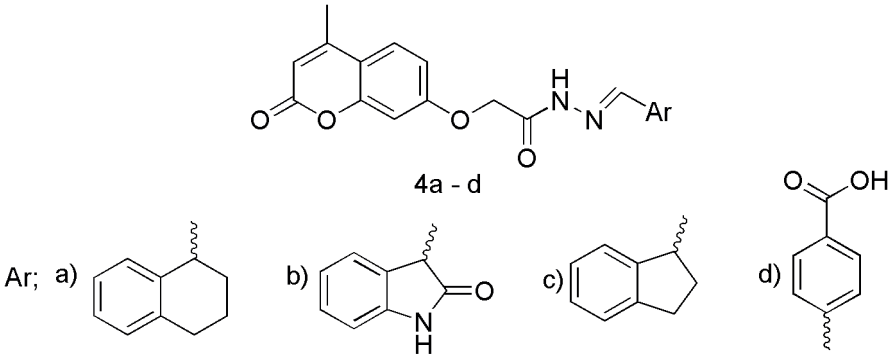

In this study, four purchased coumarin derivatives and four previously isolated from a medicinal plant by in vitro methods were used. AChE activity screening and comparison were performed. It has been stated that the most potent AChE inhibitor is thunberginol C [18].

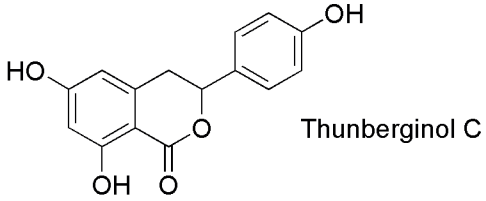

Novel ChE inhibitors, fused coumarin dihydropyridines (6a-m), were produced in a different investigation. The most promising derivatives against AChE and BChE were compounds 6b, 6f, and 6i, according to the results of in vitro analyses [30].

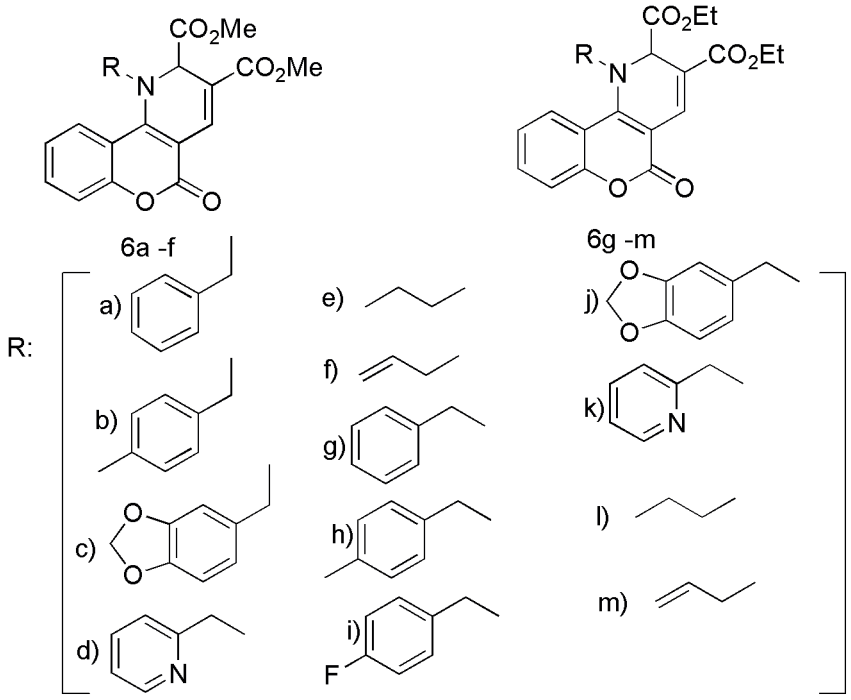

Well-characterized CouS-1 and CouS-4 were employed in a different investigation to image and block Aβ in Alzheimer's patients. According to the findings, CouS-1 and CouS-4 have a few benefits, including their excellent selectivity, strong binding affinities, good biocompatibility, and capacity to penetrate the blood-brain barrier [31].

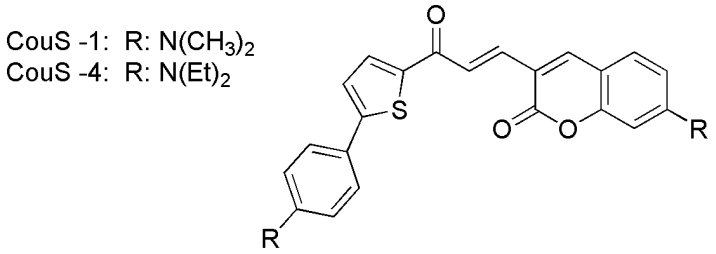

A novel fluorescent probe (XCYC-3) was found in another investigation. It was highlighted that XCYC-3 exhibited good blood-brain barrier permeability and displayed a greater fluorescence rise for aggregated Aβ than monomeric

Aβ. According to the findings, XCYC-3 is a potential agent for fluorescence imaging of Aβ [32].

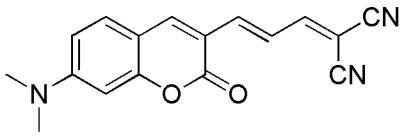

XCYC -3

Compounds (1-3) that were synthesized for the first time in this study were tested for their anti-AD properties both in vitro and in silico. They exhibited good inhibitory activities on Aβ aggregation and acetylcholinesterase (AChE), with compound 1 had the highest AChE inhibitory effect (AChE IC50=11.15 μM) [33].

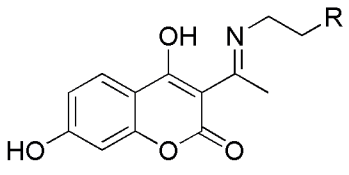

1 -3

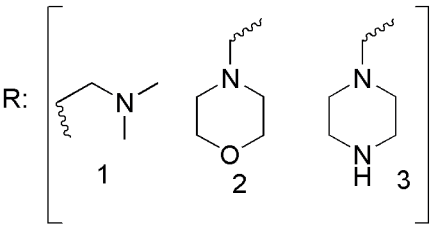

Alzheimer hastalığının (AD) tedavisine yönelik bir dizi yeni Schiff bazı-kumarin hibriti sentezlendi. Bu hibritlerin asetilkolinesteraz (AChE) inhibitör etkileri araştırıldı. Hepsi AChE'ye karşı mükemmel inhibitör aktivite sergiledi.Özellikle 13c ve 13d (IC50 değerleri sırasıyla 0,232 ± 0,011 ve 0,190 ± 0,004 μM) en güçlü aktiviteyi gösterdiler (Referans ilaç Galantamine IC50: 1,142 ± 0,027 μM) [34].

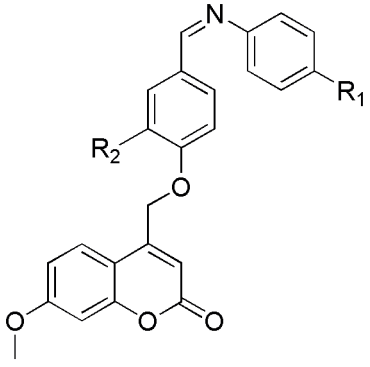

13a - f

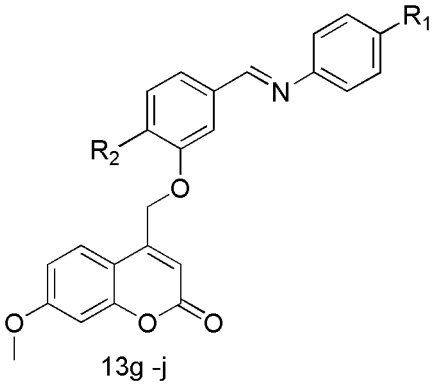

13g -j

	13a	13b	13c	13d	13e	13f	13g	13h	13i	13j
R_1	H	OCH_3	Cl	Cl	H	OCH_3	OCH_3	OCH_3	Cl	Cl
R_2	H	H	H	OCH_3	OCH_3	OCH_3	H	OCH_3	OCH_3	H

A number of coumarin-triazole hybrids were created for this investigation. It was reported that 10b (IC50 of 2.57, 3.26, and 10.65 μM, respectively) was the most active molecule in the inhibition of β-secretase-1 (BACE-1), butyrylcholinesterase (BChE), and acetylcholinesterase (AChE) [35].

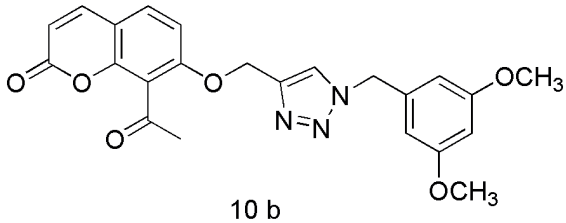

10 b

Excellent yields of a number of novel coumarin-based phosphorothioates were produced, and the new compounds' cholinesterase inhibitory properties were assessed. 7a was found to be the most effective molecule (anti-AChE activity; IC50 = 0.73 μg/ml) according to the results of the structure-activity relationship investigation [36].

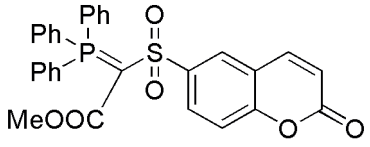

7 a

A total of fourteen novel chalcone-coumarin derivatives (8a-n) were synthesized, and examined by the Ellman method to determine whether the produced compounds might suppress the activity of acetylcholinesterase (AChE). AChE inhibition was seen in all substances tested; the IC50 values ranged from 0.201 ± 0.008 to 1.047 ± 0.043 μM. Compared to other members of the series, 8d demonstrated comparatively superior potency with an IC value of 0.201 ± 0.008 μM. Hybrid 8d has a chloro substitution on the B ring of the chalcone scaffold. The IC50 of galantamine, the reference medication, was 1.142 ± 0.027 μM [37].

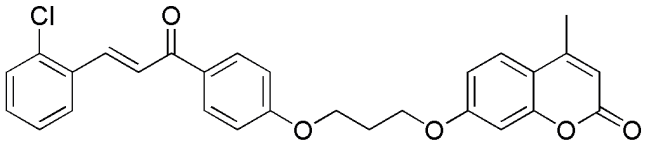

8 d

In a different work, the tris(bipyridine)ruthenium(II) complex was combined with the coumarin derivative using a formaldehyde-sensitive preservative to create a luminescence probe (Ru-COU). Ratiometric luminescence imaging of formaldehyde and Alzheimer disease brain slices in vivo is made possible by the probe [38].

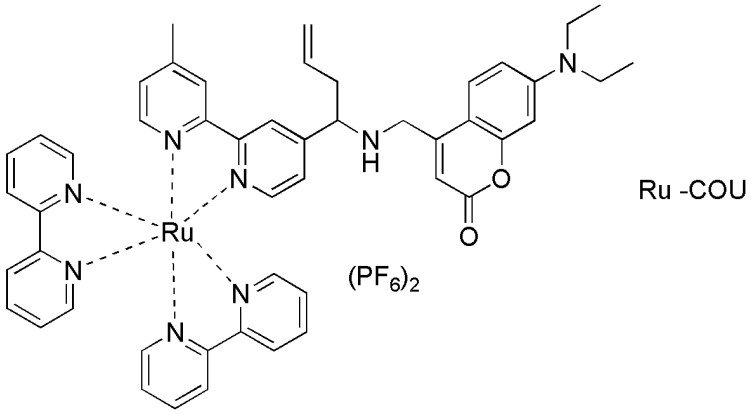

Ru -COU

This work involved the synthesis of 12 coumarin-chalcone derivatives, all of which showed potent inhibition of acetylcholinesterase. The range of Ki values for acetylcholinesterase was 2.39 ± 0.97–9.35 ± 3.95 nM, while the values for tacrine were 13.78 ± 4.36 nM [39].

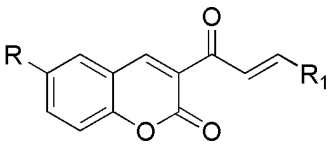

7 a -7 l

	R	R_1
7a	H	Phenyl
7b	H	4-Nitrophenyl
7c	H	4-Dimethylaminophenyl
7d	H	2-Furyl

7e	H	3-Bromphenyl
7f	H	2-Methylphenyl
7g	$C_6H_5N{=}N$	Phenyl
7h	$C_6H_5N{=}N$	4-Dimethylaminophenyl
7i	$C_6H_5N{=}N$	3-Bromphenyl
7j	$C_6H_5N{=}N$	5-[2-(4-amidophenyl)diazenyl] salicylaldehyde
7k	$H_2NCOC_6H_4N{=}N$	4-Nitrophenyl
7l	$H_2NCOC_6H_4N{=}N$	4-Dimethylaminophenyl

Three naturally occurring coumarins (1-3) that had previously been separated from Murraya paniculata leaves were examined in this study in relation to the cholinesterase enzymes AChE and BChE. Compound 1 was shown to be inert against both AChE and BChE, while compounds 2 and 3 were found to be strong inhibitors of both enzymes [40].

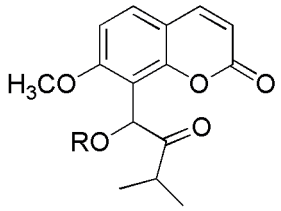

2: R=H
3: $R{=}COCH_2CH(CH_3)_2$

Based on coumarin and benzotriazole moieties, a number of fluorescent compounds were created. The compound BTAC(e) showed a strong affinity for Hcy, which has been linked to a number of illnesses, including Alzheimer's, coronary artery disease, stroke, and cardiovascular disease [41].

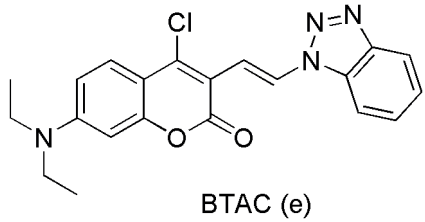

BTAC (e)

This work examined the ability of coumarins to inhibit the acetylcholinesterase enzyme (AChE) by synthesizing eight distinct dihydroxycoumarin derivatives. The outcomes demonstrated that every chemical had inhibitory efficacy against AChE. The compounds with the strongest inhibitory activity were 1 (96.83%), 3 (96.72%), and 2 (95.48%); these results were superior to those of galantamine (93.14%) [42].

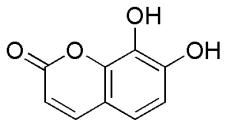

1

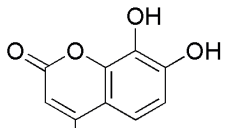

2

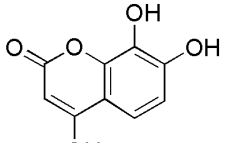

3

This work produced nine coumarin compounds (I - IX) and examined how well they inhibited AChE. I demonstrated an IC50 of 48.49 ± 4.6 nM, which was significantly higher than the IC50 of donepezil (DON), the FDA-approved medication for Alzheimer's disease (AD), which was 74.13 ± 8.3 nM. These data demonstrate compound I's unquestionably powerful potential against AChE inhibition [43].

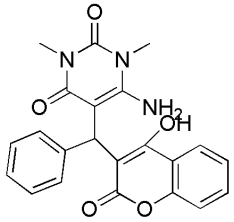

I

New coumarin thiosemicarbazone compounds and their zinc(II), nickel(II) and copper(II) metal complexes were synthesized and characterized. The inhibitory activities of these new coumarin thiosemicarbazone-based metal complexes against butyrylcholinesterase (BChE), acetylcholinesterase (AChE), αamylase and α-glucosidase were examined, and (E)-2-((7,8-dimethoxy-2-oxo-2H-chromen-3-yl)(phenyl)methylene)-N-phenyl-hydrazine-1-carbothioamide Zn complex has the best activity [44].

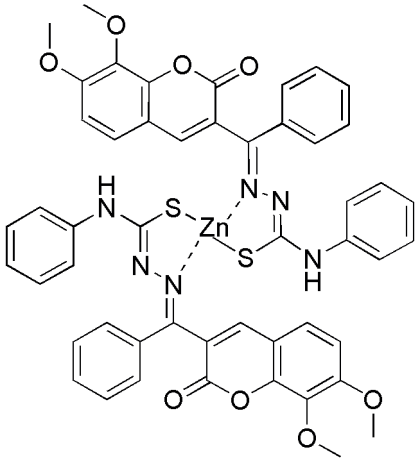

REFERENCES

1. Fries, G.R., Saldana, V.A., Finnstein, J., Rein, T., 2023. Molecular pathways of major depressive disorder converge on the synapse. Molecular Psychiatry. 28, 284–297. https://doi.org/10.1038/s41380-022-01806-1
2. Kenda, M., Koˇcevar Glavaˇc, N., Nagy, M., Sollner Dolenc, M., 2022. Medicinal plants used for anxiety, depression, or stress treatment: an update. Molecules. 27, 6021-6039. https://doi.org/10.3390/molecules27186021.
3. Pathak, A., Srivastava, A.K., Singour, P., Gouda, P., 2016. Synthetic and natural monoamine oxidase inhibitors as potential lead compounds for effective therapeutics. Central Nervous System Agents in Medicinal Chemistry. 16 :2, 81–97.
4. Akwu, N.A., Lekhooa, M., Deqiang, D., Aremu, A.O., 2023. Antidepressant effects of coumarins and their derivatives: A critical analysis of research advances. European Journal of Pharmacology. 956, 175958-175976. https://doi.org/10.1016/j.ejphar.2023.175958.
5. Simon, R.P., Greenberg, D.A., Aminoff, M.J., 2018. Clinical neurology (Tenth ed.). [New York]: McGraw Hill. p. 111. ISBN 978-1-259-86173-4.
6. Knopman, D.S., Amieva, H., Petersen, R.C., Chételat, G., Holtzman, D.M., Hyman, B.T., et al., 2021. Alzheimer disease. Nature Reviews Disease Primers. 7 (1): 1-21. https://doi.org/10.1038/s41572-021-00269-y.
7. Todd, S., Barr, S., Roberts, M., Passmore, A.P., 2013. Survival in dementia and predictors of mortality: a review. International Journal of Geriatric Psychiatry. 28 :11, 1109–1124. https://doi.org/10.1002/gps.3946.
8. Frozza, R.L., Mychael, V., Lourenco, M.V., De Felice, F.G., 2018. Challenges for Alzheimer's Disease Therapy: Insights from Novel Mechanisms Beyond Memory Defects. Frontiers in Neuroscience. 12, 1–13. https://doi.org/10.3389/fnins.2018.00037.
9. Alzheimer's Disease International, 2019. World Alzheimer Report 2019: Attitudes to Dementia. London, UK.
10. Breijyeh, Z., Karaman, R., 2020. Comprehensive Review on Alzheimer's Disease: Causes and Treatment. Molecules (Review). 25 :24, 5789-5816. https://doi.org/10.3390/molecules25245789.
11. Iqbal, K., Alonso, A., Chen, S., Chohan, M.O., El-Akkad, E., Gong, C.X., et al. 2005. Tau pathology in Alzheimer disease and other tauopathies. Biochimica et Biophysica Acta (BBA) - Molecular Basis of Disease. 1739 (2–3), 198–210. doi:10.1016/j.bbadis.2004.09.008.
12. Halder, D., Das, S., Jeyaprakash, R.S., Joseph, A., 2023. Role of multi-targeted bioactive natural molecules and their derivatives in the treatment of Alzheimer's disease: an insight into structure-activity relationship. Journal of Biomolecular Structure and Dynamics. 41:20, 11286-11323, DOI:

10.1080/07391102.2022.2158136.

13. Hasdemir, B., Yaşa, H., Onar, H.Ç., Yusufoğlu, A.S., 2016. Investigation of Antioxidant Activity of M comminus L from Turkey due to its Essential Oil Composition and Polyphenolic Content. Journal of the Turkish Chemical Society Section A: Chemistry. 3 : 3, 427-438. https://doi.org/10.18596/jotcsa.54346.

14. Hasdemir, B., Yaşa, H., Akkamış, Y., 2019. Synthesis and antioxidant activities of novel N-aryl (and N-alkyl) gamma- and delta-imino esters and ketimines. Journal of the Chinese Chemical Society. 66 :2, 197-204. https://doi.org/10.1002/jccs.201800126.

15. Biliz Y., Hasdemir B., Başpınar Küçük H., Yıldırım S., Kocabaş F., Kartop R. A., 2024. Synthesis of new pyrazolidines by [3+ 2] cycloaddition: Anticancer, antioxidant activities, and molecular docking studies. Journal of Molecular Structure 1295, 136813-136823. https://doi.org/10.1016/j.molstruc.2023.136813.

16. Onar, H.Ç., Yıldız, T., 2021. Researches on the Epilobium angustifolium L. ethanol extract, Turkey. Romanian Biotechnological Letters 26 :5, 2964-2970. https://doi.org/10.25083/rbl/26.5/2964.297.

17. Yasa, H., 2018. Synthesis, characterization, and evaluation of antioxidant activity of new gamma- and delta-imino esters. Turkısh Journal of Chemistry. 42:4, 1105-1132. https://doi.org/10.3906/kim-1801-8.

18. Şahin, H., 2023. In-vitro anti-diabetic, anti-Alzheimer, anti-tyrosinase, antioxidant activities of selected coumarin and dihydroisocoumarin derivatives. International Journal of Secondary Metabolite. 10: 3, 361–369. https://doi.org/10.21448/ijsm.1196712.

19. Abdel-Kader, N.S., Moustafa, H., El-Ansary, A.L., Sherif, O.E., Farghaly, A.M., 2021. A coumarin Schiff base and its Ag(I) and Cu(II) complexes: synthesis, characterization, DFT calculations and biological applications. New Journal of Chemistry. 45, 7714–7730. https://doi.org/10.1039/D0NJ05688J.

20. Ghalehshahi, H.G., Balalaie, S., Aliahmadi, A., 2018. Peptides Nconnected to hydroxycoumarin and cinnamic acid derivatives: synthesis and fluorescence spectroscopic, antioxidant and antimicrobial properties. New Journal of Chemistry. 42, 8831–8842. https://doi.org/10.1039/C8NJ00383A.

21. Guo, Z.L., Zhou, P., Song, H.J., Liu, Y.X., Zhang, J.J., Li, Y.Q., Wang, Q.M., 2021. Design, Synthesis, and Bioactivities of Phthalide and Coumarin Derivatives Based on the Biosynthesis and Structure Simplification of Gossypol. Journal of Agricultural and Food Chemistry. 69, 15123–15135. https://doi.org/10.1021/acs.jafc.1c05792.

22. Comert Onder, F., Durdagi, S., Sahin, K., Ozpolat, B., Ay, M., 2020. Design, Synthesis, and Molecular Modeling Studies of Novel Coumarin Carboxamide Derivatives as eEF-2 K Inhibitors. Journal of Chemical Information and Modeling. 60, 1766–1778. https://doi.org/10.1021/acs.jcim.9b01083

23. Kawai, J., Ota, M., Ohki, H., Toki, T., Suzuki, M., Shimada, T., Matsui, S., Inoue, H., Sugihara, C., Matsuhashi, N., Matsui, Y., Takaishi, S., Nakayama, K.,

2019. Structure-Based Design and Synthesis of an Isozyme-Selective MTHFD2 Inhibitor with a Tricyclic Coumarin Scaffold. ACS Medicinal Chemistry Letters. 2019, 10, 893–898. https://doi.org/10.1021/acsmedchemlett.9b00069.

24. Qin, T., Fang, F., Song, M., Li, R., Ma, Z., Ma, S., 2017. Umbelliferone reverses depression-like behavior in chronic unpredictable mild stress-induced rats by attenuating neuronal apoptosis via regulating ROCK/Akt pathway. Behavioural Brain Research. 317, 147–156. https://doi.org/10.1016/j.bbr.2016.09.039.

25. Çelik Onar, H., Mataracı Kara, E., Ceyhan, D., Erçağ, E. 2023. Molecular Docking Studies and Microbial Activities of Mono-, Di- and Tri-Substituted Simple Coumarins. European Journal of Advanced Chemistry Research. 4:1, 22–30. https://doi.org/10.24018/ejchem.2023.4.1.126.

26. Çelik Onar, H., Yaşa, H., Sin, O., 2020. Comparison of Antioxidant Activities of Mono-, Di-and Tri-substituted Coumarins. Journal of the Turkish Chemical Society Section A: Chemistry. 7 (1), 87-96. https://doi.org/10.18596/jotcsa.624265.

27. Çelik Onar, H., Anlaş, F.C., Yaşa, H., Üstün Alkan, F., Hasdemir, B., Bakırel, T., 2019. Anticancer Activities of Even Numbered Monoketo Eicosanoic Acid Anilides and Semicarbazones. Journal of the Turkish Chemical Society Section A: Chemistry. 6:3, 429-432. https://doi.org/10.18596/jotcsa.583845

28. Wang, C., Lin, H., Yang, N., Wang, H., Zhao, Y., Li, P., Liu, J., Wang, F., 2019. Effects of platycodins folium on depression in mice based on a UPLC-Q/TOF-MS serum assay and hippocampus metabolomics. Molecules. 24, 1712-1731. https://doi.org/10.3390/molecules24091712.

29. Kamel, N.N., Aly, H.F., Fouad, G.I.,. Abd El-Karim, S.S., Anwar, M.M., et al., 2023. Anti-Alzheimer activity of new coumarin-based derivatives targeting acetylcholinesterase inhibition. RSC Advances. 13, 18496-18511. https://doi.org/10.1039/d3ra02344c.

30. Zahedi, N.A., Mohammadi-Khanaposhtani, M., Rezaei, P., Askarzadeh, M., et al. 2023. Dual functional cholinesterase and carbonic anhydrase inhibitors for the treatment of Alzheimer's disease: Design, synthesis, in vitro, and in silico evaluations of coumarin-dihydropyridine derivatives. Journal of Molecular Structure. 1276, 134767-134779. https://doi.org/10.1016/j.molstruc.2022.134767.

31. Chen, X., Li, Y., Kang, J., Ye, T., Yang, Z., et al. 2023. Application of a novel coumarin-derivative near-infrared fluorescence probe to amyloid-β imaging and inhibition in Alzheimer's disease. Journal of Luminescence 256, 119661-119669. https://doi.org/10.1016/j.jlumin.2022.119661.

32. Cao, Y., Liu, X., Zhang, J., Liu, Z., Fu, Y., et al., 2023. Design of a Coumarin-Based Fluorescent Probe for Efficient In Vivo Imaging of Amyloid-β Plaques. ACS Chemical Neuroscience.14:5, 829–838. https://doi.org/10.1021/acschemneuro.2c00468.

33. Wang, H., Su, M., Shi, X., Li, X., Zhang, X., Yang, A., Shen, R., 2023. Design, Synthesis, Calculation and Biological Activity Studies Based on Privileged Coumarin Derivatives as Multifunctional Anti-AD Lead Compound. Chemistry

and Biodiversity. 20, e202200867-e202200879. doi.org/10.1002/cbdv.202200867.

34. Hasan, A.H., Abdulrahman, F.A.,Obaidullah, A.J., Alotaibi, H.F., Alanazi, M.M., Noamaan, M.A., Murugesan, S., Amran, S.I., Bhat, A.R., Jamalis, J., 2023. Discovery of Novel Coumarin-Schiff Base Hybrids as Potential Acetylcholinesterase Inhibitors: Design, Synthesis, Enzyme Inhibition, and Computational Studies. Pharmaceuticals.16, 971-1002. https://doi.org/10.3390/ph16070971.

35. Sharma, A., Bharate, S.B., 2023. Synthesis and Biological Evaluation of Coumarin Triazoles as Dual Inhibitors of Cholinesterases and β-Secretase. ACS Omega. 8, 11161−11176. https://doi.org/10.1021/acsomega.2c07993.

36. El-Hussieny, M., ElMansya, M.F., Ewies, E.F., El-Rashedy , A.A., Ibrahim, A.Y., El-Sayed, N.F., 2023. Synthesis, biological evaluation, and molecular dynamics of novel coumarin based phosphorothioates as cholinesterase inhibitors. Journal of Molecular Structure. 1272, 134214-134224. https://doi.org/10.1016/j.molstruc.2022.134214.

37. Hasan, A.H., Shakya, S., Hussain, F.H.S., Sankaranarayanan Murugesan,Chander, S., Pratama, M.R.F., et al., 2023. Design, synthesis, antiacetylcholinesterase evaluation and molecular modelling studies of novel coumarinchalcone hybrids. Journal of Biomolecular Structure and Dynamics. 41:21, 11450-11462. https://doi.org/10.1080/07391102.2022.2162583.

38. Li, B., Liu, C., Zhang, W., Ren, J., Song, B., Yuan, J., 2023. Ratiometric lysosome-targeting luminescent probe based on a coumarin-ruthenium(II) complex for formaldehyde detection and imaging in living cells and mouse brain tissues . Methods. 217, 10–17. https://doi.org/10.1016/j.ymeth.2023.06.008.

39. Çelik Onar, H., Mehtap Ozden, E., Taslak, H.D., Gülçin, İ., Ece, A., Erçag, E., 2023. Novel coumarin-chalcone derivatives: Synthesis, characterization, antioxidant, cyclic voltammetry, molecular modelling and biological evaluation studies as acetylcholinesterase, α-glycosidase, and carbonic anhydrase inhibitors. Chemico-Biological Interactions. 383, 110655-110662. https://doi.org/10.1016/j.cbi.2023.110655.

40. Khalid, A., Khan, W., Zia, K., Azizuddin Ahsan, W., Alhazmi, H.A., Abdalla, A.N., Najmi, A., Khan, A., Bouyahya, A., Ul-Haq, Z., Khan, A., 2023. Natural coumarins from Murraya paniculata as mixed-type inhibitors of cholinesterases: In vitro and in silico investigations. Frontiers in Pharmacology. 14, 1133809-1133818. https://doi.org/10.3389/fphar.2023.1133809.

41. Li, S., Feng, S., Song, X., Zheng, Q., Feng, G., Song, Z., 2023. A benzotriazole-coumarin derivative as a turn-on fluorescent probe for highly efficient and selective detection of homocysteine and its bioimaging application. Microchemical Journal. 185, 108293-108299. https://doi.org/10.1016/j.microc.2022.108293.

42. Özdemir, M., Taskın, D., Ceyhan, D., Köksoy, B., Taskın, T., Bulut, M., Yalçın, B., 2023. 7,8-Dihydroxycoumarin derivatives: In silico molecular docking and in vitro anticholinesterase activity. Journal of Molecular Structure. 1274, 134535-134547. https://doi.org/10.1016/j.molstruc.2022.134535.

43. Bhatta, A., Baruah, P., Phanrang, P.T., Basumatary, G., Bez, G., Mitra, S., 2022. Modulated photophysical properties and sequestration of potent anti-acetylcholinesterase active coumarinyl dyes in human serum albümin, Dyes and Pigments 208, 110871-110884. https://doi.org/10.1016/j.dyepig.2022.110871.

44. Çelik, E., Özdemir, M., Köksoy, B., Taskin-Tok, T., Taslimi, P., Sadeghian, N., Yalçın, B., 2023. New Coumarin Thiosemicarbazone Based Zn(II), Ni(II) and Co(II) Metal Complexes: Investigation of Cholinesterase, α- Amylase, and α-Glucosidase Enzyme Activities, and Molecular Docking Studies. ChemistrySelect. 8, e202301786 (1-13). https://doi.org/10.1002/slct.202301786.

CHAPTER 8

HOMOTHETIC MOTIONS WITH DUAL BICOMPLEX NUMBERS AT $\mathbb{D}_2^4$

Faik BABADAĞ[1]

1 Doçent Doktor. Mühendislik ve Doğa Bilimleri Fakültesi/ Matematik Bölümü/ Kırıkkale Üniversitesi, ORCID No: 0000-0001-9098-838X

1. Introduction

Dual numbers (Guggenheimer, 1963), extension of real numbers, first were defined by W. K. Clifford in 1873 as

$$\mathbb{D} = \{\mathbb{A} = a + \varepsilon a^* : a, a^* \in \mathbb{R}, \varepsilon \neq 0, \varepsilon^2 = 0\}.$$

This new number system is commutative and associative algebra over real numbers wich has dimension two. Kotelnikov (Kotelnikov, 1895), initiated the study of the first applications of dual numbers. Study used these numbers and associated vectors in line geometry and kinematics (Study, 1901). The set of dual vectors can be shown as $\mathbb{D}^3$, the set of all unit dual vectors is called unit dual sphere and shown by

$$\mathbb{S}^2 = \{\overrightarrow{\mathbb{A}} \in \mathbb{D}^3 : \ \|\overrightarrow{\mathbb{A}}\| = 1\}.$$

Dual numbers and dual complex numbers emerge in many areas in physics and mathematics such as coordinate transformation, matrix modeling, displacement analysis, rigid body dynamics, velocity analysis, static analysis, dynamic analysis, $2\mathbb{D}$ rigid transformation, mechanics, kinematics and applications of geometry. So far, there are number of studies in the literature related with dual numbers and dual complex numbers (Fjelstad et al, 1998; Matsuda et al, 2014). The Italian mathematician Gerolamo Cardano first discovered complex numbers while trying to solve a simpler state of the cubic equation. After, Leonard Euler illustrated the complex numbers as points with rectangular coordinates by using the notation $i = \sqrt{-1}$. Bicomplex numbers were defined in 1892 to improve the properties of algebra. As a result of the research, it was included in an article by Corrado Segre. Here bicomplex numbers are considered as tricomplex numbers. Rochon and Tremblay presented a study titled "II. The Hilbert Space," which was based on bicomplex quantum mechanics and then, Rochon and Shapiro gave algebraic properties of bicomplex and hyperbolic numbers (Rochon et al. 2004, 2006; Price,1991). This study presents bicomplex (hyperbolic) numbers from several perspectives on Hilbert Space in quantum physics.

The set of bicomplex numbers can be given by

$$\mathbb{C}_2 = \{A \mid A = a_0 + a_1 i_1 + a_2 i_2 + a_3 i_3 : a_{0-3} \in \mathbb{R}\}$$

where the imaginary units i_1, i_2 and i_3 satisfy

$$i_1^2 = i_2^2 = -1,\ i_1 i_2 = i_2 i_1 = i_3.$$

In this paper, we give a dual matrix which is similar to Hamilton operators for dual bicomplex numbers at $\mathbb{D}_2^4$. Thanks to this new dual matrix, we define a new dual motion and it is proven that this dual motion is homothetic. We provide some theorems for dual velocities, dual pole points, and dual pole curves for this one parameter dual homothetic motion. Moreover, we demonstrate that the motion described by the regular order n dual curve has only one acceleration center of order $(n-1)$ at every t-instant after defining dual accelerations.

Dual Bicomplex Numbers

In this section we define dual bicomplex numbers with components including bicomplex numbers and dual numbers.

Definition 1. The dual bicomplex numbers are defined as.

$$\begin{aligned}\tilde{A} = {} & \tilde{a}_0 + \tilde{a}_1 i_1 + \tilde{a}_2 i_2 + \tilde{a}_3 i_3 \\ & = (a_0 + a_0^* \varepsilon) + (a_1 + a_1^* \varepsilon) i_1 + (a_2 + a_2^* \varepsilon) i_2 + (a_3 + a_3^* \varepsilon) i_3\end{aligned}$$

where i_1, i_2, i_3 are the imaginary units and ε is the dual unit,

$$i_1^2 = i_2^2 = -1, i_1 i_2 = i_2 i_1 = i_3 \text{ and } \varepsilon^2 = 0.$$

The set of all dual bicomplex number is defined by

$$\mathbb{C}_2^{\mathbb{D}} = \left\{\tilde{A} \mid \tilde{A} = \tilde{a}_0 + \tilde{a}_1 i_1 + \tilde{a}_2 i_2 + \tilde{a}_3 i_3 : \tilde{a}_{0-3} \in \mathbb{D}\right\}.$$

Proposition 1. Let $\tilde{A}$ and $\tilde{B}$ be dual bicomplex numbers, then their addition and multiplication are

$$\tilde{A} + \tilde{B} = \left(\tilde{a}_0 + \tilde{b}_0\right) + \left(\tilde{a}_1 + \tilde{b}_1\right) i_1 + \left(\tilde{a}_2 + \tilde{b}_2\right) i_2 + \left(\tilde{a}_3 + \tilde{b}_3\right) i_3$$

and

$$\tilde{A}\tilde{B} = (\tilde{a}_0 + \tilde{a}_1 i_1 + \tilde{a}_2 i_2 + \tilde{a}_3 i_3)(\tilde{b}_0 + i_1\tilde{b}_1 + i_2\tilde{b}_2 + i_3\tilde{b}_3)$$
$$= (\tilde{a}_0\tilde{b}_0 - \tilde{a}_1\tilde{b}_1 - \tilde{a}_2\tilde{b}_2 + \tilde{a}_3\tilde{b}_3) + (\tilde{a}_0\tilde{b}_1 + \tilde{a}_1\tilde{b}_0 - \tilde{a}_2\tilde{b}_3 - \tilde{a}_3\tilde{b}_2)i_1$$
$$+(\tilde{a}_0\tilde{b}_2 - \tilde{a}_2\tilde{b}_0 + \tilde{a}_3\tilde{b}_1 - \tilde{a}_1\tilde{b}_3)i_2 + (\tilde{a}_0\tilde{b}_1 + \tilde{a}_1\tilde{b}_0 - \tilde{a}_2\tilde{b}_3 - \tilde{a}_3\tilde{b}_2)i_3,$$

according to the imaginary units i_1, i_2 and i_3, the conjugates and norms of the dual bicomplex number $\tilde{A}$, are

$$\tilde{A}^{i_1} = \tilde{a}_0 - \tilde{a}_1 i_1 + \tilde{a}_3 i_2 - \tilde{a}_3 i_3$$
$$\widetilde{A}\,\tilde{A}^{i_1} = \tilde{a}_0^2 + \tilde{a}_1^2 - \tilde{a}_2^2 - \tilde{a}_3^2 + 2i_2(\tilde{a}_0\tilde{a}_2 + \tilde{a}_1\tilde{a}_3)$$
$$\tilde{A}^{i_2} = \tilde{a}_0 + \tilde{a}_1 i_1 - \tilde{a}_3 i_2 - \tilde{a}_3 i_3$$
$$\widetilde{A}\,\tilde{A}^{i_2} = \tilde{a}_0^2 - \tilde{a}_1^2 + \tilde{a}_2^2 - \tilde{a}_3^2 + 2i_2(\tilde{a}_0\tilde{a}_1 + \tilde{a}_2\tilde{a}_3)$$
$$\tilde{A}^{i_3} = \tilde{a}_0 - \tilde{a}_1 i_1 - \tilde{a}_3 i_2 + \tilde{a}_3 i_3$$
$$\widetilde{A}\,\tilde{A}^{i_3} = \tilde{a}_0^2 + \tilde{a}_1^2 + \tilde{a}_2^2 + \tilde{a}_3^2 + 2i_2(\tilde{a}_0\tilde{a}_3 - \tilde{a}_1\tilde{a}_2)$$

and

$$\left\|\tilde{A}\right\|_{i_1} = \tilde{a}_0^2 + \tilde{a}_1^2 - \tilde{a}_2^2 - \tilde{a}_3^2$$
$$\left\|\tilde{A}\right\|_{i_2} = \tilde{a}_0^2 - \tilde{a}_1^2 + \tilde{a}_2^2 - \tilde{a}_3^2$$
$$\left\|\tilde{A}\right\|_{i_3} = \tilde{a}_0^2 + \tilde{a}_1^2 + \tilde{a}_2^2 + \tilde{a}_3^2.$$

The system $\mathbb{C}_2^{\mathbb{D}}$ is a commutative algebra. It is referred as the dual bicomplex number algebra shown with $\mathbb{C}_2^{\mathbb{D}}$, briefly one of the bases of this algebra is $\{1, i_1, i_2, i_3\}$ and the dimension is 4. It is possible to give the production similar to Hamilton operators which has defined (Agrawal, 1987; Hacısalihoglu, 1980,1983; Yayli Y,1995).

$$\phi: \tilde{A} \to \phi(\tilde{A}) = \begin{bmatrix} \tilde{a}_0 & -\tilde{a}_1 & -\tilde{a}_2 & \tilde{a}_3 \\ \tilde{a}_1 & \tilde{a}_0 & -\tilde{a}_3 & -\tilde{a}_2 \\ \tilde{a}_2 & -\tilde{a}_3 & \tilde{a}_0 & -\tilde{a}_1 \\ \tilde{a}_3 & \tilde{a}_2 & \tilde{a}_1 & \tilde{a}_0 \end{bmatrix}$$

$\mathbb{C}_2^{\mathbb{D}}$ is algebraically isomorphic to the matrix algebra

$$\mathcal{N} = \left\{ \begin{bmatrix} \tilde{a}_0 & -\tilde{a}_1 & -\tilde{a}_2 & \tilde{a}_3 \\ \tilde{a}_1 & \tilde{a}_0 & -\tilde{a}_3 & -\tilde{a}_2 \\ \tilde{a}_2 & -\tilde{a}_3 & \tilde{a}_0 & -\tilde{a}_1 \\ \tilde{a}_3 & \tilde{a}_2 & \tilde{a}_1 & \tilde{a}_0 \end{bmatrix} : \ \tilde{a}_0, \tilde{a}_1, \ \tilde{a}_2, \ \tilde{a}_3 \in \mathbb{D} \right\}$$

and $\phi(\tilde{A})$ is a faithful real matrix representation of $\mathcal{N}$. Moreover, $\forall\ \tilde{A}, \tilde{B} \in \mathbb{C}_2^{\mathbb{D}}$ and $\forall\ \lambda \in \mathbb{R}$, we obtain

$$\phi(\tilde{A} + \tilde{B}) = \phi(\tilde{A}) + \phi(\tilde{B})$$

$$\phi(\lambda\, \tilde{A}) = \lambda\, \phi(\tilde{A})$$

$$\phi(\tilde{A}\, \tilde{B}) = \phi(\tilde{A})\phi(\tilde{B}).$$

2. Homothetic Motions at $\mathbb{D}_2^4$

Definition 2. Let $\mathcal{M}$, $\mathcal{S}_2^3$ and $\mathcal{K}$ be a dual hypersurface, unit dual sphere and null dual-cone, respectively, as following,

$$\mathcal{M} = \{\gamma = (\gamma_0, \gamma_1, \gamma_2, \gamma_3) \mid \gamma_0\gamma_1 + \gamma_2\gamma_3 = 0\},$$

$$\mathcal{S}_2^3 = \{\gamma = (\gamma_0, \gamma_1, \gamma_2, \gamma_3) \mid \gamma_0^2 - \gamma_1^2 + \gamma_2^2 - \gamma_3^2 = 1\}$$

$$\mathcal{K} = \{\gamma = (\gamma_0, \gamma_1, \gamma_2, \gamma_3) \mid \gamma_0^2 - \gamma_1^2 + \gamma_2^2 - \gamma_3^2 = 0\}.$$

Let us consider the following dual curve:

$\gamma \ : I \subset R \ \to \ \mathcal{M} \subset \mathbb{D}_2^4$ given by

$t \ \to \ \gamma(t) = \gamma_0(t) + \gamma_1(t)i_1 + \gamma_2(t)i_2 + \gamma_3(t)i_3$

$= \big(a_0(t) + \varepsilon a_0^*(t)\big) + \big(a_1(t) + \varepsilon a_1^*(t)\big)i_1$

$$+\big(a_2(t) + \varepsilon a_2^*(t)\big)i_2 + \big(a_3(t) + \varepsilon a_3^*(t)\big)i_3$$

for every $t \in I$. We suppose that the curve $\gamma(t)$ is differentiable dual regular curve of order n. The operator $\mathcal{B} = \mathcal{N}$, corresponding to $\gamma(t)$, is defined by the following dual matrix

$$\mathcal{B} = \begin{bmatrix} \gamma_0 & -\gamma_1 & -\gamma_2 & \gamma_3 \\ \gamma_1 & \gamma_0 & -\gamma_3 & -\gamma_2 \\ \gamma_2 & -\gamma_3 & \gamma_0 & -\gamma_1 \\ \gamma_3 & \gamma_2 & \gamma_1 & \gamma_0 \end{bmatrix}. \tag{1}$$

Let $\|\gamma'(t)\| = 1$, $\gamma(t)$ be a unit velocity dual curve. If $\gamma(t)$ does not pass through the orijin, and $\gamma(t) \neq 0$, the matrix $\mathcal{B}$ can be rewrite as

$$\mathcal{B} = \lambda\, \mathcal{A} = \lambda \begin{bmatrix} \gamma_0/\lambda & -\gamma_1/\lambda & -\gamma_2/\lambda & \gamma_3/\lambda \\ \gamma_1/\lambda & \gamma_0/\lambda & -\gamma_3/\lambda & -\gamma_2/\lambda \\ \gamma_2/\lambda & -\gamma_3/\lambda & \gamma_0/\lambda & -\gamma_1/\lambda \\ \gamma_3/\lambda & \gamma_2/\lambda & \gamma_1/\lambda & \gamma_0/\lambda \end{bmatrix} \tag{2}$$

and

$\lambda: I \subset \mathbb{R} \to \mathbb{D}$

$t \to \lambda(t) = \| \gamma(t) \| = \sqrt{|\gamma_0^2(t) - \gamma_1^2(t) + \gamma_2^2(t) - \gamma_3^2(t)|}$ and $\gamma(t) \neq 0$.

Theorem 1. From (2), the matrix $\mathcal{A}$ is dual semi-orthogonal matrix

Proof. Let $\gamma(t) \notin \mathcal{K}$, and $\gamma_1(t)\gamma_2(t) + \gamma_3(t)\gamma_4(t) = 0$. In $\mathcal{B} = \lambda\mathcal{A}$, the matrix $\mathcal{A}$ has been shown by $\mathcal{A}^{\mathrm{T}}\varepsilon\, \mathcal{A} = \varepsilon$. Let the signature matrix, given in (Barrett, 1983), be

$$\varepsilon = \begin{bmatrix} 1 & 0 & 0 & 0 \\ 0 & -1 & 0 & 0 \\ 0 & 0 & 1 & 0 \\ 0 & 0 & 0 & -1 \end{bmatrix}$$

where, the matrix $\mathcal{A}$ is dual semiorthogonal matrix and $\det\mathcal{A} = 1$.

Theorem 2. Let $\gamma(t) \in \mathcal{S}_2^3 \cap \mathcal{M}$. The matrix $\mathcal{A}$ in (2) is a dual semi-ortogonal matrix.

Proof. From definition (2), if $\gamma(t) \in \mathcal{S}_2^3$, and $\gamma_0^2 + \gamma_1^2 + \gamma_2^2 + \gamma_3^2 = 1$,

by using (2), we obtain that $\mathcal{B}^{-1} = \varepsilon\mathcal{B}\varepsilon$ and $\det\mathcal{A} = 1$.

3. Dual motion with one parameter

Let the fixed space and the motinal space be, respectively, $\mathcal{R}_0$ and $\mathcal{R}$. In this case, one-parametric motion of $\mathcal{R}_0$ with respect to $\mathcal{R}$ will be denoted by $\mathcal{R}_0/\mathcal{R}$. This motion can be expressed by

$$\begin{bmatrix} \mathcal{X} \\ 1 \end{bmatrix} = \begin{bmatrix} \lambda\mathcal{A} & \mathcal{C} \\ 0 & 1 \end{bmatrix} \begin{bmatrix} \mathcal{X}_0 \\ 1 \end{bmatrix}$$

or equivalently

$$\mathcal{X} = \lambda\mathcal{A}\mathcal{X}_0 + \mathcal{C} \tag{3}$$

where, $\mathcal{X}$ and $\mathcal{X}_0$ represent position vectors of any point, respectively, in $\mathcal{R}$ and $\mathcal{R}_0$, and $\mathcal{C}$ represent any translation vector.

Definition 3. In dual 4-space, the one-parameter dual homothetic motion of a body is generated by the transformation given in (3). Here λ is called the homothetic scale, which is a dual scalar matrix, $\mathcal{A}$ is an 4×4 dual orthogonal matrix, $\mathcal{X}_0$ and $\mathcal{C}$ are 4×1 dual matrices, and $\mathcal{A}, \mathcal{C}$, and λ are of class $\mathcal{C}^{\mathrm{n}}$. In order not to encounter the case of affine transformation we suppose that

$$\lambda(t) = h(t) + \varepsilon h^*(t) \neq \text{constant},\ \lambda(t) \neq 0$$

and to prevent the cases of pure rotation and pure translation we also suppose that

$$\dot{\lambda}\mathcal{C} + \lambda\dot{\mathcal{C}} \neq 0, \dot{\mathcal{C}} \neq 0.$$

Corollary 1. In dual space $\gamma(t) \in \mathbb{D}_2^4$, The homothetic motions are regular and has only one instantaneous rotation centre at all time t .

Theorem 3. The motion defined by (3) is a dual homothetic motion with one parameter.

Proof. The matrix determined by (3) is a dual homothetic motion with one parameter, where $\mathcal{A} \in \mathrm{SO}(4,2)$.

Theorem 4. Let $\gamma(t)$ be a unit velocity curve and $\dot{\gamma}(t) \in \mathcal{M}$ then the derivation operator $\mathcal{B}$ of $\mathcal{B} = \lambda\mathcal{A}$ is dual semi-orthogonal matrix in $\mathbb{D}_2^4$.

Proof. Since $\gamma(\mathrm{t})$ is a dual unit velocity curve,

$$\dot{\gamma}_0^2(t) + \dot{\gamma}_1^2(t) + \dot{\gamma}_2^2(t) + \dot{\gamma}_3^2(t) = 1$$

and $\dot{\gamma}(t) \in \mathcal{M}$, then

$$\dot{\gamma}_0(t)\dot{\gamma}_1(t) + \dot{\gamma}_2(t)\dot{\gamma}_3(t) = 0.$$

Thus, $\dot{\mathcal{B}}\varepsilon\dot{\mathcal{B}}^{\mathrm{T}} = \dot{\mathcal{B}}^{\mathrm{T}}\varepsilon\dot{\mathcal{B}}$ and $\det\dot{\mathcal{B}} = 1$.

Theorem 5. If $\gamma(t)$ is a dual spherical curve on $\mathcal{M}$, then the motion is rotatin motion.

Proof. Since $\gamma(t)$ is a dual spherical curve on

$$\dot{\gamma}_0^2(t) + \dot{\gamma}_1^2(t) + \dot{\gamma}_2^2(t) + \dot{\gamma}_3^2(t) = 1$$

and $\mathcal{B}\varepsilon\mathcal{B}^{\mathrm{T}} = \mathcal{B}^{\mathrm{T}}\varepsilon\mathcal{B}$, $\mathcal{B}$ is a dual semi-orthogonal matrix and

$\det\mathcal{B} = 1$. Thus $\mathcal{B}$ is a dual rotating matrix in dual space $\mathbb{D}_2^4$.

4. Dual velocities, dual pole points and dual pole curves

From (3), we obtain

$$\mathcal{X} = \mathcal{B}\mathcal{X}_0 + \mathcal{C} \tag{4}$$

then

$$\mathcal{X}_0 = -\mathcal{B}^{-1}(\mathcal{X} - \mathcal{C}).$$

If we let $\mathcal{C}' = \mathcal{B}^{-1}\mathcal{C}$, Then ($\lambda^{-1} = \frac{1}{\lambda}\mathrm{I}$, $\lambda^{\mathrm{T}} = \lambda$) cause

$$\mathcal{X}_0 = \mathcal{B}^{-1}\mathcal{X} + \dot{\mathcal{C}} \tag{5}$$

and (4) and (5) are coordinate transformations between the fixed and moving dual spaces. Differentiating (5) with respect to t we get

$$\dot{\mathcal{X}} = \dot{\mathcal{B}}\mathcal{X}_0 + \dot{\mathcal{C}} + \dot{\mathcal{X}}_0 + \mathcal{B}\dot{\mathcal{X}}_0$$

where $\mathcal{B}\dot{\mathcal{X}}_0$ is the dual relative velocity, $\dot{\mathcal{B}}\mathcal{X}_0 + \dot{\mathcal{C}}$ is the dual sliding velocity, and $\dot{\mathcal{X}}$ is the dual absolute velocity of point $\dot{\mathcal{X}}_0$. In this case the following theorem can be given.

Theorem 6. For dual homothetic motion with one parameter, the dual absolute velocity vector of a moving system of point $\dot{\mathcal{X}}_0$ at that time t is the sum of the dual sliding velocity and dual relative velocity of $\dot{\mathcal{X}}_0$ in dual space $\mathbb{D}_2^4$. To find the pole point, we have to solve the equation

$$\dot{\mathcal{B}}\mathcal{X}_0 + \dot{\mathcal{C}} = 0, \tag{6}$$

any solution of (6) is a dual pole point of the dual motion at that t - instant, which is the only solution. In that case the following theorem can be given.

Theorem 7. If $\gamma(t)$ is a dual unit velocity curve and $\dot{\gamma}(t) \in \mathcal{M}$ in $\mathcal{R}_0$, then the dual pole point corresponding to each t-instant is the rotation by $\dot{\mathcal{B}}$ of the dual speed vector $\dot{\mathcal{C}}$ of the translation vector at that moment.

Proof. Since the matrix $\dot{\mathcal{B}}$ is dual orthogonal, then the matrix $\dot{\mathcal{B}}^{\mathrm{T}}$ is dual orthogonal. Thus, it makes a dual rotation.

5. Dual accelerations and dual acceleration centers

Definition 4. The set of the zeros of dual sliding acceleration of order n is defined the dual acceleration centre of order $(n-1)$.

By the definition (4), we have to solve the solution of

$$\mathcal{B}^{(n)}\mathcal{X}_0 + \mathcal{C}^{(n)} = \sum_{k=o}^{n} \binom{n}{k} \lambda^{(n-k)}\mathcal{A}^{(n)}\mathcal{X}_0 + \mathcal{C}^{(n)} = 0 \qquad (7)$$

where $\mathcal{B}^{(n)} = \frac{d^n\mathcal{B}}{dt^n}$ and $\mathcal{C}^{(n)} = \frac{d^n\mathcal{C}}{dt^n}$. We know that $\gamma(t)$ is a regular curve of order n and

$\gamma^{(n)} \in \mathcal{M}$. Then we have $\gamma_0^{(n)}\gamma_1^{(n)} + \gamma_2^{(n)}\gamma_3^{(n)}\tilde{\gamma}_3^{(n)} = 0$. Thus,

$$\left(\gamma_0^{(n)}\right)^2 + \left(\gamma_1^{(n)}\right)^2 + \left(\gamma_2^{(n)}\right)^2 + \left(\gamma_3^{(n)}\right)^2 \neq 0,$$

also, we have

$$det\mathcal{B}^{(n)} = \left(\left(\gamma_0^{(n)}\right)^2 + \left(\gamma_1^{(n)}\right)^2 + \left(\gamma_2^{(n)}\right)^2 + \left(\gamma_3^{(n)}\right)^2\right)^2 \neq 0.$$

Thus matrix $\mathcal{B}^{(n)}$ has an inverse in (7), the dual acceleration centre of order $(n-1)$ at every t-instant, is

$$\mathcal{X}_0 = \left[\mathcal{B}^{(n)}\right]^{-1}\left[-\mathcal{B}^{(n)}\right].$$

Example 1. Let $\gamma: I \subset R \rightarrow \mathcal{M} \subset \mathbb{D}_2^4$ be a dual curve given by

$\gamma(t) = \frac{1}{\sqrt{2}}(cosht, sinht, sinht, -cosht)$. Note that $\gamma(t) \in S_2^3$ and since $\|\dot{\gamma}(t)\| = 1$, then $\gamma(t)$ is a unit velocity curve. Moreover,

$$\dot{\gamma}(t), \ddot{\gamma}(t), , , \gamma^{(n)}(t) \in \mathcal{M}.$$

Thus $\gamma(t)$ satisfies all conditions of the above theorems.

REFERENCES

[1] Guggenheimer, H.W. (1963) Differential Geometry. McGraw-Hill, New York.

[2] Kotelnikov, A.P. (1895). Screw Calculus and Some Applications to Geometry and Mechanics, Kazan, Russia: Annals of the Imperial University of Kazan.

[3] Study, E. (1901). Geometry der dynamen, Leipzig.

[4] Fjelstad, P. & Gal, S. G. (1998). n-dimensional dual complex numbers, Advances in Applied Clifford Algebras, 8(2); 309-322.

[5] Matsuda, G., Kaji, S. & Ochiai. (2014). H. Anticommutative dual complex numbers and 2d rigid transformation, in Mathematical Progress in Expressive Image Synthesis I, 131–138.

[6] Rochon D. & Tremblay S. (2006). Bicomplex Quantum Mechanics: II. The Hilbert Space Adv. appl. Clifford alg. DOI 10.1007/s00006-003-0000, Birkhauser Verlag Basel/Switzerland.

[7] Rochon D. & Shapiro M. (2004). On algebraic properties of bicomplex and hyperbolic numbers, Anal. Univ. Oradea, fasc. math.,11; 71-110.

[8] Price, G.B. (1991). An Introduction to Multicomplex Spaces and Functions. Marcel Dekker, Inc: New York, 1; 44(1).

[9] Agrawal O.P. (1987). Hamilton operators and dual number quaternions in spatial kinematics. Mech Mach Theory, 22; 569–575.

[10] Hacısalihoglu, H. H. (1980). Yüksek Diferensiyel Geometriye Giriş. Fırat Üniversitesi Fen Yayını.

[11] Hacısalihoglu, H. H. (1983). Hareket Geometrisi ve Kuaterniyonlar Teorisi. Gazi Üniversitesi Fen Edebiyat Yayını, 78-94.

[12] Yayli Y. & Bukcu B. (1995). Homothetic motions at E^8 with Cayley numbers. Mech Mach Theory; 30; 417–420.

[13] Barrett O. (1983). Neill Semi-Riemannian Geometry, Pure and Applied Mathematics, 103 Academic Pres, Inc., New York.

CHAPTER 9

SEISMIC GAP THEORY-BASED SEISMIC RISK EVALUATION IN THE MARMARA REGION

Serpil ÜNAL[1]

1 Dr. Öğr. Üyesi, Usak University, Faculty of Arts and Sciences, Department of Mathematics, Uşak, Turkey, E-mail:serpil.unal@usak.edu.tr
ORCHID: 0000-0002-4043-6832

1. Introduction

The North Anatolian Fault (NAF) is among the most significant strike-slip fault ever discovered, with well-known seismological-seismotectonic properties, and constitutes among Turkey's most significant tectonic elements. The formation and westward migration of major earthquakes were observed semi-systematically after the 1939 Erzincan Earthquake, its ruptures towards the west continued following the Adapazarı-Mudurnu Valley earthquake of 1967 and finally on August 17 and November 12, 1999 with two catastrophic earthquakes in the Marmara region (Fig.1), situated at this fault zone's westernmost point. The fact that no significant earthquake has occurred in the region since 1999 has not provided a clear opportunity to explain and support models for the region. On the other hand, the fact that no significant earthquake has occurred in the region for a long time has led to scientific discussion of the possibility of a major earthquake (Kalafat, 2011).

The ability to predict earthquakes, whether short-term or long-term, has been a significant scientific difficulty for decades, with numerous papers supporting and disputing this claim. The contributed papers differ in terms of the area covered, time frame for forecasting, the magnitude range that can be forecasted, and of course the methodology used to establish the prediction. In parallel, a number of theories make an effort to shed light on the prediction dilemma. The 'seismic gap theory' which connects the duration since the preceding seismic event to the magnitude of the succeeding seismic event, is one such contentious idea. As per the theory, there is a positive correlation, which implies that the chance of a major earthquake occurring in an area increases when there is a prolonged period of no seismic activity. In the event that such a relationship is present, modeling these two parameters allows us to predict (statistically) the magnitude of a future earthquake. (Nikoloulopoulos & Karlis, 2008).

Copula models come into play when modeling the dependency between random variables. Copulas are functions that establish a connection between

the one-dimensional marginal distribution functions and multivariate distribution functions. Their extensive history of application in a variety of scientific domains dates back to, in economics, survival analysis, finance, insurence. Copula theory has also been investigated for many applications in the fields of geology, up to now. Nikoloulopoulos and Karlis (2008) use copulas to real data in support of the seismic gap hypothesis, which postulates a positive relationship between the magnitude of an earthquake and the amount of time that has passed since its last occurrence. In order to evaluate the joint seismic losses probability distribution, Goda and Ren (2010) employ copulas. Li, Shi and Zhang (2013) showed how copula can be used for risk assessment and bivariate return periods. Kara (2017) modeled the dependency structure for Turkey's earthquake data's magnitude and frequency with copulas and for these chosen copula models, estimated the probability of an earthquake occurring and the bivariate return periods. Karacam (2019) used conditional copula to represent the Semi-Markov model's dependent structure based on the seismic gap theory. Again, Unal (2023) showed that compared to the Semi-Markov model, the Conditional Copula has substantially higher success rates, particularly for large magnitudes in study on the seismicity of Western Anatolia.

It is now acknowledged that predicting the location, timing, and magnitude of earthquakes as well as preventing these catastrophic natural occurrences are impossible (Karacam, 2019). Owing to the intricate mechanisms and varied geographic locations of earthquakes, it is difficult to achieve high-precision predictions. However, the occurrence of earthquakes is not entirely chaotic, and partially, probability predictions can be made up (Ma, Bai & Meng, 2021).

Taking all these into consideration, the aim of this study is to evaluate seismic risk based on the Seismic Gap Theory in Marmara Region (Fig.1), located between the latitudes of 40°-41.5° N and the longitudes of 26°-32° E, using seismic data for the years 1964 to 2024 with the magnitude $M_W \geq 5$.

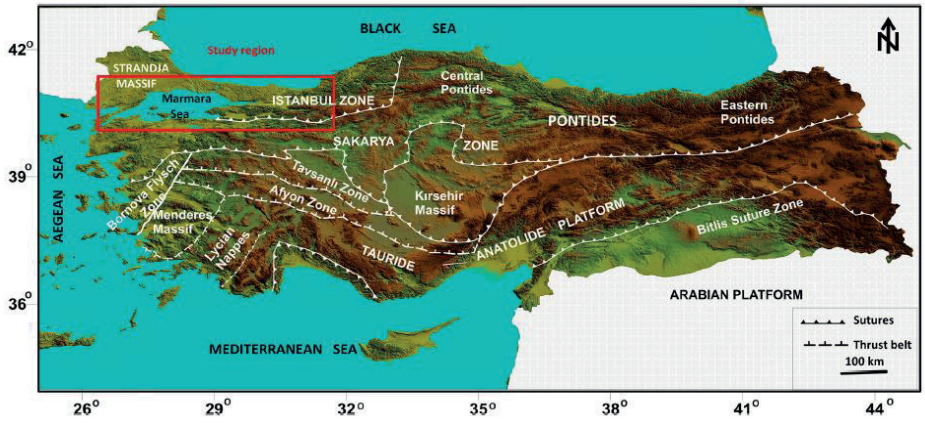

Figure 1. Turkey's simplified tectonic units (modified from Okay and Tuysuz, (1999)) and the study area (represented by red rectangle) (Kiran, Ates & Dolmaz, 2021)

2. Methods

2.1. Definition of Copula and Sklar's Theorem

A copula $C(u) = C(u_1, u_2, \dots, u_n)$ is a mapping from the unit hypercube to the unit interval, i.e. $C: [0,1]^n \rightarrow [0,1]$. Following McNeil, Frey and Embrechts (2005) for a function to be considered a copula, three requirements must be met: Firstly, $C(u_1, u_2, \dots, u_n)$ is an increasing function in each component u_i. Second, by positioning each component $u_j = 1$ with $i \neq j$ we obtain the marginal component u_i, i.e. $C(1, \dots, 1, u_i, 1 \dots, 1) = u_i$. Thirdly, for a random vector $(U_1, U_2, \dots, U_n)'$ having a distribution function C and for values $(v_1, \dots, v_n)$ and $(w_1, \dots, w_n) \in [0,1]^n$ with $v_i \leq w_i$ the probability $P(v_1 \leq U_1 \leq w_1, \dots, v_n \leq U_n \leq w_n)$ has to be non-negative (rectangle inequality). When combined, the three characteristics describe a copula and offer an alternate definition for it. As a result, any function satisfying these properties can be referred to as a copula (Fischbach, 2010).

Theorem 1. (Sklar's) Given a multivariate distribution function H with marginals $F_1, \dots F_n$, a copula C is present, for $x_1, \dots, x_n \in [-\infty, \infty]$,

$$H(x_1, \dots, x_n) = C\big(F_1(x_1), \dots, F_n(x_n)\big) \tag{1}$$

According to Embrechts, Lindskog and Mcneil (2003), Sklar's theorem is elegant because it shows us how to distinguish between the multivariate dependent structure, symbolised by the copula function, and the univariate marginal distributions. In general, there are two methods to understand Sklar's theorem. On one side, if C is a copula and $F_1, \dots F_n$ represent univariate distribution functions, then the multivariate distribution function H is defined using the formula shown above. Therefore, by combining the marginals with a copula, a joint distribution function can be produced. Conversely, a copula can be derived from the related marginal distributions and a joint distribution function. Therefore, Sklar's theorem also demonstrates that a copula is present in all multivariate distribution functions. Specifically, in the case where the marginals are continuous, the copula function C is unique (Fischbach, 2010). A few families of one-parameter copulas are given in Table 1.

Family	$C_\gamma(u, v)$	Range of γ
Clayton	$(u^{-\gamma} + v^{-\gamma} - 1)^{-1/\gamma}$	$(0, \infty)$
Frank	$-\gamma^{-1} ln\big([(e^{-\gamma} - 1) + (e^{-\gamma u} - 1)(e^{-\gamma v} - 1)]/(e^{-\gamma} - 1)\big)$	$(-\infty, \infty) - \{0\}$
Gumbel	$e^{\left(-((-\ln u)^\gamma + (-\ln v)^\gamma)^{1/\gamma}\right)}$	$[1, \infty)$
Çelebioğlu-Cuadras	$uve^{(\gamma(1-u)(1-v))}$	$[-1,1]$
FGM	$uv + \gamma uv(1-u)(1-v)$	$[-1,1]$
Galambos	$uve^{\left\{[(-\ln u)^{-\gamma} + (-\ln v)^{-\gamma}]^{-1/\gamma}\right\}}$	$[0, \infty)$
Tawn	$uve^{\left(-\gamma \frac{\ln u \ln v}{\ln(uv)}\right)}$	$(0,1)$
Joe	$1 - [(1-u)^\gamma + (1-v)^\gamma - (1-u)^\gamma(1-v)^\gamma]^{1/\gamma}$	$[1, \infty)$

Table 1. A few families of one-parameter copulas

2.2. The method of Inference Function of Margins (IFM)

In the initial phase of the approach, the marginal distribution parameters are estimated by MLE

$$\hat{\gamma}_1 = argmax_{\gamma_1} \sum_{t=1}^{T} \sum_{i=1}^{2} log f_i(x_{i,t}; \gamma_1) \quad (2)$$

in the second phase, followed by estimating of the copula parameters conditioned on the previous marginal distribution as

$$\hat{\gamma}_2 = argmax_{\gamma_2} \sum_{t=1}^{T} \log c(F_1(x_{1,t}), F_2(x_{2,t}); \gamma_2, \hat{\gamma}_1) \quad (3)$$

(Kara, 2017).

2.3. Model selection

Once the parameters of a group of copulas have been estimated using IFM approach, the following stage of copula fitting to empirical data is to select the best copula from among those under consideration. In this context, it is important to emphasize that there is no one test that allows us to choose which copula best suits the data under examination. An apparent requirement is to compare the log likelihood function if there are the same number of estimated parameters for all maximum likelihood functions and the same data are utilized for each model specification during the estimation process. In this case, the copula with the maximized log-likelihood value is the one that most closely matches the observed data (Fischbach, 2010).

2.4. Performance criteria

A bootstrap approach was presented by Allcroft and Glasbey (2003) to test the hypothesis, for $k = 1, \ldots, m$,

$H_0: C = C_k$ versus $H_1: C \neq C_k$ (4)

Mahalanobis squared distance is adequate for the aforementioned comparisons, because the central limit theorem indicates that the log-likelihoods' joint distributions are nearly multivariate normal. To be the vector of log-likelihoods δ at the original data and the vector of average log-likelihoods $\bar{\delta}_k$ at the kth copula's simulated data, the distant between these two vectors is calculated as follows,

$$D_k^2 = \left(\delta - \bar{\delta}_k\right)' S^{-1} \left(\delta - \bar{\delta}_k\right) \quad (5)$$

where S represents these log-likelihood's sample covariance matrix. Considering that the log-likelihoods are normal, the quantity D_k^2 follows an $mF_{m,B-1}$, distribution under the null hypotheses that kth copula is true (Nikoloulopoulos & Karlis, 2008).

2.5. Return Periods

It is common practice to characterize and quantify risk using the return period and return levels. The return level is equivalent to the variable's $100p\%$ quantile and p is the probability that a variable will surpass the return level within a year; that is, $P\{X_{t_i} \geq Z_p\} = p$. The return period $1/p$ is the average time when the variable surpasses the return level for the second time (Ma et al, 2021).

3. An Application for Earthquake Data in the Marmara Region

3.1. The study area

The Marmara region is situated on the nortwestern part of Turkey, locating in the western end of the North Anatolian Fault Zone (NAFZ) which is one of the most significant fault systems in Turkey (Fig. 2). This fault zone, the pattern of occurrence of major earthquakes on it, and their migration to the west were observed semi-systematically after the 1939 Erzincan Earthquake, and its rupture towards the west continued with the 1967

Adapazari-Mudurnu Valley earthquake and finally the 1999 Golcuk and Duzce earthquakes. The primary northern branch of the NAF, which is clearly traced up to Bolu, extends to the Gulf of Izmit, passes through the Sea of Marmara, connects to the Ganos Fault, and extends to the Gulf of Saros and reaches the Northern Aegean Sea. The southern branch passes south of Lake Iznik and reaches Gemlik Bay. Along the line passing from the north of the Marmara Sea, Sarkoy- Murefte - Guzelkoy - Tekirdag - M.Eregli - Silivri (West Marmara Fault) and in the south along the Gemlik Gulf-Bandırma Gulf - Erdek Gulf descending from the south of Iznik Lake to Gemlik Gulf, it is seen that there is earthquake activity and earthquake clustering and these faults produce significant earthquakes (Kalafat, 2011).

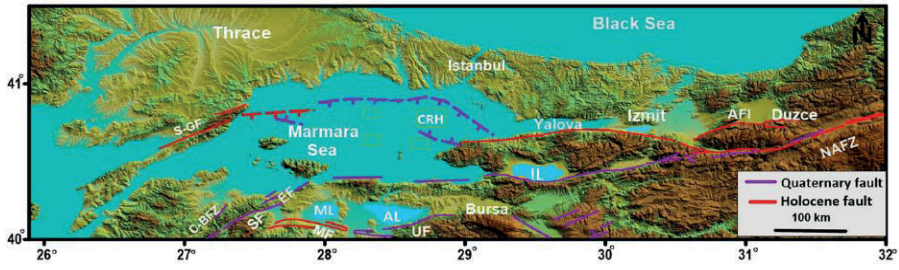

Figure 2. A simplified active fault map of northwest Turkey's Marmara region (modified from Emre et al (2013), Ates et al (2009), Saroglu, Emre and Kuscu (1992)). Sarikoy Fault (SF), Saros-Gazikoy Fault (S-GF), Edincik Fault (EF), Can Biga Fault Zone (C-BFZ), Manyas Fault (MF), Ulubat Fault (UF), North Anatolian Fault Zone (NAFZ), Almacık Flake (AFI), Iznik Lake (ML), Manyas Lake (ML), Apolian Lake (AL), and Central Ridge Horst (CRH). Holocene faults are red, and Quaternary faults are purple. Green rectangles in the Marmara Sea also show the approximate locations of the horsts (Kiran et al, 2021)

3.2. Earthquake records of Marmara Region

All statistical analyses are based on data collected during the modern instrumental period (1964-2024). The information, which included the timing,

latitude, longitude, and magnitude of the earthquakes, was gathered from the National Earthquake Monitoring Centre and Earthquake Research Institute at Bogazici University's Kandilli Observatory. While they may be felt, earthquakes with the magnitude $M_W < 5$ typically do not cause structural damage to buildings. Strong earthquakes are defined as those having a magnitude $M_W \geq 5$, and they have the potential to destroy structures. For this reason, earthquakes with the magnitude $M_W \geq 5$ were chosen for examination in order to provide more substantial application and practical significance. (Ma et al, 2021). Tan (2021) transformation equations were used to homogenize the data according to the single earthquake scale (M_W). Additionally, throughout the study, X_{t_i} and Y_i were defined as the earthquake magnitude at time t_i and the time elapsed between successive earthquakes, respectively.

3.3. Construction of Marginal distribution

The first step in modeling is to determine the marginal distributions of the elapsed time between subsequent earthquakes Y_i and their magnitudes X_{t_i}. Table 2 lists goodness of fit test results and the estimated parameters. According to the Kolmogorov-Smirnov test results, Weibull distributions (Fig. 3) and Gen-Extreme Value distributions (Fig. 4) are the best fitting distributions for Y_i and X_{t_i}, respectively.

Two-Parameter Weibull Cumulative Distribution

$$F(x) = 1 - \exp\left(-\left(\frac{x}{\beta}\right)\right)^{\alpha} \tag{6}$$

where α and β are continuous shape and scale parameters, respectively and $\alpha,\ \beta > 0$.

Gen-Extreme Value (GEV) Cumulative Distribution

$$F(x) = \exp\left(-\left(1 + k\left(\frac{x-\mu}{\sigma}\right)\right)^{-1/k}\right) \tag{7}$$

where k, σ and μ are continuous shape, scale and location parameters, respectively and $\sigma > 0$.

Table 2. The marginal distributions

Goodness of fit summary	$Y_i \approx \boldsymbol{Weibull}$	$\boldsymbol{.}\ \boldsymbol{X_{t_i}} \approx \boldsymbol{GEV}$
Kolmogrov-Smirnov test p-value	0.0423	0.0407
Estimated parameters	$\alpha = 0.25234, \beta = 0.13254$	$k = 0.37834, \sigma = 0.18487, \mu = 5.1229$

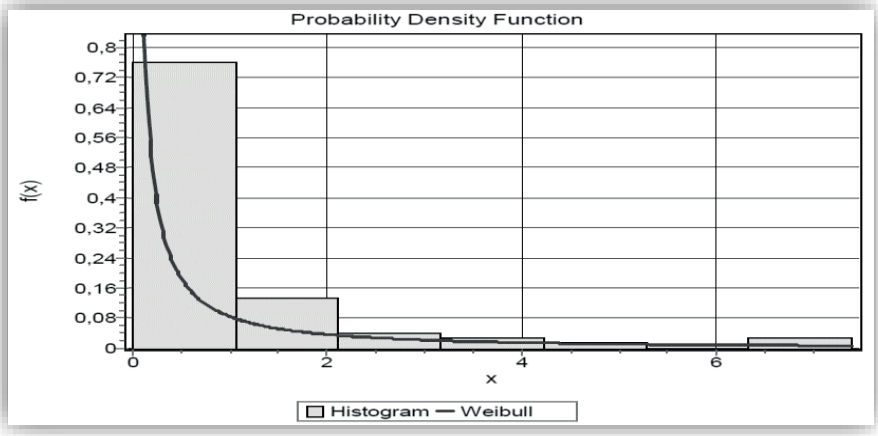

Figure 3. Histogram of the elapsed time between successive earthquakes

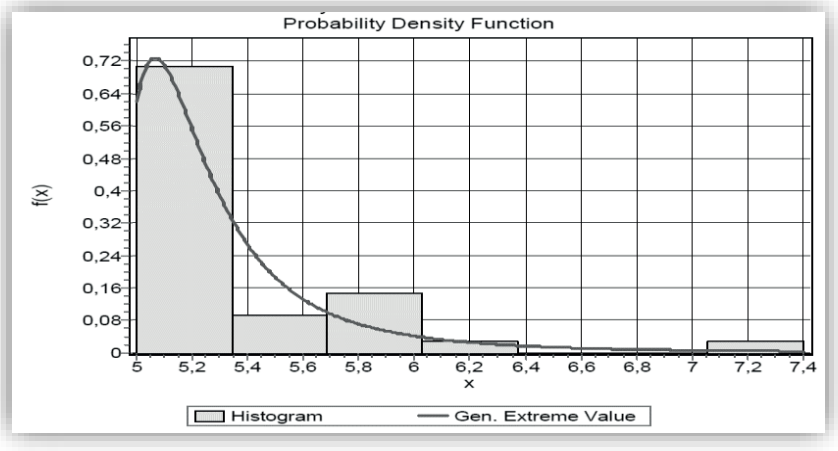

Figure 4. Histogram of the earthquake magnitudes

3.4. Risks Based on Copula Models

Selecting the best relevant copula to express the dependence between the variables X_{t_i} and Y_i is the next step in the modelling process. Therefore, estimations of copula parameters and the values of log-likelihood are as follows:

Table 3. Copula parameter estimations and the log-likelihood values

	X_{t_i} Y_i	
Family	$\hat{\gamma}$	$Log-likelihood$
$C_\gamma^{\text{Clayton}}$	0.14509e-006	-80.9936
C_γ^{Frank}	0.1355	-80.9505
C_γ^{Gumbel}	1.0266	-80.9133
$C_\gamma^{\text{Çelebioğlu}}$	-0.0605	-80.9732
C_γ^{FGM}	-0.0670	-80.9708
$C_\gamma^{\text{Galambos}}$	0.0009	-80.9936
C_γ^{Tawn}	0.0500	-80.9595
C_γ^{Joe}	1.7756	-91.1028

The goodness of fit results in Table 3 showed that the Gumbel copula with $\hat{\gamma} = 1.0266$ and Frank copula with $\hat{\gamma} = 0{,}1355$ best represent the dependence structure between X_{t_i} and Y_i. According to the result, we also report the Mahalanobis squared distance D_k^2 and its p-value for each family to evalute performance (Table 4). In order to calculate D_k^2 for the observed data, the number of simulated datasets from each fitted copula distribution that we utilize is B=1000.

Table 4. Performance evaluation

Family	Mahalanobis		
	Log-likelihood	D_k^2	p-value
Frank	-80.9505	0.1686	0.377
Gumbel	-80.9133	0.0860	0.415

According to the results obtained from Table 3 and Table 4, to be among a number of copula families, the one that best illustrates dependent structure between X_{t_i} and Y_i is Gumbel copula with $\hat{\gamma} = 1.0266$, $X_{t_i} \approx$ Gen-Extreme Value $(k = 0.37834, \sigma = 0.18487, \mu = 5.1229)$ ve $Y_i \approx$ Weibull $(\alpha = 0.25234, \beta = 0.13254)$, the joint distribution $H(x, y)$ is as follows:

$$H(x,y) = exp\left(-((-\ln F_1(x))^{1.0266} + (-\ln F_2(y))^{1.0266})^{1/1.0266}\right) \quad (8)$$

With the help of the joint distribution given in (8), the conditional probability distributions given in (9) and (10) can be obtained and various predictions regarding the Marmara region can be made with these distributions.

$$P\{X_{t_i} \geq x | Y_i \leq y\} = 1 - \frac{exp\left(-((-\ln F_1(x))^{1.0266} + (-\ln F_2(y))^{1.0266})^{1/1.0266}\right)}{F_2(y)} \quad (9)$$

$$P\{X_{t_i} \geq x | y_1 \leq Y_i \leq y_2\} = 1 - \frac{H(x,y_2)-H(x,y_1)}{F_2(y_2)-F_2(y_1)} \quad (10)$$

Based on (9), the probabilities of the earthquakes having magnitude M_W greater than or equal to 5, 5.5, and 7 in the region within 2 years are estimated to be approximately 88%, 20%, and 2%, respectively, with the starting time being December 4, 2023. Moreover, again from (9), the probabilities of the earthquakes having magnitude M_W greater than or equal to 5, 5.5, 6 and 7 in the region at all times are estimated to be approximately 88%, 20%, 6% and 2%, respectively.

3.5. Return periods

Table 5. The Marmara Region's earthquake magnitude's parametric models' return level and 95% bootstrap confidence interval

Return Period	GEV model
2 years	5.2 (5.14,5.31)
5 years	5.5 (5.39,5.72)
25 years	6.3 (5.95,6.72)
50 years	6.8 (6.24,7.38)
100 years	7.4 (6.53,8.16)

Table 6 lists the most significant historical earthquakes that occurred in the Marmara Region between 1964 and 2024. Numerous fatalities and substantial financial losses were caused by the earthquakes in the table. From Table 5, we discovered that the 100-year return level was approximately 7.4. This indicates that seismic events with a magnitude of $M_W = 7.4$, like the one that struck Izmit-Golcuk-Yalova-Adapazarı-Eastern Marmara on August 17, 1999, have a return time of approximately 100 years in the region. Moreover, there is a 1% probability of such a disastrous earthquake occurring in any given year. On the other hand, with copulas, while the probability of

experiencing a magnitude $M_W \geq 7{,}4$ earthquake in the Marmara Region in any given year is 1% for the first 12 years, this probability increases to 2% during and after the 13th year, and during and after the 46th year, this probability increases to 3%.

Table 6. Historical the major earthquakes from 1964 to 2024 in Marmara Region

Time	Location	M_w
22 July 1967	Adapazarı-Mudurnu Valley	6.2
17 August 1999	Izmit-Golcuk-Yalova-Adapazarı-Eastern Marmara	7.4
12 November 1999	Duzce-Kaynasli	7.2

4. Conclusion

The Marmara Region is located in the northwestern part of Turkey and is located at the western end of the North Anatolian Fault Zone (NAFZ), one of the most significant fault systems in Turkey. Especially in July 22, 1967 Adapazarı, August 17, 1999 Marmara and November 12, 1999 Duzce earthquakes that have occurred in the region since 1964, when the modern instrumental era began, there were hundreds of thousands of buildings damaged, tens of thousands of injuries, and thousands of deaths. Our historical experiences show that we will continue to encounter such devastating disasters. Since earthquakes or seismic activities are devastating natural disasters that cannot be prevented, it is of great importance to prepare to survive such dangerous events. (Causapin, 2018). With some statistical analyzes and predictions we made in this study, we also wanted to show that loss of life and damage can be prevented to some extent by predicting earthquakes that may occur in the Marmara Region and its surroundings. For this purpose, with the help of the seismic gap theory, which is based on the probability of a large earthquake occurring in a region where there has been no seismic activity for

a long time, the earthquake magnitude and the time variables between two successive earthquakes were modeled with copulas and the return periods were also calculated, thus approaching the issue of seismic risk and it has been possible to contribute to earthquake prediction studies to some extent. According to the results obtained, considering the return period, the probability of experiencing an earthquake with a magnitude of $M_W = 7.4$ in the Marmara Region in any year is approximately 1/100. On the other hand, with copulas, while the probability of experiencing a magnitude $M_W \geq 7{,}4$ earthquake in the Marmara Region in any given year is 1% for the first 12 years, this probability increases to 2% during and after the 13th year, and during and after the 46th year, this probability increases to 3%.

REFERENCES

Allcroft, D.J. and Glasbey, C.A. (2003). A simulation-based method for model evaluation. Statistical Modelling, 3(1):1-13.

Ates, A., Buyuksarac, A., Bilim, F., Bektas, O., Sendur, C., Komanovali, G. (2009). Spatial correlation of the aeromagnetic anomalies and seismogenic faults in the Marmara region, NW Turkey. Tectonophysics, 478:135–142.

Causapin, H. P. A. (2018). Semi-Markov chain modeling on earthquake occurrences in selected areas in Luzon. TILAMSIK: The Southern Luzon Journal of Arts and Sciences, 10 (1): 67-90.

Embrechts, P., Lindskog, F., & Mcneil, A. (2003). Modelling dependence with copulas and applications to risk management, Elsevier.

Emre, O., Duman, T.Y., Ozalp, S., Elmaci, H., Olgun, S., Saroglu, F. (2013). Active fault map of Turkey with an Explanatory Text. 1/1,250,000 scale, General Directorate of Mineral Research and Exploration, Special Publication Series-30, Ankara, Turkey.

Erbek Kiran, E., Ates, A., Dolmaz, M.N. (2021). Upper crustal structure of the Marmara region, northwest Turkey from aeromagnetic anomalies: western segment of the North Anatolian Fault. Marine Geophysical Research 42 (3): 1-8.

Fischbach, P. (2010). Copula-Models in the Electric Power Industry", Dissertation, University of St. Gallen.

Goda, K., Ren, J. (2010). Assessment of Seismic Loss Dependence Using Copula. Risk Analysis, 30(7): 1076-1091.

Kalafat, D. (2011). Marmara Bölgesi'nin Depremselliği ve Deprem Ağının Önemi, 1. Türkiye Deprem Mühendisliği ve Sismoloji Konferansı, Middle East Technical University, Ankara (in Turkish).

Kızılok Kara, E. (2017). The Earthquake Risk Analysis Based on Copula Models for Turkey. Sigma J Eng & Nat Sci 35 (2), 187-200.

Li, Y., Shi, B., Zhang, J. (2013). Copula joint function and its application in probability seismic hazard analysis. Acta Seismologica Sinica, 21(3): 296-305.

Ma, N., Bai, Y.B., Meng, S.W. (2021) Return period evaluation of the largest possible earthquake magnitudes in mainland China based on extreme value theory. Sensors 21: 3519.

McNeil, A., Frey, R. & Embrechts, P. (2005). Quantitative risk management – Concepts, techniques and tools. Princeton University Press.

Nikoloulopoulos, A.K., Karlis, D. (2008). Fitting copulas to bivariate earthquake data: The Seismic Gap Hypothesis revisited. Environmetrics, 19: 251-269.

Okay, A.L., Tuysuz, O. (1999). Tethyan sutures of northern Turkey, in the Mediterranean Basins: tertiary extension within the Alpine Orogen. Geol Soc Lond Spec Publ 156:475–515.

Saroglu, F., Emre, O., Kuscu, I. (1992). Active fault map of Turkey. 1/1,000,000 scale, general directorate of mineral researh and exploration. Publication of MTA, Ankara.

Unal Karacam, S. (2019). Investigation of the dependence structure in seismic hazard analysis: an application for Turkey. Communications Faculty of Sciences University of Ankara Series A1 Mathematics and Statistics, 68(2), 1528-1542.

Unal, S. (2023). Semi-Markov vs Conditional Copulas: A comparative Study in Seismic Hazard Analysis, international academic research and reviews in science and mathematics, serüven yayınevi, Ankara, 127-145.

Tan, O. (2021). A homogeneous earthquake catalogue for Turkey, Nat. Hazards Earth Syst. Sci., 21, 2059–2073.

CHAPTER 10

PHENOLIC COMPOUNDS, EXTRACTION METHODS AND SOME METHODS USED IN THEIR ANALYSIS

Zeynep DEMİRKAN[1]
Bülent KAYA[2]

1 Zeynep Demirkan Doktora Öğrencisi Bingöl Üniversitesi Orcıd: 0000-0002-8101-8194
2 Bülent Kaya Doç. Dr. Bingöl Üniversitesi Orcıd: 0000-0002-1216-6441

1. Introduction

Plants have been among the basic sources of life since the existence of humanity. Plants are used not only for nutrition but also for the treatment of many diseases. Alternative medicine practices are included in the culture and traditions of developing countries for treatment and prevention purposes (Njume *et al*., 2009). Plants used as herbal medicine in modern medicine and alternative medicine practices are called 'Medical Plants'. (Baydar, 2007). The most important factor in the use of plants for therapeutic purposes is the high antioxidant capacity of the phenolic substances they contain. The most effective method to protect against diseases and gain resistance against them is to strengthen the immune system. There is increasing interest in the consumption of foods rich in antioxidant properties resulting from phenolic compounds that can replace the high toxicity of synthetic antioxidants. The determination and quantity of phenolic compounds in food has become very important, with the perception that the more phenolic compounds in the plant content, the higher the antioxidant value.

2. Phenolic Compounds

Polyphenols were first defined by Bate-Smith and Swain in 1962 as water-soluble phenolic compounds with molecular weights between 500-3,000 (Da) that, in addition to forming ordinary phenolic reactions, have special properties such as precipitating gelatin, alkaloids and other proteins in solution (Bate-Smith 1954). Phenolic compounds are compounds found in the seeds, fruits, leaves, flowers, branches and stems of plants and originating from the shikimate, phenylpropanoid and pentose phosphate pathways in plant metabolism (Balasundram *et al*., 2006; Harborne and Williams, 2000). Phenolic compounds in plant parts are secondary metabolites that are formed through metabolic activities as well as synthesized under various stress conditions such as infection, tissue damage, exposure to UV light and radiation, and they are generally found in the form of glycosides (Naczk & Shahidi, 2004; Saldamlı, 1998). Today, the structures of approximately more than 8000 plant phenolic compounds have been reported, and newly identified phenolic compounds continue to be added (Alu'datt *et al*., 2017). Phenolic compounds are phytochemical substances that are effective in the formation of different characteristic properties such as taste, color and smell of fruits, vegetables, grains and various herbal products (Bohn, 2014). Phenolic compounds are structurally formed by an aromatic ring and one or more –OH groups attached to this ring. The carbon skeleton of phenolic compounds is the C6-C3-C6 ring structure, which contains flavonoids, partial phenolic acids and condensed tannins, and the C6-C1 structures, which mainly contain partial phenolic acids and hydrolyzed tannins. They are classified according to the bonding of benzo-γ-pyrone derivatives carrying phenol and pyran rings to the ring (Ringli *et al*., 2008; Yao *et al*., 2004; Heim *et al*., 2002). Phenolic

compounds are classified as flavonoids, phenolic acids, lignans, tannins and stilbenes according to their chemical structures (Alu'datt *et al*., 2017).

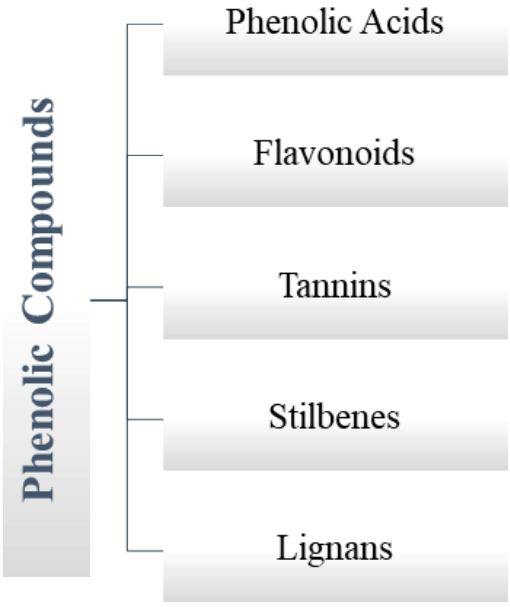

Figure 1. *Classification of Phenolic Compounds (Atak and Uslu, 2018)*

In addition to their chemical classification, it is possible to classify them as water-soluble and insoluble compounds (Rispail *et al*., 2005). Phenolic compounds exist in three different forms within the cell: free, extractable and non-extractable (Nayak *et al*., 2015). Phenolic compounds in free form are trapped inside cell vacuoles. Phenolic compounds in extractable form can be esterified into low molecular weight compounds or glycosides thanks to the aromatic ring and –OH groups in their structure (Saura-Calixto, 2012). Phenolic compounds that cannot be extracted are bound covalently to structures such as protein, pectin and cellulose in the cell wall via acetal, ether or ester bonds. The -OH groups in the aromatic ring of phenolic compounds form ether bonds with lignin in the cell walls of plants; -COOH groups are bonded to carbohydrates and proteins via ester bonds (Acosta-estrada *et al*., 2014). The antioxidant properties of phenolic compounds are related to the atoms in their rings, structural function relationships and glycosylation (Bendary *et al*. 2013; Wang *et al*., 2018a).

According to recent studies, due to the high bioactivity of phenolic substances, they are used for prevention and treatment of many different diseases such as cardiovascular diseases, diabetes and oxidative stress-related

diseases due to their antioxidant, anti-inflammatory and anticarcinogenic effects (Yasir *et al*., 2016). Phenol compounds can protect important biomolecules such as proteins and nucleic acids against oxidative damage (Heleno *et al*., 2015). The basis of the antioxidative mechanism of phenolic compounds; It is related to the reducing properties of these compounds that scavenge free radicals, such as hydrogen or electrons. Due to their free radical scavenging effect and chelating activity on metals such as iron and copper, they prevent the formation of free radicals by the catalysis of metals (Vuolo *et al*., 2019). These compounds have different effects such as taste, odor and color formation of fruits and vegetables, positive effects on human health, as well as enzyme inhibition (Saldamlı, 1998). Recent studies have proven that phenolic substances inhibit the enzymes of α-amylase and α-glucosidase and therefore have a positive effect in the treatment of type 2 diabetes (Mccue & Shetty, 2004). They also play an important role in protecting plants against pesticides and play a role in the defense mechanism of plants and are effective against various pests such as parasitic viruses (Alasalvar *et al*., 2001; Bohn, 2014). Plants rich in secondary metabolites are used in different application areas such as medicine, agriculture, cosmetics and food (Tepe *et al* 2005).

2.1. Phenolic Acids

Phenolic acids; They are phytochemicals that contain an aromatic ring containing an acidic group and one or more -OH groups and are widely included in diets (Zhang *et al*., 2019; Sevgi *et al*., 2015). These phytochemicals constitute an important class of phenolic compounds in plants, found in bound or free states (Zhang *et al*., 2016). Phenolic acids account for approximately one-third of the phenolic compounds found in vegetables, fruits, nuts, herbs, tea and coffee (Li *et al*., 2020). Phenolic acids; They can be divided into 2 subclasses: hydroxybenzoic acid and hydroxycinnamic acid. Hydroxybenzoic acids have a C6-C1 chemical structure and protocatechuic, syringic, gallic and vanillic acids are compounds in this class (Zhang *et al*, 2016). These compounds are abundant in oilseeds, coffee, currants, black-eyed peas, cereals, raspberries, pumpkins and blackberries (Zhang *et al*., 2022). Hydroxycinnamic acid, coumaric, synaptic, ferulic and caffeic acid are some examples of this class, and they are aromatic compounds with a three-carbon side chain in the C6-C3 chemical structure (Zhang *et al*, 2016). These compounds are abundant in grains, coffee, cherries, spinach, peaches, citrus fruits, plums, tomatoes, potatoes and almonds (Zhang *et al*., 2022). Unlike other phenolic compounds, hydroxycinnamic and hydroxybenzoic acids behave acidic due to the presence of the -COOH group in the molecule (Annie & Jean-Jacques, 2003).

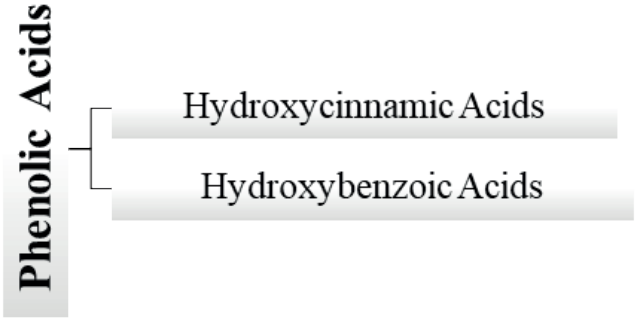

Figure 2. *Classification of phenolic acids.*

Phenolic acids play a role in different physiological activities such as photosynthesis, protein synthesis, enzyme activities, involvement in the cytoskeleton, and nutrient uptake from leaves, seeds and roots (Heleno *et al*., 2015). Phenolic acids have metal chelating and redox properties, acting as reducing agents, hydrogen donors, or singlet oxygen quenchers. It has been reported that they have various pharmacological activities such as anticarcinogenic, vasoprotective, antiallergenic and antiviral, which are attributed to phenolic compounds as antioxidants (Rao *et al*., 2018). Previous studies have reported that phenolic acids have very high biological activities such as anticancer, antimutagenic and antioxidant. In addition, previous studies have shown that dietary intake of plant foods rich in phenolic compounds is associated with a reduction in the risk of many chronic diseases such as neurodegenerative and cardiovascular disorders, some types of cancer and osteoporosis. For this reason, it has been demonstrated that phenolic acids can be used as ingredients that offer positive effects on health, such as functional foods and cosmetic products. (Li *et al*., 2020).

2.2. Flavonoid

Flavonoids derived from the Latin word flavus, meaning yellow; They are phenolic compounds containing diphenyl propane with 15 C atoms and arranged in a C6 - C3 -C6 configuration (Kahraman *et al*., 2002). The carbon skeleton of flavonoids is formed as a result of the bonding of two phenyl rings with the propane chain (Kumar & Pandey, 2013). Flavonoids generally consist of two aromatic rings, A and B, joined by a three-carbon bridge in the C-shaped form, which is a heterocyclic ring. The A aromatic ring is derived from the acetate/malonate pathway, while the B ring is derived from phenylalanine via the shikimate pathway (Merken & Beecher, 2000). High and low antioxidant capacities are related to their ability to absorb UV rays and their different ring structures. While flavonoids with dihydroxy B rings have higher antioxidant capacity, flavonoids with monohydroxy B rings absorb UV

waves better (Işık, 2005; Kumar & Pandey, 2013). Flavonoids constitute the majority of dietary phenolic compounds (Robbins, 2003). In addition to free compounds, they are often found as glycosides and partly as esters (Vermerris & Nicholson, 2006). While flavonoids were thought to be among vitamins until the 1930s, they are now studied as a class of phenolic compounds (Kumar & Pandey, 2013). Flavonoids are synthesized in different stress situations such as drought, injury, heavy metal exposure and starvation (Işık, 2005; Kumar & Pandey, 2013). Flavonoid compounds are found in all parts of plants such as leaves, roots, flowers, stems, seeds and fruits (Işık, 2005). They play a role in many important events such as color formation of flowers and fruits, attracting pollinators to the plant, protecting plants from harmful rays such as UV-A and UV-B, inhibiting enzyme activity and antioxidant (Işık, 2005; Kumar & Pandey, 2013). They also protect plants against oxidative cell damage, fungal parasites and pathogens (Cook & Samman, 1996). Flavonoids consumed regularly in the diet significantly reduce the risk of serious diseases such as heart diseases and cancer. (Beecher, 2003 ; Liu *et al*., 2008). Flavonoids are divided into 6 classes as a result of the 3-carbon propane chain taking different shapes, variable positions of the phenyl groups and forming a third ring (Kumar & Pandey, 2013).

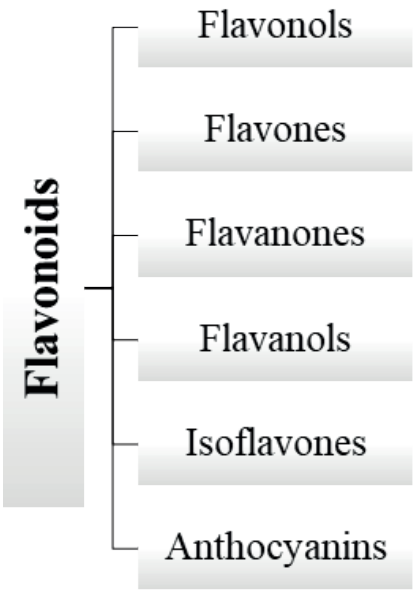

Figure 3. *Flavonoid Classification*

2.2.1. Flavonols

Flavonols are a class of flavonoids with double bonds between C2-C3 carbons and usually exist in glycoside form. The contents of flavonols, which

are commonly found in fruits and vegetables, vary depending on many different environmental factors such as season, growing conditions, cooking conditions and storage processes (Caridi *et al*., 2007). Among its flavonols, the most well-known compounds are myricetin, kaempferol, quercetin and quercetin derivatives (Durazzo *et al*., 2019).

2.2.2. Flavones

Flavones have a similar structure to flavonols, but differ by a double bond at C3 that does not contain an -OH group (Bianca *et al*., 2021). The most well-known compounds of flavones are luteolin and apigenin (Durazzo *et al*., 2019; Mark *et al*., 2019).

2.2.3. Flavanones

Flavanones are a class of slimming flavonoids with no double bonds between C2-C3 and being in the carboxyl group in all four conformations (Durazzo *et al*., 2019). In other words, flavanones are characterized by the presence of a saturated three-carbon chain and one oxygen atom (Ignat *et al*., 2011). Flavanones are the precursors of many flavonoids, although there are flavanone species belonging to most plant families (Durazzo *et al*., 2019; Mark *et al*.,2019). In addition to being found in high amounts in citrus fruits, flavanones are also found in aromatic plants such as tomatoes and mint. To give some examples of flavanones, naringenin in grapefruit, hesperetin in orange and eriodiktyol in lemon are the best examples (Ignat *et al*., 2011).

2.2.4. Flavanols (Catechins)

Flavanols, which are formed as intermediate products in the biosynthesis of flavonoids and are most commonly found in foods, are colorless compounds seen in almost all fruits. Flavanols are systematically called flavan-3-ols because they have a hydroxyl group at the C3 atom (Yeşilada, 2019.)

2.2.5. Isoflavone

Isoflavones are a class of flavonoids known as phytoestrogens, which are abundant in soybeans (Büyüktuncer ve Başaran, 2005). Isoflavones, which have structural similarities with estrogens, have hydroxyl groups in the C7-C4 positions, like the estradiol molecule. They are found in many plants and plant-derived foods in both aglycone (natural) form and acetyl- or malonyl-form. Isoflavones are used for the treatment and prevention of common diseases such as cancer and atherosclerosis. (Klejdus *et al*., 2007; D'Archivio *et al*., 2007). Among the isoflavone compounds, daidzein, genistein and glycitein stand out (Büyüktuncer and Başaran, 2005).

2.2.6. Anthocyanins

Anthocyanin, which means flower and blue in Latin, is the basic building block of flavylium ion (Kolaç *et al*., 2017). Anthocyanins derived from

flavonols with a –OH group at position 3 have two double bonds, one between the oxygen atom and carbon and the other between carbon 3 and 4. (Durazzo *et al*., 2019; Mark *et al*., 2019). Anthocyanin compounds are located in all plant tissues such as flowers, fruits, leaves, roots and stems. Anthocyanins are vacuole pigments that are water soluble and can appear in different colors such as red, purple or blue at varying pH (Ignat *et al*., 2011). Anthocyanins are plant pigments that color plant organs in blue and red (Gould & Lister, 2006). In addition to the bioactivities demonstrated by anthocyanins, they are frequently used as natural colorants, especially in the food industry (Durazzo *et al*., 2019; Mark *et al*., 2019). Anthocyanins, which are abundant in flowers and ripe fruits, play an important role in attracting the attention of pollinators for pollination and seed dispersal (Gould & Lister, 2006). Anthocyanins have strong biological functions with their pharmacological properties, antioxidant and anti-inflammatory activities (Ignat *et al*., 2011). Fermentation and heat treatments increase the release of anthocyanins in the fruit (Kolaç *et al*., 2017).

Table 1. *Food sources of some flavonoids.*

Class	Flavonoid	Nutritional Source
Flavanol	(+)-Catechin, (-)-Epicatechin, Epigallocatechin	Tea varieties, grapes, apples.
Flavone	Sirisin, apigenin, routine, luteolin and luteolin glucosides	Fruit peels, red wine, olive oil, grapefruit.
Flavonol	Kaempferol, quercetin, myricetin and tamarixetin	Leafy vegetables, onion, grapefruit, olive oil, strawberries, red wine.
Flavanone	Naringin, naringenin, taxifolin and hesperidin	Citrus fruit
Isoflavone	Genistein, daidzein	Soybean.
Anthocyanin	Apigenin, cyanidin	Cherry, raspberry, strawberry.

Source: Aktaş and Çölgeçen, 2017; Theodoratou *et al*., 2007.

2.3. **Tannins**

Tannins, also called tannic acid, are amorphous substances in flake, powder or sponge-like structure with different colors from light yellow to brown. Tannins, which are seen in the bark, root, leaf, wood and fruit tissues of plant parts, generally play an important role in regulating the development of these tissues. The tannins found in the buds protect the roots from freezing, the ones found in the leaves protect the leaves from being eaten by herbivorous animals by spoiling the taste of the leaves, and the ones found in the roots protect the roots against plant pathogens. Tannins contained in the seed tissue provide bactericidal and allelopathic effects as well as ensuring the survival of plant species (Aydın and Üstün, 2007). Hydrolyzable tannins

contain -OH groups esterified with carbohydrate and phenolic groups in the center, and they decompose into carbohydrate and phenolic acid as a result of easy hydrolysis with weak acid, weak base, hot water or enzymes such as tannase (Aydın and Üstün, 2007). Tannins are found primarily in grains, legume seeds, and many fruit and vegetable tissues. Tannins have antibacterial, antioxidant, antiviral, antiparasitic, anti-inflammatory, etc. properties. It has various biological activities such as (Smeriglio *et al*., 2017). Tannins, which are among the leading antiseptic compounds, are included in many drug compositions used in medicine due to their astringent effects on mucosa and vessels. Pharmaceutical preparations used for eczema treatment contain synthetic tannins (Aydın and Üstün, 2007).

2.4. **Stilbenes**

Another class of phenolic compounds are stilbenes, characterized by a C6–C2–C6 molecular structure with two benzene rings connected by double bonds (Durazzo *et al*., 2019; Mark *et al*., 2019). Plants produce stilbenes in response to pathogenic infection and most stress conditions (Bavaresco, 2003). The most well-known and widely researched compound of stilbenes due to their bioactivity is resveratrol (Göçmez and Seferoğlu, 2014). Resveratrol compound exists in both cis and trans isomeric forms, mostly in glycosylated forms (Ignat *et al*., 2011). Black grape fruit produces the compound resveratrol to protect itself under adverse conditions (Göçmez and Seferoğlu, 2014). Stilbenes are frequently found naturally in a wide variety of food sources such as grapes, strawberries, peanuts and some medicinal plants (Tsai *et al*., 2017). Resveratrol has an antiaging effect as it shows 50 times more antioxidant activity than vitamin E and 30 times more than vitamin C. In addition, the resveratrol compound has effects on the production of lipoproteins in the liver, suppressing fat secretion and reducing blood fats (Xie *et al*., 2013).

2.5.**Lignans**

Lignans are the largest phenolic compounds obtained by oxidative dimerization of two phenylpropane units (Pietrofesa *et al*, 2016). The basic structure of lignans consists of a combination of phenylpropanoid dimers (C6-C3) that bond with the central carbons of the side chains (Durazzo, 2019). Although lignans are mostly in free form, glycoside derivatives are also found in small numbers (Saleem *et al*., 2005). The basic lignan compounds found in plant tissues, such as secoisolariciresinol, matairesinol, isolariciresinol and lariciresinol, have a similar structure to the enterolactone and enterodiol compounds that show estrogenic activity in humans (Özkaynak and Ova, 2008). In addition to most of the bioactivities demonstrated by lignans, they also have estrogenic and anti-estrogenic activities (Bianca *et al*., 2021). Although the richest source of lignans is flaxseed, they are found in most vegetables and fruits, nuts,

oilseeds and coffee. They have been used for a long time in both ethnic and traditional medicine due to their antioxidant, antibacterial, anti-inflammatory and antiviral properties (Pietrofesa *et al*., 2016). Interest in lignans and their synthetic derivatives is increasing day by day due to their potential applications in various cancer chemotherapy and other pharmacological effects (Saleem *et al*., 2005).

3. Extraction Methods of Phenolic Compounds

The extraction process can be defined as the process of taking one or more compounds in the solid or liquid phase into a new liquid phase by taking advantage of their solubility properties (Nakilcioğlu and Ötleş, 2014). In its most general terms, extraction is the process of passing the plants and other materials to be extracted through a solvent and removing the soluble compounds contained in the material (Öztekin and Soysal, 1998). The method and solvent used in the extraction process are the first step to ensure the optimal concentration of natural compounds in the extract (Zhang *et al*., 2022). Extraction processes are applied with different methods depending on the final product to be obtained from the raw material (Öztekin and Soysal, 1998). The extraction process is the most important step in identifying and utilizing phenolic compounds. There are many different techniques and methods to extract phenolic compounds from plant materials, including fruits and vegetables (Bleve *et al*., 2008; Fredj *et al*., 1990). New extraction techniques are needed due to the need for large amounts of solvent and long periods of time in the most preferred solvent extraction method. New extraction techniques that shorten extraction times, reduce the solvent rate and are environmentally friendly are preferred (Wang & Weller, 2006). While the solvent extraction method and extraction with supercritical fluids are the most preferred techniques for the isolation of phenolic compounds, traditional and different methods such as enzyme-assisted extraction, ultrasound-assisted extraction, solid-liquid extraction, supercritical fluid extraction, microwave-assisted extraction, and pressure extraction are also used (Nahar & Sarker, 2005; Palma & Taylor, 1999; Zhang *et al*., 2022). The concentration of the desired components in the extract is determined by various factors such as the choice of different temperatures, contact times, particle size of the material, liquid-solid ratio. For example, three times higher content of phenolic compounds in almond shell extraction was determined in the liquid-solid extraction method at 50 °C compared to 25 °C (Hayouni *et al*., 2007; Pinelo *et al*., 2005 ; Rubilar *et al*., 2003). There is no generally accepted and standard solvent for the extraction of phenolic compounds. However, it is generally believed that it shows high performances in phenolic compound extraction due to the high solubility of phenolic compounds in solvents with higher polarities (Zhang *et al*., 2022).

3.1. **Liquid-liquid extraction**

The liquid-liquid extraction method is a mass transfer process in which a solution containing one or more solutes is first thoroughly mixed with an immiscible or slightly immiscible solvent. This mixture consists of two parts: the extract, which contains the extracted solute and plenty of solvent, and the waste, which contains very little solute (Müller *et al*., 2008). Liquid-liquid extraction is frequently used in the purification of metal ions and phenolic compounds and in the beverage industry (Görgülü *et al*., 2017; Ignat *et al*., 2011).

3.2.**Solid-Liquid Extraction**

Solid-liquid extraction is the process of direct extraction of fresh or dried plant materials in polar or non-polar solvents. Solid-liquid extraction is one of the easy and common methods preferred for the extraction of phenolic compounds from plant parts (Gadkari *et al*., 2014). The liquid-liquid extraction method, which is the most common and simple method, has various disadvantages due to low efficiency, long extraction time, and the use of dangerous solvents at high rates (Zhang *et al*., 2022).

3.3.**Ultrasound Assisted Extraction**

Ultrasonic sound waves are sound waves that are above what humans can hear (Cavuldak *et al*., 2016). Although the ultrasound-assisted extraction method involves close contact between the sample matrix and the solvents, it is a frequently used method to increase the efficiency of extraction of lipids, proteins and phenolic compounds in plants (Ignat *et al*., 2011). The ultrasound-assisted extraction method is an alternative technique to the traditional method because it is simpler, more efficient and cheaper than the traditional extraction method (Jing *et al*., 2008). In addition to the increase in extraction efficiency by improving mass transfers, the ultrasound-assisted method has many advantages such as the low amount of solvent used, less equipment used, less working time and simplicity of working principles (Ameer *et al*., 2017). Ultrasound-assisted extraction method is frequently used in the extraction of phenolic compounds as it is a very simple, effective and economical method.

3.4. **Supercritical Fluid Extraction**

There are three different states of matter: liquid, solid and gas. However, when the temperature and pressure of the substances are increased above their critical values, a new region is formed, this supercritical region, and the fluids in this region are defined as supercritical fluids (McHugh *et al*., 1994). Supercritical fluids are neither liquid nor gaseous. Since the fluid density decreases at low pressure and high temperatures, it will behave like a gas, and at high pressure and low temperatures, the fluid will behave like a liquid because its density will increase. The basic principle of this method is based on

the use of supercritical solvents in fluid form (Başer, 2010). Supercritical fluids preferred in biochemical materials are carbon dioxide, ammonia, ethane, propane, chlorotrifluoromethane, ethylene, trifluoromethane, propylene and hexane (Çolak & Tülek, 2003; Başer, 2010). Although there are many different fluids, the most preferred by far is supercritical carbon dioxide (SC-CO2), which is the first choice due to its low toxicity, positive effects on the environment, easy removal from solutes, compatibility with foodstuffs and cheapness. Thanks to modern technologies, it helps in the extraction of natural products with various polarities by regulating the changes in temperature and pressure (Nahar & Sarker, 2005). Supercritical fluids are replacing most organic solvents traditionally used in industrial extraction, purification and recrystallization processes. Supercritical fluids have similar dissolving power to organic solvents, but have higher diffusivity, lower surface tension, and lower viscosity (Ignat *et al*., 2011). Reasons for choosing supercritical fluid extraction; It is very fast, does not use high amounts of toxic solvents, is selective and environmentally friendly. In addition, the absence of light and air entry during extraction minimizes the degradation processes that may occur in traditional solvent extraction techniques (Bleve *et al*., 2008).

3.5. **Mikrodalga Destekli Ekstraksiyon**

Microwaves are defined as high frequency (300-300000 MHz) electromagnetic waves (Büyüktuncel, 2012). Microwave energy has been used in the field of chemistry for many years for sample thawing, drying, solvent extraction, desorption and absorption, moisture measurement, chromogenic reactions, and analytical sample preparation (Tokkan *et al*., 2012). The basic principle of the microwave-assisted extraction method is based on the direct effects of microwaves on molecules by ion conduction and dipole rotation (Büyüktuncel, 2012). In other words, it is based on the direct use of microwave frequencies to facilitate the vibration of molecules and the separation of solvents from the sample (Zhang *et al*., 2022). Factors such as reducing the harmful solvent rate and shortening the extraction time have allowed this method to become widespread (Tokkan *et al*., 2012). Important physical parameters of this method include microwave power, dielectric constant, extraction time, solubility and solvent properties (Zhang *et al*., 2022). If this method is preferred, it provides many advantages such as low working time, low amount of solvent consumed, production cost and high efficiency (Hosseini *et al*., 2016).

4. **Analysis Methods of Phenolic Compounds**

The amount of phenolic compounds in the biomolecule varies depending on many different parameters such as the preferred extraction method, chemical structure of the compounds, particle size, solvent selection and impurities. With the development and progress in analytical science, there are methods

that use spectrophotometry, High performance liquid chromatography (HPLC), Gas Chromatography (GC) and Liquid chromatography-mass spectrometry (LC-MS) and combinations of these methods in the amount and determination of phenolic compounds in biomolecules (Zhang *et al*., 2022).

4.1. **Spectrophotometry**

Spectrophotometry is a very simple and rapid technique used in the quantification of phenolic compounds in biomolecules (Gogia *et al*., 2014). Due to the low cost and simplicity of this method, it is a common technique used for the determination of different classes of phenolic compounds in biomolecules (Zhang *et al*.,2022). Folin-Ciocalteu and Folin-Denis assays have been widely preferred for many years in the determination of phenolic compounds in plant tissues. The basic principle of both methods is based on chemical reduction procedures of substances containing molybdenum and tungsten. In the presence of phenolic compounds, the products formed in the reaction appear blue at a wavelength of 760 nm (Gogia *et al*., 2014; Khoddami *et al*., 2013).

4.2. **Gas Chromatography (GC-MS)**

The term chromatography, which originates from Greek, means "color writing". The term chromatography is the name given to the process steps in which the substances contained in the mixture placed in the appropriate solvent are dissolved and separated according to their chemical and physical properties (Eser & Sepici-Dinçel, 2018). Gas chromatography; It is the technique used to identify and quantify phenolic compounds such as phenolic acids, anthocyanins, flavonoids and tannins found in plant tissues. The principle of the method is based on passing the samples through a heated column under pressure between inert gas and the non-volatile liquid layer inside the column and using different evaporation temperatures for different compounds (Balas & Popa, 2007). In this technique, the column preferred for the analysis of phenolic compounds is 30 m long, with an outer diameter of 0.25-0.30 mm and an inner diameter of 0.25 μm in capillary form. Helium gas is generally used as carrier gas in this technique. (Zhang *et al*., 2022).

4.3.**High Pressure Liquid Chromatography (HPLC)**

All compounds that can pass into soluble form (amino acids, vitamins, antibiotics, pesticides, phenolic compounds, etc.) are detected reliably and quickly by high-pressure liquid chromatography. The HPLC device consists of 8 parts, but its main parts are; It consists of pump, column and furnace, mobile phase, autosampler, deaerator, injector and detector parts (Bengü, 2021). Various advantages of the HPLC technique, such as high selectivity, precision, sensitivity, resolution and sample behavior, make it the most preferred method for the determination and separation of plant phenolic

compounds (Naczk & Shahidi, 2006). The basic principle of the method is based on the separation of the desired compounds in complex mixtures based on their solubility or interactions between the stationary phase and mobile phase (Coskun, 2016). Many factors such as selected column types, mobile phase, applied detectors and characteristics of the samples are effective in the determination of phenolic compounds. To obtain information about a particular phenolic compound, it is necessary to compare the retention time with the standard (Ignat *et al*., 2011).

4.4.**Liquid Chromatography-Mass Spectrometry (LC-MS/MS)**

Although it can be defined as a subtype of HPLC device based on liquid chromatography, it is recognized as a different method or device due to the high features provided by the mass detector (Eser & Sepici-Dinçel, 2018). Mass spectrometers are devices based on the principle of quantifying charged particles moving in an electrical or magnetic field by distinguishing them from other charged particles according to their mass and charge ratios (Biberoğlu, 2003; Aguilar, 2004). LC-MS/MS is a technique that can obtain results with high sensitivity and specificity in the determination of unknown compounds and the structural properties of organic-inorganic molecules (İşlekel, 2011). In the Mass Spectrometer, there is a capture time and mass-charge values for each molecule. Although molecules have the same mass-charge ratio, the number of molecules with the same fragmentation ions is 1/10000 in nature, allowing the quantification of contents even at very low concentrations (Eser & Sepici-Dinçel, 2018).

4.5.**Colorimetric Analysis**

The analysis method based on the color change that occurs as a result of the interaction of samples with different chemicals is called colorimetric methods (Martinez *et al*., 2008). Colorimetric analysis is another method used to determine the total phenolic compound content of organic solvents, phenols or aqueous solutions, and hydrocarbon mixtures. In colorimetric analysis, although the functional group affects hydrocarbons containing water, mineral, acidic inorganic bases, it is a successful process in determining monophenols and diphenols (Lykken *et al*., 1946).

5. **Conclusion**

Polyphenols are a class of secondary metabolites that are common in various plant organs such as dietary vegetables, fruits and spices, and play a role in the emergence of various properties of the material such as color and taste. Considering the potential health benefits of phenolic compounds, they attract the attention of researchers as natural antioxidant sources. Although synthetic antioxidants have high toxicity, studies on the use of antioxidants obtained from natural sources have increased considerably, with the belief that products

from nature will not be harmful. Internal and external factors that we are exposed to in our daily routine, such as sunlight and chemicals, are the main reasons that lead to the formation of free radicals and the acceleration of the aging process. Antioxidant compounds have highly bioactive properties such as delaying the formation of oxidative stress against free radicals and stopping or preventing the activities of free radicals. Natural phenolic compounds can also be used to extend the shelf life of foods and replace synthetic antioxidants in cosmetic products. The first step in determining the amount and content of phenolic compounds is the extraction process. In addition to the lack of a generally acceptable extraction method, parameters such as standard solvent, time and temperature vary depending on each product. However, the selected extraction method should be preferred as it is low cost, low toxicity, high efficiency and environmentally friendly. After the extraction step, natural antioxidant substances are identified and quantified using the appropriate analysis method. This analysis can be performed with the standard use of known phenolic substances in analysis methods. But what should we do about a phenolic compound that is not found in the newly obtained literature? This should be our real question. For this reason, biologists interested in this subject must have high knowledge of instrumental chemistry. In this case, analysis can be carried out up to a point with the effective use of ms/ms detectors. However, methods such as C-NMR and H-NMR must be used effectively. This is already a field of research in itself. An experimental setup and knowledge that require purification stages must be possessed and their skillful use must be ensured.

REFERENCES

Acosta-Estrada, B.A., Gutiérrez-Uribe, J.A., SernaSaldívar, S.O. (2014). Bound phenolics in foods, a review, *Food Chemistry*, 152, 46-55.

Aguilar, M.I. (2004). HPLC of Peptides and Proteins Methods and Protocols, *Methods Mol Biol,* 251:3-8.

Aktaş, T., Çölgeçen, H. (2017). Farklı Bitki Türlerinden Bitki Doku Kültürü Teknikleriyle Flavonoidlerin Üretimi, *Karaelmas Fen ve Müh. Derg.* 7(**2**), 665-673,

Alasalvar, C., Grigor, J.M., Zhang, D., Quantick, P.C., Shahidi, F. (2001). Comparison of volatiles, phenolics, sugars, antioxidant vitamins, and sensory quality of different colored carrot varieties, *J Agric Food Chem* 9(**3**),1410-6.

Alu'datt, M.H., Rababah, T., Alhamad, M.N., et al. (2017). A review of phenolic compounds in oil-bearing plants: istribution, identification and occurrence of phenolic compounds, *Food Chem*. 218(**0308-8146**),99-106

Ameer, K., Shahbaz, H.M., Kwon, J.H. (2003). Green extraction methods for polyphenols from plant matrices and their byproducts: a review, *Compr Rev Food Sci Food,* 16(**2**), 295-315.

Annie, F., Jean-Jacques, M. (2003). Flavonoids İn Health And Disease , 2. baskı . New York, ABD: CRC Press.

Atak, E., Uslu, M.E. (2018). Fenolik Bileşikler, ekstraskiyon Metodları ve Analiz Yöntemleri, *Soma Meslek Yüksekokulu Teknik Bilimler Dergisi.* 27,3.

Aydın, S.A., Üstün, F. (2007). Tanenler 1. Kimyasal Yapıları, Farmakolojik Etkileri, Analiz Yöntemleri. *İstanbul Üniv. Vet. Fak. Derg.,* 33 (**1**),21-31.

Balas, A., Popa, V.I. (2007). On characterization of some bioactive compounds extracted from *Picea abies* bark. *Rom Biotechnol Lett*, 12(**3**), 3209-3215.

Balasundram, N., Sundram, K., Samman, S. (2006). Phenolic compounds in plants and agri-industrial by-products: antioxidant activity, occurrence, and potential uses, *Food Chem*, 99(**1**), 191-203.

Başer, K.H.C. (2010). Tıbbi ve Aromatik Bitkisel Ürünlerin Üretimi ve Kalite Kontrolü, Anadolu Üniversitesi Yayınları, Eskişehir, Eylül 2010.

Bate-Smith E.C., Swain T. Flavonoid compounds. In: Mason H.S., Florkin A.M., editors. *Comparative Biochemistry.* Volume 3 Academic Press; New York, NY, USA: 1962.

Bavaresco, L. (2003). Role of viticultural factors on stilbene concentrations of grapes and wine Drugs under, *Experimental and Clinical Research*, 29 pp. 181-187.

Baydar, H., (2007). Tıbbi, Aromatik ve Keyf Bitkileri Bilimi ve Teknolojisi. *Süleyman Demirel Üniversitesi Ziraat Fakültesi, S.D.Ü.* 51, 216 s.

Beecher, G.R. (2003). Overview of dietary flavonoids: nomenclature, occurrences and intake *American Society for Nutrition and Sciences*, 133 (**10**), 3248-3254

Bendary, E., Francis, R.R., Ali, H.M.G., Sarwat, M.I., Hady, S.E. (2013). Antioxidant and structure -activity relationships (SARs) of some phenolic and anilines compounds. *Ann Agric Sci.*,58,173–81.

Bengü, A.Ş. (2021). HPLC Tekniği ve Kullanım Alanları, *BÜSAD* 2(**1**), 64 – 69.

Bianca, R.A., Sandrina, A.H., Oliveira, M.B.P.P., Barros, L., Ferreira I.C.F.R. (2021). Phenolic compounds: current industrial applications, limitations and future challenges, *Food Funct***.12,** 14-29.

Biberoğlu, G. (2003). Kütle Spektrometresi ve Tıp Alanında Kullanımı, *T Klin Tıp Bilimleri,* 23, 491-498 10.

Bleve, M., Ciurlia, L., Erroi, E., Lionetto, G., Longo, L., Rescio, L., Schettino, T. and Vasopollo, G. (2008). An innovative method for the purification of anthocyanins from grape skin extracts by using liquid and sub-critical carbon dioxide, *Seperation and Purification Technology*, 64, 192-197,

Bohn, T. (2014). Dietary factors affecting polyphenol bioavailability. Nutrition Reviews, 72(7), 429-452.

Büyüktuncel, E., (2012). Gelişmiş Ekstraksiyon Teknikleri I. *Hacettepe Üniversitesi Eczacılık Fakültesi Dergisi*, 32(**2**), 209-242.

Büyüktuncer, Z., Başaran, A. (2005). Fitoöstrojenler ve Sağlıklı Yaşamdaki Önemleri. Hacettepe Üniversitesi, *Eczacılık Fakültesi Dergisi,* 25(**2**), 79-94.

Caridi, D., Trenerry, V.C., Rochfort, S., Duong, S., Laugher, D., Jones, R. (2007). Profiling and quantifying quercetin glucoşides in onion (*Allium cepa* L.) varieties using capillary zone electrophoresis and high performance liquid chromatography, *Food Chemistry*, 105,691-699.

Cavuldak, Ö.A.,Vural, N., Anlı, R. E. (2016) Bitki Kaynaklı Fenolik Bileşiklerin Ultrasonik Dalga Destekli Ekstraksiyonu, *Gıda*, 41 (**1**), 53-60.

Cook, N.C., Samman, S. (1996). Flavonoids–chemistry, metabolism, cardioprotective effects, and dietary sources *Nutritional Biochemistry*, 7, 66-76.

Coskun, O. (2016). Separation techniques: chromatography, *North Clin Istanb*, 3(**2**), 156-160.

Çolak, N., Tülek Y., (2003). Süperkritik Akışkan Ekstraksiyonu, *Gıda dergisi* 28(**3**), 313-320.

D'Archivio, M., Filesi, C., Di Benedetto, R., Gargiulo, R., Giovannini, C., Masella ,R. (2007). Polyphenols, dietary sources and bioavailability Annali dellIstituto Superiore di Sanità, 43(**4**), 348-361.

Durazzo, A., Caiazzo, E., Lucarini, M., Cicala, C., Izzo, A., Novellino, E., Santini, A. (2019). Polyphenols: a concise overview on the chemistry, occurrence, and human health, *Phytother. Res.*, **33**, 2221- 2243.

Eser, B., Sepıcı-Dınçel, A. (2018). Kromatografiye Giriş, Yüksek Performanslı Sıvı Kromatografi Kullanımında Basit İpuçları, *Journal of Health Services and Education* 2(**2**), 51-57.

Fredj, D., Francois, D. (1990). *Purification of colored substances, especially anthocyanosides, from berries.* Patent No. FR 2641283.

Gadkari, P.V., Kadimi, U.S., Balaraman, M. (2014). Catechin concentrates of garden tea leaves (*Camellia sinensis* L.): Extraction/isolation and evaluation of chemical composition, *J Sci Food Agric*., 94(**14**), 2921-2928.

Gogia, N., Gongadze, M., Bukia, Z., Esaiashvili, M., Chkhikvishvili, I. (2014). Total polyphenols and antioxidant activity in different species of apples grown in Georgia. *Georgian Med News*., 232-233(1512-0112),107-112.

Gould, K.S., Lister, C. (2006). Flavonoid functions in plants. In: . M. wusen & K.R. Markham (Eds), Flavonoids. Chemistry, Biochemistry and Applications, *CRC Press, Boca Raton*, pp. 397–442.

Göçmez, A.,, Seferoğlu, H.G. (2014). Asmalarda Resveratrol İçeriğini Etkileyen Faktörler Ve İnsan Sağlığına Faydaları. Adnan Menderes Üniversitesi Ziraat Fakültesi Dergisi, 11(**1**),31- 38.

Görgülü, G., Ulu, B., Dede, B. (2017). Aminoketooksim Bileşiklerinin Sıvı-Sıvı Ekstraksiyon ve Boya Renk Giderim Özelliklerinin İncelenmesi, *Akademia Disiplinlerarası Bilimsel Araştırmalar Dergisi* 3 (**2**), 46-54, 2017.

Harborne, J.B., Williams, C.A., (2000). Advances in flavonoid research since 1992. *Phytochemistry*, 55(**6**), 481-504.

Hayouni, E.A., Abedrabba, M., Bouix, M., Hamdi, M. (2007). The effects of solvents and extraction method on the phenolic contents and biological activities in vitro of Tunisian *Quercus coccifera* L. and *Juniperus phoenicea* L. fruit extracts, *Food Chemistry*, 105,1126-1134.

Heim, K.E., Tagliaferro, A.R., Bobilya, D.J. (2002). Flavonoid antioxidants: chemistry, metabolism and structure-activity relationships. *J Nutr Biochem,*13(**10**), 572-84.

Heleno, S.A., Martins, A., Queiroz, M.J.R.P., Ferreira, I.C.F.R. (2015). Bioactivity of phenolic acids: metabolites versus parent compounds: a review. **Food Chemistry**, 173, 501-513.

Hosseini, S.S., Khodaiyan, F., Yarmand, M.S. (2016). Optimization of microwave assisted extraction of pectin from sour orange peel and its physicochemical properties. *Carbohydr Polym*., 140(0144-8617), 59-65.

Ignat, I., Volf, I., Popa V.I. (2011). A critical review of methods for characterisation of polyphenolic compounds in fruits and vegetables. *Food Chem*.,126(**4**), 1821-1835.

Işık, F.E. (2005). Edirne Bölgesinde Yetişen *Trifolium resupinatum* L. var. *microcephalum* Bitkisinin Fitokimyasal İncelenmesi. Doktora tezi. Trakya Üniversitesi.

İşlekel, H., (2011). LC-Tandem MS-MRM Temel Araştırma ve Klinik Laboratuvarda Kullanım. Dokuz Eylül Üniversitesi Tıp Fakültesi.

Jing, W., Baoguo, S., Yanping, C., Yuan, T., Xuehong, L. (2008). Optimisation of ultrasound-assisted extraction of phenolic compounds from wheat bran *Food*

Chemistry, 106 pp. 804-810.

Kahraman, A., Serteser, M., Köken T. (2002). Flavonoidler. ***Kocatepe Tıp Der****gisi*, 3:01-08.

Khoddami, A., Wilkes, M. A., Roberts, T. H. (2013). Techniques for analysis of plant phenolic compounds. *Molecules*, 18(**2**), 2328-2375.

Klejdus, B., Vacek, J., Benešová, L., Kopecký, J., Lapčík, O., Kubáň, V. (2007). Rapid-resolution HPLC with spectrometric detection for the determination and identification of isoflavones in soy preparations and plant extracts, *Analytical and Bioanalytical Chemistry*, 389, 2277-2285.

Kolaç, T., Gürbüz, P., Yetiş, G. (2017). Phenolic Content And Antioxidant Characteristics Of Natural Products, *İ.Ü. Sağlık Hizmetleri Meslek Yüksekokulu Dergisi*, 5,1.

Kumar, S., Pandey, A.K. (2013). Chemistry and Biological Activities of Flavonoids: An Overview. *Bio. of Plants*, 6, 34.

Li, T., Li, X., Dai, T., Hu, P., Niu, X., Liu, C. (2020). Binding mechanism and antioxidant capacity of selected phenolic acid - β-casein complexes. *Food Research International*, 129.

Liu, Q., Cai, W., Shao, X. (2008). Determination of seven polyphenols in water by high performance liquid chromatography combined with preconcentration, *Talanta*, 77, 679-683.

Lykken,L.,Treseder,R.S., Zahn,V. (1946). Colorimetric Determination of Phenols. Application to Petroleum and Allied Products. *Industrial & Engineering Chemistry Analytical Edition*, 18(**2**), 103-109.

Mark, R., Lyu, X., Lee, J.J.L., Parra-Saldívar,R., Chen, W.N. (2019). Sustainable production of natural phenolics for functional food applications, *J. Funct. Foods*, **57**, 233-254.

Martinez, A.W., Phillips, S.T., Carrilho, E., Thomas, S.W., Sindi, H., Whitesides, G.M., (2008). Simple telemedicine for developing regions: Camera phones and paper-based microfluidic devices for real-time, off-site diagnosi, *Analytical Chemistry*, 80(10): 3699–3707.

Mccue, P., Shetty, K. (2004). Inhibitory effects of rosmarinic acid extracts on porcine pancreatic amylase in vitro. *Asia Pac. J. Clin. Nutr.,* 13,101–106.

McHugh, M.A., Krukonis, V.J., (1994). Supercritical Fluid Extraction Principles and Practice, 2nd Ed. McGraw Hill, Butterwort-Heinemann, Boston Mass, 5-18 .

Merken, H.M., Beecher, G.R. (2000). Measurement of food flavonoids by high-performance liquid chromatography: A review *Journal of Agricultural and Food Chemistry*, 48 pp. 577-599

Müller, E., Berger, R., Blass, E., Sluyts, D., Pfennig, A. (2008). Ullmann's encyclopedia of industrial chemistry, *Liquid–Liquid Extraction*.

Naczk, M., Shahidi, F. (2004). Extraction and analysis of phenolics in food, *J. Chromatography A*. 1054, 95-111.

Naczk, M., Shahidi, F. (2006). Phenolics in cereals, fruits and vegetables: occurrence, extraction and analysis. *J Pharm Biomed Anal*., 41(**5**):1523-1542.

Nahar, L., Sarker, S.D., (2020). Supercritical fluid extraction, *Natural Products Isolation*, 20,(2005),47-76.

Nakilcioğlu, E., Ötleş, S. (2014). Basınçlı Çözgen Ekstraksiyonu ve Gıda Sanayiindeki Uygulamaları. *Akademik Gıda*, 12(**2**).88-94.

Nayak, B., Liu, R.H., Tang, J. (2015). Effect of processing on phenolic antioxidants of fruits, vegetables, and grains-a review. *Critical Reviews in Food Science and Nutrition*, 55(**7**), 887-918.

Njume, C., Afolayan, A.J., Ndip, R.N. (2009). An overview of antimicrobial resistance and the future of medicinal plants in the treatment of Helicobacter pylori Infections. *Afr. J. Pharm. Pharmacol*., 3, 685-699.

Özkaynak, E., Ova, G. (2008). Lignanlar ve Sağlık Üzerine Etkileri. *Türkiye 10. Gıda Kongresi*, 21-23 Mayıs, Erzurum

Öztekin, S., Yurtsever S.(1998). Tıbbi Ve Aromatik Bitkilerde Ekstraksiyon Yöntemler, *Tarımsal Mekanizasyon* 18. Ulusal Kongresi, Tekirdağ

Palma, M., Taylor, L.T. (1999). Extraction of polyphenolic compounds from grape seeds with near critical carbon dioxide Journal of Chromatography A, 849, 117-124.

Pietrofesa, R.A., Velalopoulou, A., Arguiri, E., et al. (2016). Flaxseed lignans enriched in secoisolariciresinol diglucoside prevent acute asbestos-induced peritoneal inflammation in mice. *Carcinogenesis*, 37(**2**),177-187.

Pinelo, M., Del Fabbro, P., Manzocco, L., Nunez, M.J. (2005). Nicoli M.C. Optimization of continuous phenol extraction from *Vitis vinifera* byproducts *Food Chemistry*, 92, 109-117.

Rao, Y., Zhao, X., Li, Z., Huang, J. (2018). Phenolic acids induced growth of 3D ordered gold nanoshell composite array as sensitive SERS nanosensor for antioxidant capacity assay. *Talanta*,190,174-181.

Ringli, C., Bigler, L., Kuhn, B.M., et al. (2008). The modified flavonol glycosylation profile in the Arabidopsis rol1 mutants results in alterations in plant growth and cell shape formation. *Plant Cell*.,20(**6**),1470-1481.

Rispail, N., Morris, P., Webb, K. (2005). Phenolic compounds: extraction and analysis. In: *Lotus Japonicus Handbook* (edited by A. Márquez). 349–354.

Robbins, R.J.,(2003). Gıdalardaki Fenolik Asitler:Analitik Metodolojiye Genel Bakış. *Tarım ve Gıda Kimyası Dergisi*, 51, 2866-2887 .

Rubilar, M., Pinelo, M., Franco, D., Sineiro, J., Nunez M.J. (2003). Residuos agroindustriales como fuente de antioxidants, *Afinidad*, 60, 153-160.

Saldamlı, İ. (1998). Gıda Kimyası, Hacettepe Üniversitesi Yayınları, 527 ss, Ankara.

Saleem, M., Kim, H.J., Ali, M.S., Lee, Y.S. (2005). An update on bioactive plant lignans *Natural Product Reports*, 22,696-716.

Saura-Calixto, F. (2012). Concept and healthrelated properties of nonextractable polyphenols: the missing dietary polyphenols, *Journal of Agricultural and Food Chemistry*, 60(**45**),11195-11200

Sevgi, K., Tepe, B., Sarikurkcu, C. (2015). Antioxidant and DNA damage protection potentials of selected phenolic acids, *Food and Chemical Toxicology*, 77, 12-21.

Smeriglio, A., Barreca, D., Bellocco, E., Trombetta, D. (2017). Proanthocyanidins and hydrolysable tannins: occurrence, dietary intake and pharmacological effects. *Br J Pharmacol*.,174(**11**),1244-1262.

Tepe, B., Daferera, D., Sökmen, A., Sökmen, M., Polıssıou, M. (2005). Antimicrobial and antioxidant activities of the essential oil and various extracts of Salvia tomentosa Miller (Lamiaceae). *Food Chemistry*, 90 (**3**), 333-340.

Theodoratou, E., Janet, K., Cetnarskyj, R., Farrington, S. M., Tenesa, A., Barnetson, R., Porteous, M., Dunlop, M. and Campbell, H. (2007). Dietary flavonoids and the risk of colorectal cancer. *Cancer Epidemiol. Biomarkers,* 16(**4**),684-693.

Tokkan, D., Kuşlu, S., Çalban, T., Çolak, S., (2012). Anod Çamurundaki Gümüşün Amonyum Tiyosülfat Çözeltilerinde Mikrodalga Enerjisi ile Ekstraksiyonunun Optimizasyonu. *10. Ulusal Kimya Mühendisliği kongresi.*

Tsai, H.Y., Ho, C.T., Chen, Y.K. (2017). Biological actions and molecular effects of resveratrol, pterostilbene, and 3′ -hydroxypterostilbene. *J Food Drug Anal*., 25(**1**),134-147.

Vermerris, W., Nicholson, R. (2006 . Fenolik bileşik aileleri ve sınıflandırılma yolları. *Fenolik Bileşik Biyokimyası*. 1,34. Berlin: Springer.

Vuolo, M.M., Lima, V.S., Maróstica Junior, M.R. (2019). Chapter 2-Phenolic compounds: structure, classification, and antioxidant power. In: MRS C, editor. Bioactive Compounds. Duxford: Woodhead Publishing; p. 33–50.

Wang, L., Weller, C.L. (2006). Recent advances in extraction of nutraceuticals from plants, *Trends in Food Science & Technology*, 17, 300-312.

Wang, T., Li, Q., Bi, K. (2018a). Bioactive flavonoids in medicinal plants : structure, activity and biological fate. *Asian J Pharma Sci.,* 13,12–23.

Xie, H., Han, H.P., Chen, Z., He, J.P. (2013). A Study on the Effect of Resveratrol on Lipid Metabolism in Hyperlipidemic Mice. *Afr J Tradit Complement Altern Med.*, 11(**1**), 209-12.

Yao, L.H., Jiang, Y.M., Shi, J., Tomás-Barberán, F.A., Datta, N., Singanusong, R., et al. (2004). Flavonoids in food and their health benefits. *Plant Foods Hum Nutr*, 59(**3**), 113-22.

Yasir, M., Sultana, B., Amicucci, M. (2016). Biological activities of phenolic compounds extracted from Amaranthaceae plants and their LC/ESI-MS/MS profiling. *J Funct Foods*., 26(1756-4646), 645-656.

Yeşilada, E. (2019) İzoflavonlar Menopoz Dönemi Şikâyetlerinde Etkili ve Güvenilir Bir Çözüm Sağlayabilir Mi? Http://Www.Pharmetic.Org/Fitoterapi/İzoflavonlar.Html

Zhang, L., Li, Y., Liang, Y., Liang, K., Zhang, F., Xu, T., *et al*. (2019). Determination of phenolic acid profiles by HPLC-MS in vegetables commonly consumed in China. *Food Chemistry*, 276, 538-546.

Zhang, Y., Cai, P., Cheng G., Zhang Y., (2022). A Brief Review of Phenolic Compounds Identified from Plants: Their Extraction, Analysis, and Biological Activity, *Natural Product Communications*,17, 1.

Zhang, Z., Wu, X.Y., Cao, S.Y., et al. (2016). Caffeic acid ameliorates colitis in association with increased Akkermansia population in the gut microbiota of mice. *Oncotarget*., 7(**22**), 31790-31799.